GREAT AUSTRALIAN BIGHT
RESEARCH PROGRAM

RESEARCH REPORT SERIES

Spatial and temporal variability in shelf microbial and plankton communities in the Great Australian Bight

Final Report GABRP Project 2.1

van Ruth, P.D., Patten, N.L., Bailleul, F., Chapman, P., Doubell, M., Everett, J., Goldsworthy, S.D., Harcourt, R.G., McGarvey, R., McMahon, C.R., Middleton, J.F., Redondo Rodriguez, A., Richardson, A.J., Richardson, L., Ward, T.M.

GABRP Research Report Series Number 27

October 2017

bp CSIRO Government of South Australia Primary Industries and Regions SA SARDI South Australian Research and Development Institute THE UNIVERSITY of ADELAIDE Flinders UNIVERSITY

DISCLAIMER

COPYRIGHT

THIS PUBLICATION MAY BE CITED AS:

van Ruth, P.D., Patten, N.L., Bailleul, F., Chapman, P., Doubell, M., Everett, J., Goldsworthy, S.D., Harcourt, R.G., McGarvey, R., McMahon, C.R., Middleton, J.F., Redondo Rodriguez, A., Richardson, A.J., Richardson, L. and Ward, T.M. (2017). Spatial and temporal variability in shelf microbial and plankton communities in the Great Australian Bight. Final Report GABRP Project 2.1. Great Australian Bight Research Program, GABRP Research Report Series Number 27, 106pp.

CONTACT

Dr Paul van Ruth
SARDI
e: paul.VanRuth@sa.gov.au

FOR FURTHER INFORMATION

www.misa.net.au/GAB

GREAT AUSTRALIAN BIGHT RESEARCH PROGRAM

The Great Australian Bight Research Program is a collaboration between BP, CSIRO, the South Australian Research and Development Institute (SARDI, the University of Adelaide, and Flinders University. The Program aims to provide a whole-of-system understanding of the environmental, economic and social values of the region; providing an information source for all to use.

CONTENTS

LIST OF FIGURES

LIST OF TABLES

GLOSSARY

GAB	Great Australian Bight
IMOS	Integrated Marine Observing System
MNF	Marine National Facility
NRS	National Reference Station
SAIMOS	South Australian Integrated Marine Observing System
SARDI	South Australian Research and Development Institute
Shelf	Continental margin seabed depths from 0 m to the shelf break or nominally 200 m

ACKNOWLEDGEMENTS

Physical, chemical and biological data were sourced from the Integrated Marine Observing System (IMOS) – IMOS is a national collaborative research infrastructure, supported by the Australian Government.

We thank Ian Moody (SARDI) for processing and analysis of archived samples through the Laser Optical Particle Counter.

Finally, we thank the Great Australian Bight Research Program, a collaboration between BP, CSIRO, SARDI, the University of Adelaide and Flinders University, for funding and support.

1. EXECUTIVE SUMMARY

Project 2.1 in the Pelagic Ecosystem and Environmental Drivers Theme of the Great Australian Bight Research Program (GABRP) represents the first detailed study of the influence of variations in enrichment processes on lower trophic ecosystem dynamics in shelf waters of the GAB. We focused on three key knowledge gaps in the pelagic ecology of GAB shelf waters that were identified in the review of Rogers et al. (2013), through investigations into: 1) macro-nutrient concentrations, sources and sinks, and their influence on; 2) microbial, phytoplankton, and zooplankton abundance and community composition and; 3) microbial food web dynamics and the timing of shifts in food web structure. The work was primarily aimed at the analysis of temporal patterns in existing data from the eastern GAB region (Chapters 3.1 and 4.1). However, we also examined available datasets for the central GAB, to complement work conducted in project 2.2 to investigate spatial patterns in food web dynamics across the GAB (Chapters 3.2 and 4.2). We used a suite of physical, chemical and biological datasets, including long-term data collected as part of the Australian Integrated Marine Observing System (IMOS), wind and irradiance data from the Bureau of Meteorology, and datasets associated with SARDI sardine biomass surveys, which covered a range of spatial and temporal scales. Conceptual and quantitative models of pelagic ecosystem processes were developed which provide new insights into lower trophic ecosystem dynamics in the GAB that are critical for the development of trophodynamic models for the region.

Variations in meteorology, oceanography and biogeochemistry were investigated to assess the influence of upwelling and downwelling on enrichment and primary productivity. We discovered that the length of an upwelling season did not dictate its intensity or productivity, and that long, intense seasons were not necessarily the most productive. A key finding was the importance of differentiating between upwelling events and enrichment events. The former occurred in the early upwelling season (November-December) and drew cold, nutrient rich water onto the shelf, but not into the euphotic zone. The latter only occurred in the late upwelling season (January – April), and drew water upwelled in the early season into the euphotic zone where it was available for primary producers. We identified the importance of this November-December preconditioning period in governing the intensity of enrichment of the euphotic zone during the late upwelling season, and suggest that the number, intensity and duration of upwelling events that occur during pre-conditioning will dictate levels of enrichment associated with late season upwellings. Our analyses confirmed that the upwelled water mass, and thus significant enrichment of waters in the euphotic zone, was restricted to the eastern GAB. Water mass characteristics revealed no evidence of upwelled water on the central GAB shelf. We used this information to develop a conceptual model for five different meteorological/oceanographic scenarios that are likely to occur in the eastern GAB, and their influence on enrichment, lower trophic ecosystem dynamics and productivity. Scenarios include winter mixing, preconditioning, moderate upwelling, strong upwelling and suppression of upwelling. We hypothesise that total ecosystem productivity depends on the combination of these scenarios which may occur in the region in a given season/year.

Patterns in microbial and plankton biomass, abundance and community composition from long-term datasets were compared, with predictions made for each scenario in the conceptual model, to test the hypothesis that spatial and temporal shifts in the influence of upwelling and downwelling trigger shifts in food web dynamics in the eastern GAB. During winter-mixing, small phytoplankton dominated, zooplankton biomass and abundance were high, and the community was dominated by zooplankton taxa known to preferentially feed on small pico- and nano-plankton. During preconditioning, moderate phytoplankton biomass was present, with nano- and micro-

phytoplankton comprising the bulk of the autotrophic community. Peaks in diatoms and flagellates at this time occurred in response to the winter-spring transition, where irradiances and stratification of the water column increase, promoting elevated levels of primary production. Coincident high abundances and biomass of zooplankton indicate strong trophic transfer from primary to secondary producers at this time. During moderate upwelling, pico- and micro-phytoplankton made similar contributions to moderate levels of phytoplankton biomass. Zooplankton abundances and biomass were low, proposed to result from significant grazing on copepods and their eggs during preconditioning. Highest autotrophic biomass occurred during strong upwelling, and was dominated by micro-plankton (specifically diatoms). High zooplankton biomass, with dominant taxa known to respond to enriched waters and enhanced micro-phytoplankton biomass, suggests strong trophic transfer from primary producers to secondary consumers. The dominance of smaller pico-phytoplankton during suppression was coincident with low zooplankton biomass and abundance, indicating a food web more reliant on microbial recycling processes.

Patterns in microbial and plankton abundance, biomass, and size distributions, and sardine egg densities were examined, together with key environmental drivers of observed variations, to test the hypothesis that shifts in food web dynamics will have implications for the size structure of the zooplankton community, and patterns in sardine egg density. Differences in meso-zooplankton size between the eastern and central GAB shelf reflected the food webs that underpinned these systems. Our results reveal positive links between cold upwelled water and efficient trophic biomass transfer from phytoplankton to meso-zooplankton to sardines, culminating in high sardine egg densities.

Our findings indicate that enrichment via upwelling is the key environmental driver of variation in food web dynamics in the eastern GAB. However, the situation is more complex than first thought, and our findings deviated somewhat from our original hypotheses. There are three food webs operating in the eastern GAB, all of which vary significantly in their influence on productivity in the region, and are enhanced by enrichment via upwelling. The microbial food web is present year-round in the eastern GAB, but as a background signal underlying other important food webs in the region, effectively "keeping the lights on" in productivity terms. The dominant food web in the eastern GAB, supporting moderate rates of primary productivity year-round, is a food web previously undocumented in the region, based on nano-phytoplankton and heterotrophic dinoflagellates. The efficient, classic food web only occurs during upwelling, when enrichment drives high rates of primary productivity that are comparable to highly productive eastern boundary current upwelling systems.

We have detailed the importance of the preconditioning period that characterises the early upwelling season in governing the intensity of enrichment in the euphotic zone during the late upwelling season. In addition, we have discovered a previously undocumented "spring bloom" scenario which develops during the winter-spring transition, and provides a critical "kick-start" for productivity and trophic transfer in the system. Physical and chemical drivers of this phenomenon are yet to be described. Future studies should focus on examining the influence of variations in the duration and intensity of individual upwelling/downwelling events (i.e. within scenario variation) on enrichment, primary productivity, and food web dynamics in the eastern GAB, and the physical, chemical, and biological processes underlying the region's spring bloom.

Through this project, we have also discovered that meso-zooplankton size distributions and the parameters of the Normalised Biomass Size Spectrum (NBSS) provide valuable information that improves our understanding of the drivers of sardine egg density distributions. The analysis of plankton samples collected systematically during sardine biomass surveys will provide additional

information that will assist in the management of this valuable fishery and the GAB marine ecosystem.

2. INTRODUCTION

2.1 Overview

The Great Australian Bight (GAB) is part of the world's only northern boundary current system, the Flinders Current System, which extends from western Tasmania to south-western Western Australia. The eastern GAB is characterised by enhanced primary and secondary productivity supported by coastal upwelling in the austral summer (Middleton and Cirano 2002, Kämpf et al. 2004, McClatchie et al. 2006, Middleton and Bye 2007, van Ruth et al. 2010a, b). Increased productivity supports large populations of small pelagic fish, including sardine and anchovy (Ward et al. 2001a, b, 2006, 2011), and important populations of large marine species, including southern bluefin tuna (Hobday et al. 2009, Fujioka et al. 2010, Basson et al. 2012), Australian sea lions (Goldsworthy et al. 2013) and pygmy blue whales (Gill et al. 2011). The GAB is a region of global conservation significance, supporting valuable fishing, aquaculture and ecotourism industries (Ward et al. 2006, Goldsworthy et al. 2013, Rogers et al. 2013). Future management of this economically and ecologically important local region requires a thorough understanding of variations in the lower trophic levels of the food web which support ecosystem productivity (microbes, phytoplankton, zooplankton) in an area under increasing pressure from anthropogenic activities and a changing climate.

Important information about ecosystem structure and function can be derived from the taxonomic composition and size distribution of microbial and plankton assemblages and their variations in response to such key ecosystem drivers as nutrient enrichment through upwelling. In other systems, high autotrophic biomass and productivity in response to enrichment of the euphotic zone is associated with the dominance of large phytoplankton (diatoms), and the prevalence of an efficient 'classical' food web (i.e. diatoms to zooplankton to fish; Ryther 1969, Cushing 1989). In the absence of significant enrichment through physical processes, when well-lit waters become devoid of nutrients, a less efficient 'microbial' food web underpinned by picophytoplankton dominates, with high rates of nutrient recycling by microbes providing minimal enrichment via biological means. This study represents the first investigation of the influence of variations in physical/biological enrichment processes on primary productivity and food web dynamics in the GAB, and the implications these changes may have for overall ecosystem productivity.

Empirical evidence suggests that inter-annual changes in the species composition and size distribution of the plankton assemblage can have major implications for key components of the ecosystem. For example, a change in the zooplankton assemblage, combined with fishing pressure, may have contributed to the decline in the jack mackerel stock off northeast Tasmania in the 1980s (Young et al. 1993, 1996). Information on zooplankton abundance and ecosystem dynamics are critical to understanding the effects of potential future anthropogenic impacts on ecosystem structure and function.

This project was primarily focused on the analysis of temporal patterns in existing physical, chemical and biological data from the data rich eastern GAB region (Chapters 3.1 and 4.1). However, we also examined available datasets for the central GAB, to complement work conducted in project 2.2 to investigate spatial patterns in food web dynamics across the GAB (Chapters 3.2 and 4.2). This work has provided new insights into lower trophic ecosystem dynamics in the GAB that are critical for the development of trophodynamic models for the region. We developed conceptual and quantitative models of pelagic ecosystem processes that will provide a basis for understanding potential future changes or environmental impacts in ecosystem structure and function. We focused on two key hypotheses:

1. That the microbial loop is the dominant planktonic food web in shelf waters of the eastern GAB and that the more efficient classic food web only occurs in the eastern GAB during periods of nutrient-rich upwelling. Spatial and temporal shifts in the influence of upwelling and downwelling in the eastern GAB trigger shifts in food web structure between the microbial loop and the classic diatom dominated food web.

2. That shifts in food web structure will have implications for the size structure of the zooplankton community in shelf waters of the GAB and, consequently, the biomass of upper trophic levels.

This project further addressed the following knowledge gaps identified in the literature review (Rogers et al. 2013):

1. Macro-nutrient concentrations, sources and sinks
2. Microbial, phytoplankton, and zooplankton abundance and community composition
3. Microbial loop dynamics and the timing of shifts in food web structure

2.2 Objectives

1. Identify and compare inter-annual, seasonal and spatial variability in the taxonomic composition and size distribution of the microbial, phytoplankton and zooplankton assemblage in shelf waters of the eastern GAB to test the hypothesis that spatial and temporal shifts in the influence of upwelling and downwelling in these regions trigger shifts in food web structure between the microbial loop and the classic diatom dominated food web.

2. Derive empirical relationships between taxonomic composition and size structure of plankton to test the hypothesis that shifts in food web structure will have implications for the size structure of the zooplankton community and, consequently, the biomass of upper trophic levels.

3. Identify key environmental drivers of observed variability in species composition and size spectrum of microbes and plankton (e.g. upwelling strength, nutrient concentrations, primary productivity).

4. Compare inter-annual patterns in microbial and planktonic ecosystem structure and sardine egg densities.

References

Basson, M., Hobday, A., Eveson, J., and Patterson, T. 2012. Spatial Interactions Among Juvenile Southern Bluefin Tuna at the Global Scale: A Large Scale Archival Tag Experiment FRDC Report 2003/002.

Brown, J. H., Gillooly, J. F., Allen, A. P., Savage, V. M., and West, G. B. 2004. Toward a metabolic theory of ecology. Ecology, 85: 1771-1789.

Cushing, D. 1989. A difference in structure between ecosystems in strongly straified waters and those that are only weakly stratified Journal of Plankton Research, 11: 1-13.

Gill, P. C., Morrice, M. G., Page, B., Pirzl, R., Levings, A. H., and Coyne, M. 2011. Blue whale habitat selection and within-season distribution in a regional upwelling system off southern Australia. Marine Ecology Progress Series, 421: 243-263.

Goldsworthy, S. D., Page, B., Rogers, P. J., Bulman, C., Wiebkin, A., McLeay, L. J., Einoder, L., et al. 2013. Trophodynamics of the eastern Great Australian Bight ecosystem: Ecological change associated with the growth of Australia's largest fishery. Ecological Modelling, 255: 38-57.

Hobday, A., Kawabe, R., Takao, Y., Miyashita, K., and Itoh, T. 2009. Correction factors derived from acoustic tag data for a juvenile southern bluefin tuna abundance index in southern Western Australia. Tagging and tracking of marine animals with electronic devices. In Tagging and Tracking of Marine Animals with Electronic Devices. Reviews: Methods and Technologies in Fish Biology and Fisheries. Ed. by Nielsen J.L., Arrizabalaga H., Fragoso N., Hobday A., Lutcavage M., and S. J. Springer Publishing, Dordrecht.

Kämpf, J., Doubell, M., Griffin, D., Matthews, R., L., and Ward, T. M. 2004. Evidence of a large seasonal coastal upwelling system along the southern shelf of Australia. Geophysical Research Letters, 31: 31:doi:1029/2003GL019221.

McClatchie, S., Middleton, J. F., and Ward, T. M. 2006. Water mass analysis and alongshore variation in upwelling intensity in the eastern Great Australian Bight. Journal of Geophysical Research: Oceans, 111: doi:10.1029/2004JC002699.

Middleton, J. F., and Bye, J. A. T. 2007. A review of the shelf-slope circulation along Australia’s southern shelves: Cape Leeuwin to Portland. Progress in Oceanography, 75: 1-41.

Middleton, J. F., and Cirano, M. 2002. A northern boundary current along Australia's southern: The Flinders Current shelves. Journal of Geophysical Research: Oceans, 107: doi:10.1029/2000JC000701,002002.

Richardson, A., Wolne, W., John, A. W. G., Jonas, T. D., Lindley, A., Sims, D. W., Stevens, D., et al. 2006. Using continuous plankton recorder data. Progress in Oceanography, 68: 27-74.

Rogers, P. J., Ward, T. M., van Ruth, P. D., Williams, A., Bruce, B. D., Connell, S. D., Currie, D. R., et al. 2013. Physical processes, biodiversity and ecology of the Great Australian Bight region: a literature review.

Ryther, J. H. 1969. Photosynthesis and fish production in the sea. Science, 166: 72-76.

van Ruth, P. D., Ganf, G. G., and Ward, T. M. 2010a. Hot-spots of primary productivity: An Alternative interpretation to Conventional upwelling models. Estuarine, Coastal and Shelf Science, 90: 142-158.

van Ruth, P. D., Ganf, G. G., and Ward, T. M. 2010b. The influence of mixing on primary productivity: A unique application of classical critical depth theory. Progress in Oceanography, 85: 224-235.

Ward, T., M., McLeay, L. J., Dimmlich, W. F., Rogers, P., J., McClatchie, S. A. M., Matthews, R., Kampf, J., et al. 2006. Pelagic ecology of a northern boundary current system: effects of upwelling on the production and distribution of sardine (*Sardinops sagax*), anchovy (*Engraulis australis*) and southern bluefin tuna (*Thunnus maccoyii*) in the Great Australian Bight. Fisheries Oceanography, 15: 191-207.

Ward T.M., Burch, P., and Ivey, A. R. 2012. South Australian Sardine (*Sardinops sagax*) Fishery: Stock Assessment Report 2012. Report to PIRSA Fisheries and Aquaculture. South Australian Research and Development Institute (Aquatic Sciences), Adelaide. 111 pp.

Ward, T. M., Burch, P., McLeay, L. J., and Ivey, A. R. 2011. Use of the Daily Egg Production Method for stock assessment of sardine, *Sardinops sagax*; lessons learnt over a decade of application off southern Australia. Reviews in Fisheries Science, 19: 1-20.

Ward, T. M., Hoedt, F., McLeay, L. J., Dimmlich, W. F., Jackson, G., Rogers, P. J., and Jones, K. 2001a. Have recent mass mortalities of the sardine *Sardinops sagax* facilitated an expansion in the distribution and abundance of the anchovy *Engraulis australis* in South Australia. Marine Ecology Progress Series, 220: 241-251.

Ward, T. M., Hoedt, F., McLeay, L. J., Dimmlich, W. F., Kinloch, M., Jackson, G., McGarvey, R., et al. 2001b. Effects of the 1995 and 1998 mass mortality events on the spawning biomass of sardine, *Sardinops sagax*, in South Australian waters. ICES Journal of Marine Science, 58: 865-875.

Young, J., W., Bradford, R., W., and al., e. 1996. Biomass of zooplankton and micronekton in the southern bluefin tuna fishing grounds off eastern Tasmania, Australia. Marine Ecology Progress Series, 138: 1-14.

Young, J. W., Jordan, A. R., Bobbi, C., Johannes, R. E., Haskard, K., and Pullen, G. 1993. Seasonal and interannual variability in krill (*Nyctiphanes australis*) stocks and their relationship to the fishery for jack mackerel (*Trachurus declivis*) off eastern Tasmania, Australia. Marine Biology, 116: 9-18.

3. VARIATIONS IN PHYSICAL AND CHEMICAL DRIVERS OF FOOD WEB DYNAMICS

3.1 Drivers of change in lower trophic ecosystems: the influence of temporal variations in upwelling on enrichment and primary productivity in the eastern GAB (van Ruth, P.D., Patten, N.L., Doubell, M.J., Chapman, P., Redondo Rodriguez, A., and Middleton, J,F.)

3.1.1 Introduction

The productivity of an upwelling region typically depends on the periodicity of upwelling favourable winds. While upwelling enriches illuminated surface waters with macronutrients necessary for phytoplankton growth, thus stimulating primary production, continuous advection as a result of upwelling can result in reduced productivity, as nutrients and phytoplankton are forced offshore (Marra 1978). Relaxation of upwelling through the reversal or calming of upwelling favourable winds during periods of quiescence allows stratification to develop, creating a surface layer of nutrient rich water with optimal conditions for phytoplankton production (Small & Menzies 1981, Tilstone et al. 1999, Richardson et al. 2003). However, long periods of stratification may lead to decreased production, as nutrients used up in the surface layer are not replenished, and phytoplankton sink out of the photic zone (Cushing 1989). The highest levels of productivity are typically achieved during alternations between strong upwelling events and periods of relaxation/quiescence (Peterson et al. 1988, Mann 1993, Mann and Lazier 1996, Tilstone et al. 1999, Richardson et al. 2003).

Shelf waters of the eastern Great Australian Bight (GAB), southern Australia, support Australia's largest fishery by weight, the Australian Sardine Fishery, and the valuable Commonwealth Southern Bluefin Tuna Fishery, as well as the highest densities of seabirds and marine mammals in the Australian region (Goldsworthy et al. 2013, Rogers et al. 2013). The enhanced pelagic productivity of this ecosystem is underpinned by seasonal upwelling, which occurs as a series of two to four events between November and May (Kämpf et al. 2004a, Middleton and Bye 2007). The upwelling system in the eastern GAB is globally unique. The region is characterised by a wide zonal shelf that is influenced by the world's only northern boundary current, the Flinders Current, flowing east-west along the continental slope (Bye 1972, Middleton and Cirano 2002). Previous studies have identified the mechanisms that contribute to the two-step process that characterises the eastern GAB upwelling system. The first step sees water drawn from ~ 300 m depth onto the shelf through the interaction between the Flinders Current, shelf edge canyons, and upwelling favourable (south easterly) winds (Middleton and Bye 2007, Kämpf 2010) leading to the formation of the Kangaroo Island pool, a large volume of cold, nutrient rich water sitting in a bottom layer on the continental

shelf (McClatchie et al. 2006, Middleton and Bye 2007, Kämpf 2010, van Ruth et al. 2010b, a). Water from the Kangaroo Island pool is then brought into the euphotic zone in the second step through subsequent periods of upwelling favourable winds (McClatchie et al. 2006, Middleton and Bye 2007, van Ruth et al. 2010a, b). In contrast to typical eastern boundary current upwelling systems, there are rarely, if ever, periods of quiescence in the eastern GAB. Through the November to April upwelling season, conditions are either upwelling favourable, or downwelling favourable, with upwelling driving significant volumes of nutrient rich waters above the euphotic depth, and downwelling suppressing that enrichment (van Ruth et al. 2010a, b). Upwelling characteristics in the eastern GAB are highly variable both within and between seasons, and play a significant role in influencing variability in enrichment in the region (van Ruth et al. 2010a, b).

Previous studies of enrichment and productivity in the eastern GAB ecosystem have used spot measurements that may not have been representative of overall seasonal conditions to make assertions about seasonal primary productivity. This study provides the first detailed examination of long time series data to assess enrichment and primary productivity at the scale of upwelling/downwelling events. We aimed to improve our understanding of the influence of between- and within-season variations in upwelling and downwelling on enrichment and primary productivity in the eastern GAB. We addressed this aim in the context of two key hypotheses:

- That the duration and intensity of an upwelling season influences seasonal primary productivity by dictating seasonal enrichment;

- That within-season variations in the number of upwelling/downwelling events drives between-season variations in enrichment and primary productivity.

Herein, we used a decade of wind data and remote sensed primary productivity data (2002-2012) to examine variations in upwelling and primary productivity in the eastern GAB at a seasonal scale. These data also provide long-term context to our investigations of event scale variations in the influence of upwelling/downwelling on enrichment and primary productivity, which were focussed on 5 years of *in-situ* data (2008-2012) collected from the Kangaroo Island reference station (NRSKAI), part of the National Reference Station Network of the Australian Integrated Marine Observing System (IMOS, http://imos.org.au/).

3.1.2 Methods

Characterisation of upwelling/downwelling seasons

Hourly wind data from 2002 to 2012 were obtained from the Australian Bureau of Meteorology's automatic weather station on Neptune Island (N.I., 35.12 ° S, 136.12 ° E, Fig. 3.1-1; www.bom.gov.au). Alongshore winds were used as an indicator of the timing and intensity of upwelling and downwelling seasons in the eastern GAB. All wind data were standardized to 10 m height (Large and Pond 1981) and vector averaged to provide daily values of wind speed and direction. The alongshore component of the wind speed which drives coastal upwelling was determined by rotation of the principal axis relative to the orientation of the coastline consistent with previous analysis of coastal upwelling in the region (Kämpf et al. 2004b, Middleton and Bye 2007).

The daily alongshore windstress (τ) was then estimated as described in Pond and Pickard (1983):

$$\tau = \rho_a C_d V^2$$

where V^2 is the alongshore component of the daily average wind speed, ρ_a is the air density and C_d is a variable dimensionless drag coefficient described by Trenberth et al. (1989).

Determination of the start/finish, duration and intensity of upwelling and downwelling seasons was then made following the objective criteria described in Bylhouw er et al. (2013). This included first minimizing high-frequency variability in the daily wind stress using a simple 30-day running mean (RM) filter. The timing of the start and end of each season was then determined by association with a percentage of the total cumulative τ for each year. Cut off percentages (COP) of 5% and 95% of the total cumulative τ were used for the demarcation of each season. For summer upwelling periods, the start and end of the upwelling season were associated with the lower and upper COP's for the total cumulative positive τ between July 1 and June 30 of consecutive years (see Fig. 3.2-2B). Winter downwelling was associated with the timing of COP with the total cumulative negative τ estimated from the day following the conclusion of the preceding summer upwelling period. The intensity of an upwelling (downwelling) season was the cumulative positive (negative) τ for that season.

Physical and chemical water column characteristics

In-situ physical and chemical data were collected between November 2008 and April 2012 at NRSKAI, which is situated on the 100 m isobath west of Kangaroo Island (Fig. 3.1-1). NRSKAI consists of a mooring collecting time series data, which is supplemented by semi-regular spot sampling for physical and chemical parameters. Moored instruments include FSI/Teledyne Conductivity, Temperature, Depth recorders (CTDs) at ~35 m and ~100 m, each sampling every hour for 15 seconds @ 2 Hz, without averaging. A string of 12 Aquatec loggers runs between the CTDs, at 5 m intervals from ~40 m to ~95 m. Of the 12 loggers, three are temperature/pressure loggers (at 40 m, 70 m, 95 m), and nine are temperature loggers. The loggers burst sample for 32 seconds every 20 minutes, with the data averaged for analysis. Spot sampling occurred on board the *RV* Ngerin at one to four month intervals with increased sampling effort over the upwelling season (November – April). CTD profiles were recorded at 140 sites across the region (Fig. 3.1-1). Temperature, salinity, and irradiance data were acquired with a SeaBird SBE 19*plus* CTD equipped with a Biospherical QSP-2300 underwater PAR sensor with log amplifier (Biospherical Instruments Inc., San Diego, CA, USA), and a Wet Star fluorometer (WetLabs). Water samples for the analysis of nutrient concentrations were taken from surface waters (~15 m depth), the depth of the chlorophyll maximum (as determined from CTD fluorescence), and deep waters (~90 m depth), using 5 L Niskin bottles. Samples were filtered through 0.45 μm syringe filters, and stored at -20 °C prior to analysis. Concentrations of dissolved oxides of nitrogen (NO_x) were determined by flow injection analysis with a QuickChem 8500 Automated Ion Analyser (detection limit 0.071 μM).

Mixed Layer Depths (Z_m) were calculated using CTD-derived potential density profiles and a hybrid method modified from the algorithm of Holte and Talley (2009). The algorithm models the general shape of the profile and selects Z_m from a number of possible values, including the de Boyer Montégut et al. (2004) threshold criteria (a density difference of 0.03 kg m^{-3} and the measurement closest to the 10 dbar as the reference value) and Dong et al. (2008) gradient method criteria (0.0005 kg m^{-3} $dbar^{-1}$).

The coefficient of downwelled irradiance (K_d) was derived from the slope of the semi-log plot of irradiance versus depth. The euphotic depth (Z_{eu}) was calculated by substituting K_d into the Beer-Lambert equation (Kirk, 1994):

$$Z_{eu} = 1/K_d \times Ln(100/1)$$

Linear regressions were used to characterise relationships between temperature, salinity and NO_x. These types of analyses have previously been used to monitor upwelling in the Benguela Current (Waldron and Probyn 1992), the California Current (Strickland 1970, Traganza et al. 1980) and globally (Switzer et al. 2003). Prior to regression, data were filtered to remove samples with NO_x concentrations below the detection limit of the analytical method (i.e. <0.071 µM).

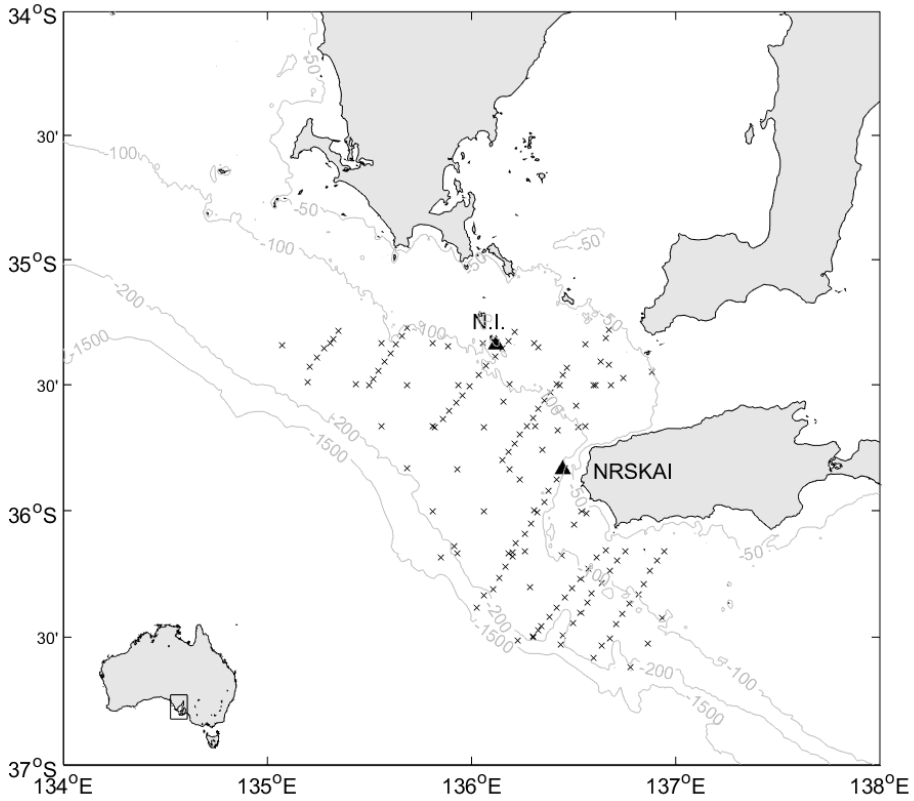

Figure 3.1-1 Regional map showing the location of the IMOS national reference station NRSKAI (◢), the location of the Neptune Island weather station (N.I.) and CTD profiling sites (×).

Remote sensed primary productivity

Daily primary productivity data were obtained from the IMOS Australian Ocean Data Network portal (AODN; https://portal.aodn.org.au/) from 2002 to 2012. The primary productivity product is a level-4 data product derived from the MODerate-resolution Imaging Spectroradiometer (MODIS) onboard the NASA Aqua satellite. The model used is based on the standard vertically generalised production model (VGPM; Behrenfeld and Falkowski 1997) which estimates primary productivity as a function of chlorophyll (standard OC3M algorithm), available irradiance, and the temperature-dependant optimal specific rate of photosynthesis. The latter is described using an exponential function to account for variation on rates of photosynthesis due to photo-acclimation (Eppley 1972, Carr et al. 2006). The daily values of primary productivity were averaged for the study area (a polygon within the limits: 135.26E-34.16S; 133.93E-35.015S; 130.62E-36.68S; 136.95E-35.28S) and further used to create seasonal means for the 2002-2012 time period, based on the upwelling season start/finish dates which were determined as detailed above. Event scale variations in primary productivity were

examined using a 3-day running mean for the study area for comparison with *in-situ* data from 2008-2012.

3.1.3 Results

Overall, seasonal mean τ was positive during the upwelling season and negative during the downwelling season (Fig. 3.1-2A). The duration and intensity of upwelling seasons was highly variable through the study period (Fig. 3.1-2C-D), with associated variations in primary productivity (Fig. 3.1-2E). Mean (± standard error) durations and intensities, across the 10 upwelling seasons from 2002-2012, were 154 (± 1.4) days and 5.2 (± 0.3) Pa, respectively. Mean (± standard error) seasonal primary productivity across that time was 452.5 (± 7.9) mg C m^{-2} d^{-1}. The 2002/03 season was the longest (239 days) and most intense (7.0 Pa), yet had a relatively low mean daily integral primary productivity (424.1 mg C m^{-2} d^{-1}). The 2005/06 season was the shortest (84 days) and least intense (3.5 Pa), yet had a similar mean daily integral primary productivity to 2002/03 (440.0 mg C m^{-2} d^{-1}). Highest mean daily integral primary productivity occurred in 2007/08 (500.9 mg C m^{-2} d^{-1}). This season was the second shortest in duration (124 days) and only moderate in intensity (5.7 Pa). Lowest mean daily integral primary productivity occurred in 2011/12 (420.2 mg C m^{-2} d^{-1}), which was also relatively short in duration (138 days), with only moderate intensity (5.3 Pa).

Mean Z_m and Z_{eu} calculated from *in-situ* data for each month sampled during this study indicated that Z_{eu} was always deeper than Z_m in the eastern GAB (Fig. 3.1-3). Z_{eu} was ~30 – 40 m deeper than Z_m in January and February, with the gap decreasing to ~10-20 m from March through to July. In August Z_m and Z_{eu} are nearly concurrent, with the difference within the margin of error around the mean. The difference in depths then began to widen again from ~10 – 20 m in October to ~30 – 40 m in November and December.

NO_x concentrations at NRSKAI varied greatly throughout the study period (Fig. 3.1-4), both within and between seasons, with maximum concentrations observed during the upwelling season differing by up to three-fold (2008/09 = 3.1 µM, 2009/10 = 10.2 µM, 2010/11 = 6.9 µM, and 2011/12 = 3.5 µM). The maximum winter NO_x concentration was 2.0 µM (Fig. 4.1-4). Regressions demonstrated a better relationship between salinity and NO_x ($y = -10.357x + 371.011$, $r^2 = 0.65$, $p < 0.0001$, Fig. 4.1-4A) than temperature and NO_x ($y = -0.973x + 17.463$, $r^2 = 0.50$, $p < 0.0001$, Fig. 4.1-4B), with salinities <35.6 psu and temperatures <15 °C associated with NO_x concentrations generally >2 µM.

Event-scale analysis of τ through three day running means highlighted high variability both between and within upwelling seasons, with downwelling events (demonstrated by negative τ) observed within upwelling seasons (Fig. 5A). The time series of temperature and salinity in bottom waters (Fig. 5.1B-C) and the euphotic zone (Fig. 5.1-5E-F) indicated that despite episodes of upwelling favourable positive τ between November and December, water <15 °C and <35.6 psu was not found in the bottom layer at NRSKAI until late in the upwelling season (~January – March). The appearance of this water at NRSKAI was associated with increased nitrate concentrations in the euphotic zone (up to ~ 10 µM, Fig. 5.1-5G), and spikes in mean daily integral primary productivity (up to ~700 mg C m^{-2} d^{-1}, ~250 mg C m^{-2} d^{-1} more than the long-term mean, Fig. 5.1-5D). Enriched water did not need to reach the surface (Fig. 5.1-5G) for increased primary productivity to occur (Fig. 5.1-D).

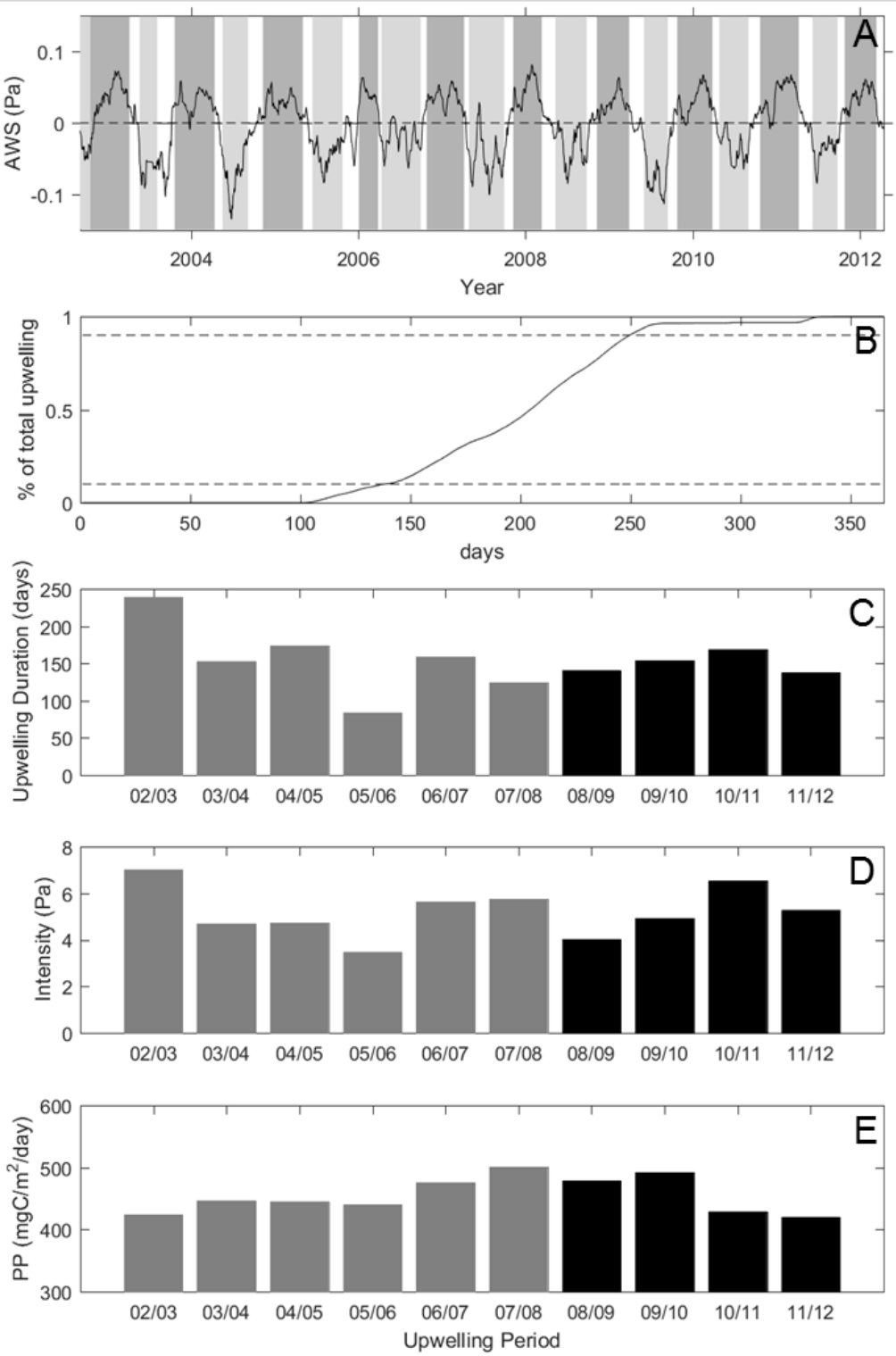

Figure 3.1-2 Ten-year time series of the 30-day running mean of alongshore wind stress (AWS, black line) at Neptune Island. Positive values indicate upwelling favourable wind and negative values indicate downwelling favourable wind. Dark and light grey shaded regions indicate summer upwelling and winter downwelling seasons. (B) The percentage of cumulative total upwelling as a function of time (days) during the summer upwelling season beginning in 2010. Dashed lines indicate the 5% and 95% COP's used to demarcate the start and end of the upwelling season, respectively. (C) The duration (days) and (D) intensity (Pa) of upwelling seasons in the eastern GAB from 2002 to 2012. Black shaded years correspond with collection of IMOS data presented in this paper. (E) Mean remote sensed daily integral primary productivity for the duration of upwelling seasons in the eastern GAB from 2002 to 2012 (as indicated in C).

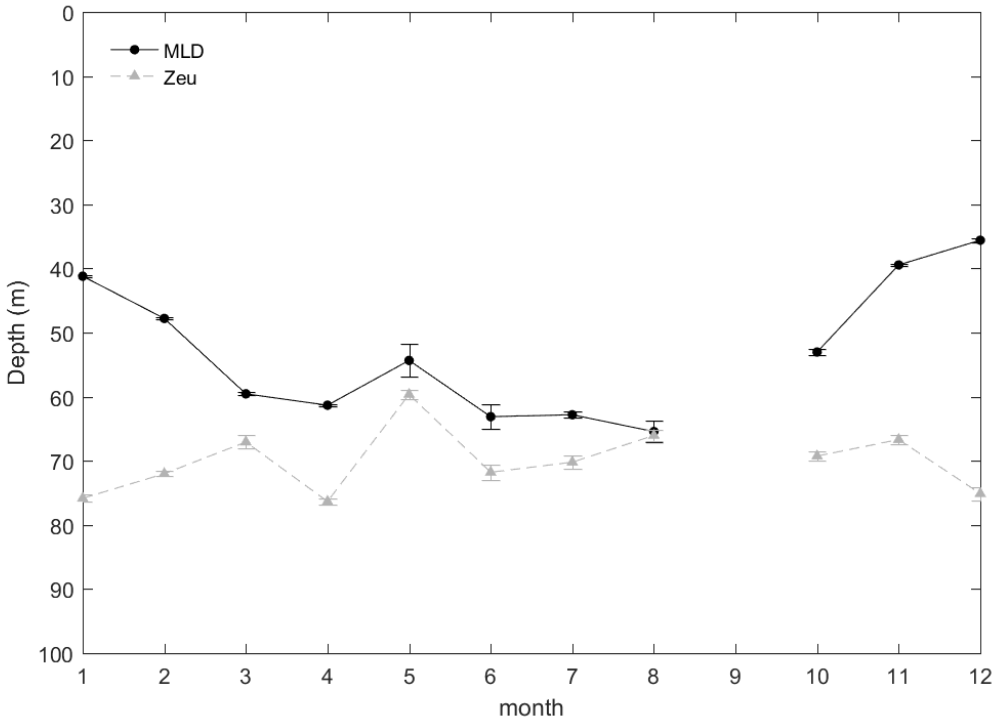

Figure 3.1-3 Mean (± se) mixed layer depth (MLD) and euphotic depth (Z_{eu}) for each month sampled during the 5 years of this study (2008-2012).

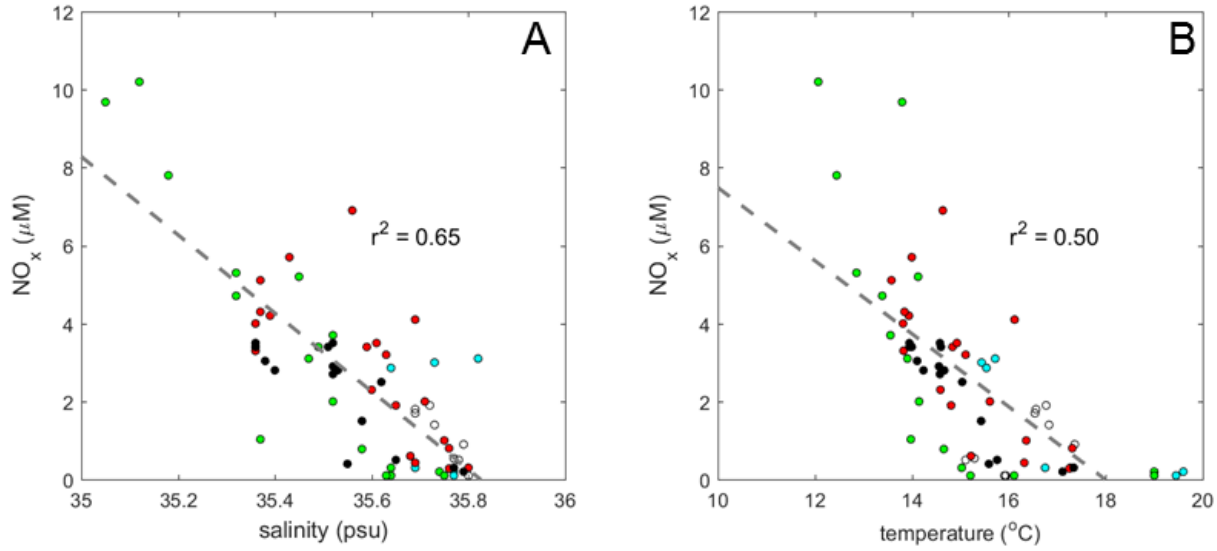

Figure 3.1-4 Linear regression models of (A) salinity (psu) versus NO_x (µM) and (B) temperature (°C) versus NO_x (µM) for data collected between 2008 and 2012 for samples where S < 35.82 psu and [NO_2^- + NO_3^-] = or > 0.071 µM. Dashed lines show the least-squares. Symbol colours denote upwelling seasons: light blue = 08/09, green = 09/10, red = 10/11, black = 11/12. White symbols = winter.

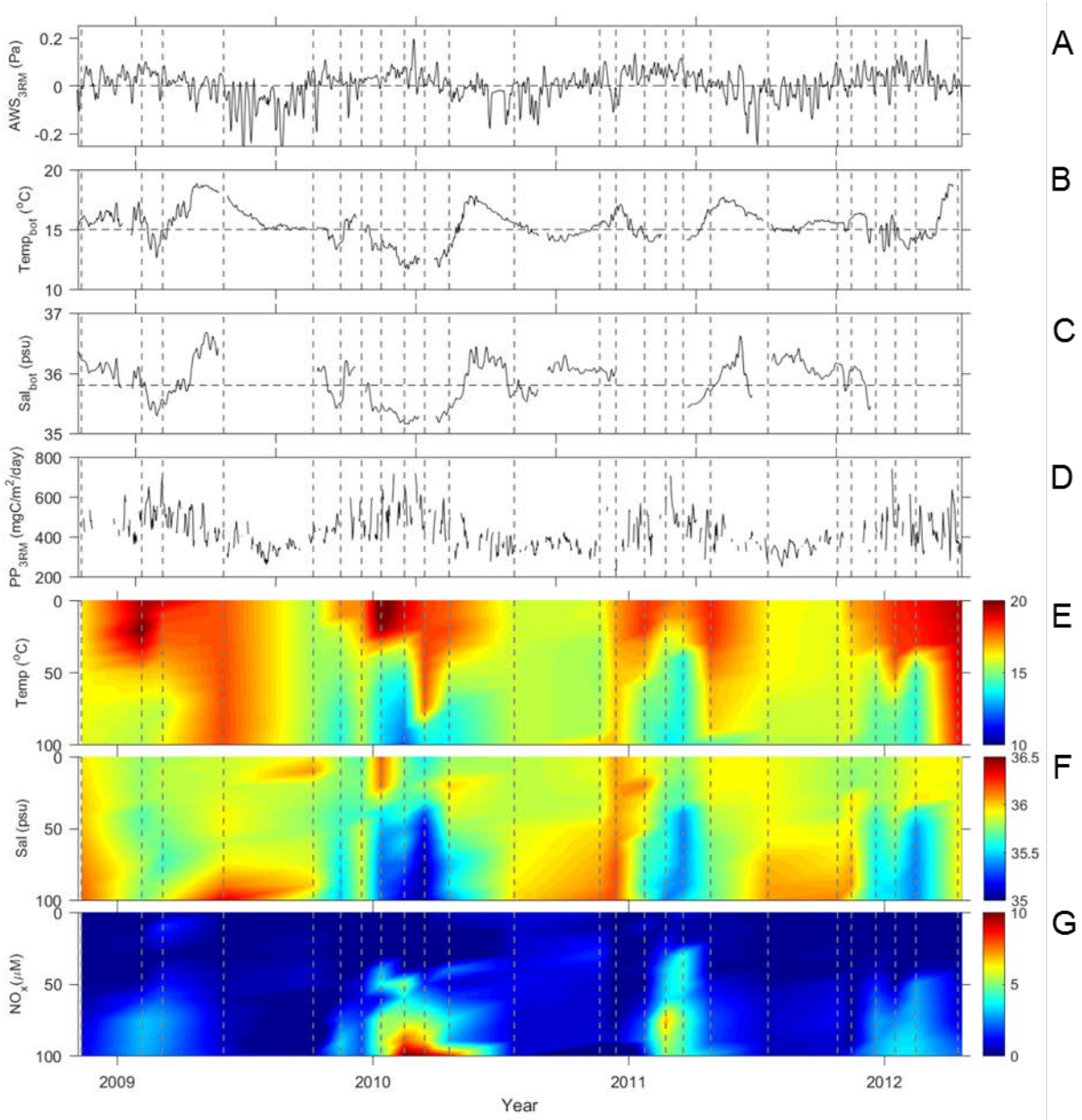

Figure 3.1-5 Time series of AWS, hydrographic parameters and nutrients (NO_x µM) measured at the NRSKAI site between November 10, 2008 and April 15, 2012. (A) 3-day running mean of AWS (Pa) determined from wind data collected on Neptune Island. (B) and (C) bottom temperature and salinity measured at NRSKAI at 100 m depth. Dashed lines show the salinity (35.8 psu) and temperatures (15°C) values below which increased NO_x values are expected (see Fig. 4). (D) three day running mean of remote sensed primary productivity. (E), (F) and (G) interpolated vertical distribution of temperature (°C) and salinity (psu) measured by CTD profiling, and NO_x (µM) measured by discrete water sampling. Vertical dashed lines indicate the timing of sampling events.

3.1.4 Discussion

Consistent with previous studies (Kämpf et al. 2004, Middleton and Bye 2007, van Ruth et al. 2010a, b), we found that upwelling/downwelling seasons can be characterised by the dominant alongshore wind stress, with upwelling favourable winds prevailing through summer (November-April), and downwelling favourable winds dominant in winter (May-October). Consistent with previous studies (van Ruth et al. 2010a, b), there was a high degree of inter- and intra-seasonal variability in wind stress that drove variation in seasonal primary productivity. However, our results also provide new insights into the influence of temporal variations in meteorological and oceanographic forcing on enrichment and productivity in the eastern GAB. The length of an upwelling season did not dictate its intensity or productivity, with long, intense seasons not always the most productive. For example, seasons 2003/04 and 2004/05 were similar in intensity and productivity, despite the fact that 2004/05 was longer in duration by around 25 days. In contrast, while the 2006/07 and 2007/08 seasons were similar in intensity, the 2007/08 season was the more productive, despite being shorter by 35 days. Clearly, an understanding of the drivers of seasonal variability in primary productivity in the eastern GAB requires careful consideration of the influence of within season variations in the number and intensity of upwelling events on enrichment of waters in the euphotic zone.

A key finding of this study was the importance of differentiating between upwelling events and enrichment events. Within upwelling seasons, wind stress was found to be a poor indicator of enrichment of waters in the euphotic zone (Fig. 5.1-5A vs Fig. 5.1-5G), particularly in the early upwelling season (November/December). Temperature and salinity were found to be better indicators of enrichment of shelf waters than wind stress, with temperatures <15 °C and salinities <35.6 psu associated with elevated concentrations of NO_x. Regardless of the occurrence of upwelling favourable winds, it was not until water temperatures below 15 °C, and salinities less than 35.6 psu, were observed in shelf waters, that significant enrichment of the euphotic zone transpired. Enrichment was not seen until the late upwelling season (January – April), despite the fact that several upwelling events may have occurred through November and December (as indicated by wind stress). This suggests that a sustained period of positive τ is required before sufficient Ekman pumping can be generated to draw significant volumes of enriched water onto the shelf and above Z_{eu}. The early upwelling season seems to represent a preconditioning period that, while not responsible for enrichment of waters above Z_{eu}, is critical to the development of the Kangaroo Island pool which facilitates late season enrichment events and drives overall seasonal productivity. Enrichment events saw NO_x concentrations in the euphotic zone elevated to levels greater than 2 µM, which was the maximum observed during winter. Peak NO_x concentrations during enrichment (3-10 µM) were higher than the range reported for the Ningaloo Current upwelling off south-west Western Australia (2 – 6 µM, Hanson et al. 2005) but lower than values reported for the major eastern boundary current upwelling regions off Peru, north-west and south west Africa, and California (15 – 19 µM, Messié et al. 2009). Thus, the eastern GAB can be considered a region subject to moderate enrichment on a global scale. However, levels of enrichment in the eastern GAB varied greatly between seasons, in a manner unrelated to the duration and intensity of upwelling. The characteristics of the preconditioning period are likely to be a more important factor governing the degree of enrichment in a given upwelling season than the duration and intensity of the upwelling season itself. The intensity and number of upwelling/downwelling events through the pre-conditioning period will significantly influence the volume of water drawn onto the shelf in the Kangaroo Island pool, and the depth from which it comes, thus impacting the magnitude of enrichment of waters above Z_{eu} through subsequent late season upwelling events.

Enrichment events in the eastern GAB drove bursts of primary productivity, but the enriched water did not need to reach the surface for high levels of primary productivity to occur. *In-situ* density and irradiance data demonstrated that Z_{eu} was always deeper than Z_m. This means that, particularly through the November to April upwelling season, there was a significant volume of enriched upwelled water in a bottom layer on the shelf, within the euphotic zone but below the surface mixed layer. Several prior studies have highlighted the presence of subsurface peaks in chlorophyll *a* in the eastern GAB during the upwelling season, associated with the upwelled water mass below the surface mixed layer (Kämpf et al. 2004, van Ruth et al. 2010a, b, van Dongen-Vogels et al. 2011, 2012, Paterson et al. 2013). The presence of enhanced phytoplankton biomass in subsurface waters has implications for the accuracy of remote sensed estimates of primary productivity for the GAB region, as these rely on surface measurements of phytoplankton biomass (van Ruth et al. 2010a, b). Remote sensed estimates of daily integral primary productivity peaked at ~700 mg C m^{-2} d^{-1}, around half to a quarter the level of rates previously reported for the region using in-situ data (van Ruth et al. 2010a, b). It is likely that remote sensed values under estimate primary productivity in the eastern GAB by not accounting for enhanced productivity in enriched waters below the surface mixed layer yet still within the euphotic zone. Despite this, the spatial and temporal resolution offered by remote sensed data makes it a critically important tool for examining long term patterns in primary productivity.

The productivity of an ecosystem will depend on the food webs that support it. In the marine environment food webs vary in complexity, and in the efficiency of energy transfer from autotrophs to higher trophic levels, according to the nutrient status of surrounding waters. Low nutrient waters typically support a long microbial food web based on picophytoplankton, and are relatively unproductive (Azam 1983, Stockner 1988). Nutrient rich systems, however, generally support high productivity via an efficient classic food web underpinned by diatoms (Sommer et al. 2002). The mechanisms that drive the upwelling system of the eastern GAB, and thus variations in enrichment of the euphotic zone, are likely to influence food web dynamics in the region, which will have implications for seasonal ecosystem productivity.

With a clearer understanding of the influence of event scale variations in upwelling and downwelling on enrichment and primary productivity in the eastern GAB we propose a refined conceptual model for the region, building on the work of van Ruth et al. (2010a, b). The model details five different meteorological/oceanographic scenarios that are likely to occur in the eastern GAB, and their influence on lower trophic ecosystem dynamics and productivity (Fig. 5.1-6). Scenario 1 depicts winter (downwelling) conditions with south westerly winds, a well-mixed water mass present in shelf waters, deep mixing and, in the absence of enrichment, low primary productivity, with a microbial food web underpinned by picophytoplankton expected to dominate. Scenario 2 describes conditions during the pre-conditioning stages of the summer upwelling season when upwelling favourable south easterly winds influence the region, but not enough to drive significant enrichment of waters above Z_{eu} (i.e. upwelling events, not enrichment events). In this scenario, primary productivity would remain low, and it is expected that the microbial food web would continue to dominate. Scenario 3 details conditions during a moderate enrichment event in the mid-late upwelling season, when nutrient rich water is drawn onto the shelf in a bottom layer that intrudes above Z_{eu} but is constrained below the surface mixed layer. This upwelled water likely supports moderate bursts of primary productivity, expected to be underpinned by increased abundances of micro-phytoplankton and a classic food web, with a microbial food web persisting above Z_m. Scenario 4 is similar to Scenario 3 but depicts a more intense enrichment event when upwelled water is forced closer to the surface near the coast, with high primary productivity and a classic food web supported by the large volume of nutrient rich water on the shelf above Z_{eu}. Scenario 5 depicts

the suppression of upwelling during a late summer downwelling/relaxation event, post enrichment. Enhanced mixing due to south westerly winds during these events is expected to seed surface waters with both previously upwelled nutrients, and micro-phytoplankton from the classic food web. In this case, moderate levels of primary productivity would persist. Total ecosystem productivity in the eastern GAB will depend on the combination of these scenarios that occurs in the region in a given season/year. Enrichment through the late upwelling season will be heavily influenced by the characteristics of the pre-conditioning period.

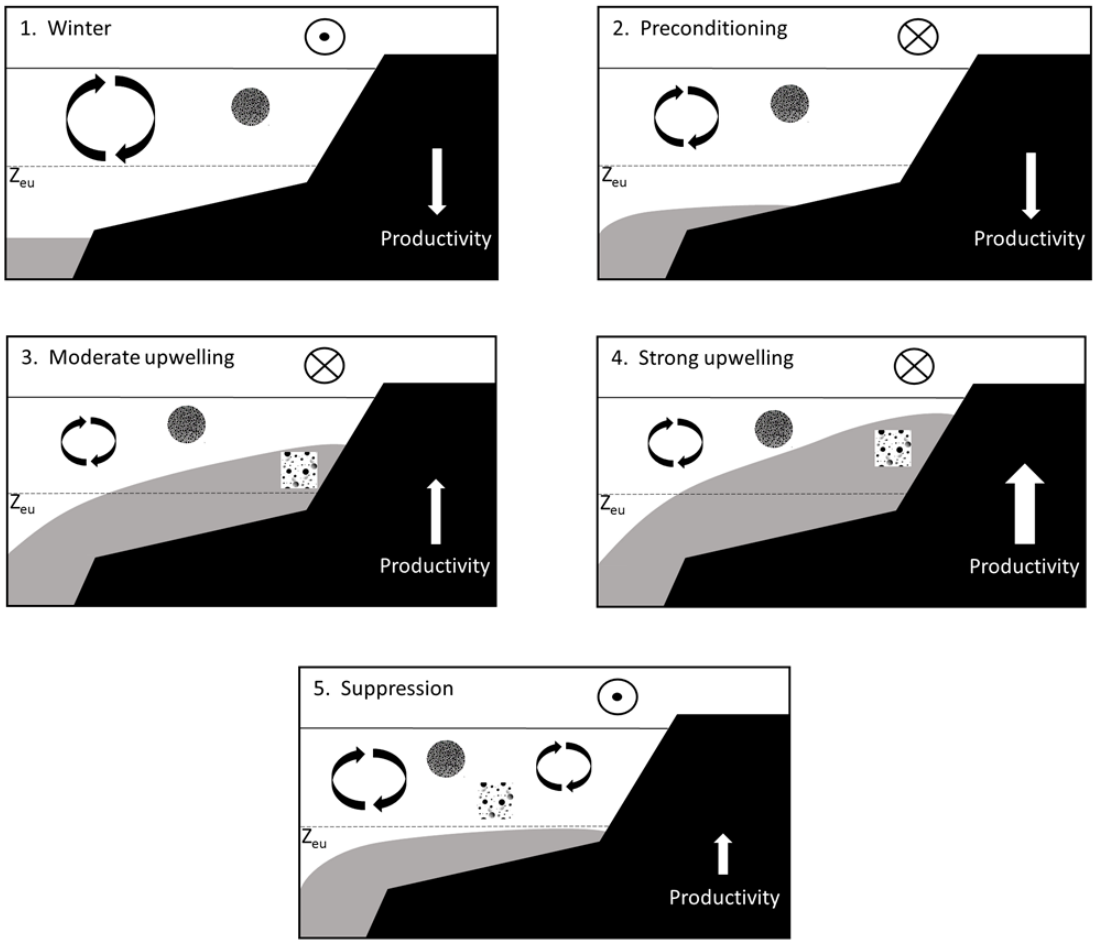

Figure 3.1-6 A refined conceptual model of variation in the influence of upwelling/downwelling on mixing, water mass characteristics, primary productivity and food web dynamics in shelf waters of the eastern Great Australian Bight. ⊙ = wind coming out of the page (i.e. south westerly), ⊗ = wind going into the page (i.e. south easterly). ● = pico-phytoplankton, ⁘ = microphytoplankton. Black shading indicates the shoreline and shelf, grey shading denotes enriched upwelled water. The dashed line indicates the euphotic depth (Z_{eu}). Black arrows indicate depth of mixing, white arrows indicate the expected level of primary productivity.

3.1.5 Summary and conclusions

This work represents the first use of long term datasets to characterise the influence of seasonal and event-scale variations in upwelling and downwelling on enrichment and primary productivity in the GAB. We discovered that the length of an upwelling season did not dictate its intensity or productivity, and that long, intense seasons were not necessarily the most productive. A key finding of this study was the importance of differentiating between upwelling events and enrichment events, with the latter only occurring in the late upwelling season (January – April). We have identified the importance of the November - December pre-conditioning period in governing the intensity of enrichment during the late upwelling season. The number, intensity and duration of upwelling events that occur during the preconditioning period (i.e. within scenario variations) will dictate the volume of nutrient rich water drawn onto the shelf in the Kangaroo Island pool that is available to be brought into the euphotic zone during subsequent, late season upwellings. We have proposed a conceptual model that details five different meteorological/oceanographic scenarios that are likely to occur in the eastern GAB, and their influence on lower trophic ecosystem dynamics and productivity, and hypothesise that total ecosystem productivity will depend on the combination of these scenarios that occurs in the region in a given season/year. This hypothesis is tested in chapter 4.1, using long-term IMOS datasets to characterise the planktonic food webs present in the eastern GAB under the different scenarios proposed in our conceptual model.

References

Azam, F. 1983. The ecological role of water-column microbes in the sea. Marine Ecology Progress Series, 10: 257-263.

Behrenfeld, M. J., and Falkowski, P. 1997. Photosynthetic rates derived from satellite-based chlorophyll concentrations. Limnology and Oceanography: 1-20.

Bye, J. A. T. 1972. Oceanographic circulation South of South Australia. Antarctic Oceanology II. The Australian-New Zealand Sector. Hayes, D.E. (ed) Antarctic Research Series: American Geophysics Union No. 19. 95-100 pp.

Bylhouwer, B., Ianson, D., and Kohfeld, K. 2013. Changes in the onset and intensity of wind-driven upwelling and downwelling along the North American Pacific coast. Journal of Geophysical Research: Oceans, 118: 2565-2580.

Carr, M.-E., Friedrichs, M. A. M., Schmeltz, M., Noguchi Aita, M., Antoine, D., Arrigo, K. R., Asanuma, I., et al. 2006. A comparison of global estimates of marine primary production from ocean color. Deep Sea Research Part II: Topical Studies in Oceanography, 53: 741-770.

Cushing, D. 1989. A difference in structure between ecosystems in strongly straified waters and those that are only weakly stratified Journal of Plankton Research, 11: 1-13.

de Boyer Montégut, C. B., G. , Madec, G., Fischer, A. S., Lazar, A., and D., L. 2004. Mixed layer depth over the global ocean: An examination of profile data and a profile-based climatology. Journal of Geophysical Research, 109: doi:10.1029/2004JC002378.

Dong, S., Sprintall, J., Gille, S. T., and Talley, L. 2008. Southern Ocean mixed-layer depth from Argo float profiles. Journal of Geophysical Research, 113: C06013, doi:06010.01029/02006JC004051.

Dugdale, R. C., and Goering, J. J. 1967. Uptake of new and regenerated forms of nitrogen in primary productivity. Limnology and Oceanography, 12: 196-206.

Eppley, R. W. 1972. Temperature and phytoplankton growth in the sea. Fish. Bull, 70: 1063-1085.

Goldsworthy, S. D., Page, B., Rogers, P. J., Bulman, C., Wiebkin, A., McLeay, L. J., Einoder, L., et al. 2013. Trophodynamics of the eastern Great Australian Bight ecosystem: Ecological change associated with the growth of Australia's largest fishery. Ecological Modelling, 255: 38-57.

Hanson, C. E., Pattiaratchi, C. B., and Waite, A. M. 2005. Sporadic upwelling on a downwelling coast: Phytoplankton responses to spatially variable nutrient dynamics off the Gascoyne region of Western Australia. Continental Shelf Research, 25: 1561-1582.

Holte, J., and Talley, L. 2009. A New Algorithm for Finding Mixed Layer Depths with Applications to Argo Data and Subantarctic Mode Water Formation. Journal of Atmospheric and Oceanic Technology, 26: 1920-1939.

Kämpf, J. 2010. On preconditioning of coastal upwelling in the eastern Great Australian Bight. . Journal of Geophysical Research: Oceans, 115: doi:10.1029/2010JC006294.

Kämpf, J., Doubell, M., Griffin, D., Matthews, R., L., and Ward, T. M. 2004. Evidence of a large seasonal coastal upwelling system along the southern shelf of Australia. Geophysical Research Letters, 31: 31:doi:1029/2003GL019221.

Mann, K. H. 1993. Physical oceanography, food chains, and fish stocks: A review. ICES Journal of Marine Science Bulletin, 50: 105-119.

Mann, K. H., and Lazier, J. R. N. 1996. Dynamics of Marine Ecosystems: Biological-physical interactions in the oceans. 2nd edn. Blackwell Science, Oxford.

Marra, J. 1978. Phytoplankton photosynthetic response to vertical movement in a mixed layer. Marine Biology, 46: 203-208.

McClatchie, S., Middleton, J. F., and Ward, T. M. 2006. Water mass analysis and alongshore variation in upwelling intensity in the eastern Great Australian Bight. Journal of Geophysical Research: Oceans, 111: doi:10.1029/2004JC002699.

Messié, M., Ledesma, J., Kolber, D. D., Michisaki, R. P., Foley, D. G., and Chavez, F. P. 2009. Potential new production estimates in four eastern boundary upwelling ecosystems. Progress in Oceanography, 83: 151-158.

Middleton, J. F., and Bye, J. A. T. 2007. A review of the shelf-slope circulation along Australia’s southern shelves: Cape Leeuwin to Portland. Progress in Oceanography, 75: 1-41.

Middleton, J. F., and Cirano, M. 2002. A northern boundary current along Australia's southern: The Flinders Current shelves. Journal of Geophysical Research: Oceans, 107: doi:10.1029/2000JC000701,002002.

Paterson, J. S., Nayar, S., Mitchell, J. G., and Seuront, L. 2013. Population-specific shifts in viral and microbial abundance within a cryptic upwelling. Journal of Marine Systems, 113–114: 52-61.

Peterson, W. T., Arcos, D. F., McManus, G. B., Dam, H., Bellantoni, D., Johnson, T., and Tiselius, P. 1988. The nearshore zone during coastal upwelling: Daily variability and coupling between primary and secondary production off central Chile. Progress in Oceanography, 20: 1-40.

Pond, S., and Pickard, G. L. 1983. Introductory dynamical oceanography, 2nd ed, Pergamon Press.

Richardson, A., J. , M. Verheye, H., Mitchell-Innes, B., A. , Fowler, J., L. , and Field, J., G. 2003. Seasonal and event-scale variation in growth of *Calanus agulhensis* (Copepoda) in the Benguela upwelling system and implications for spawning of sardine *Sardinops sagax*. Marine Ecology Progress Series, 254: 239-251.

Rogers, P. J., Ward, T. M., van Ruth, P. D., Williams, A., Bruce, B. D., Connell, S. D., Currie, D. R., et al. 2013. Physical processes, biodiversity and ecology of the Great Australian Bight region: a literature review.

Ryther, J. H. 1969. Photosynthesis and fish production in the sea. Science, 166: 72-76.

Small, L. F., and Menzies, D. W. 1981. Patterns of primary productivity and biomass in a coastal upwelling region. Deep Sea Research, 28: 123-149

Sommer, U., Stibor, H., Katechakis, A., Sommer, F., and Hansen, T. 2002. Pelagic food web configurations at different levels of nutrient richness and their implications for the ratio fish production:primary production. Hydrobiologia, 484: 11-20.

Stockner, J. G. 1988. Phototrophic picoplankton: an overview from marine and freshwater ecosystems. Limnology and Oceanography, 33: 765-775.

Stolte, W., McCollin, T., Noordeloos, A. A. M., and Riegman, R. 1994. Effect of nitrogen source on the size distribution within phytoplankton populations. Journal of Experimental Marine Biology and Ecology, 184: 83-97.

Stolte, W., and Riegman, R. 1995. Effect of phytoplankton cell size on transient state nitrate and ammonium uptake kinetics. Microbiology, 141: 1221-1229.

Stolte, W., and Riegman, R. 1996. A model approach for size-selective competition of marine phytoplankton for fluctuating nitrate and ammonium. Journal of Phycology, 32: 732-740.

Strickland, J. D. H. (Ed). 1970. The Ecology of the Plankton off La Jolla, California, in the Period April Through September, 1967*,* University of California, Berkeley, California.

Switzer, A. C., Kamykowski, D., and Zentara, S.-J. 2003. Mapping nitrate in the global ocean using remotely sensed sea surface temperature. Journal of Geophysical Research: Oceans, 108: 3280, doi:10.1029/2000JC000444, C8.

Tilstone, G. H., Figueiras, F. G., Fermín, E. G., and Arbones, B. 1999. Significance of nanophytoplankton photosynthesis and primary production in a coastal upwelling system (Ría de Vigo, NW Spain). Marine Ecology Progress Series, 183: 13-27.

Traganza, E. D., Nestor, D. A., and McDonald, A. K. 1980. Satellite observations of a nutrient upwelling off the coast of California. Journal of Geophysical Research: Oceans, 85: 4101-4106.

Trenberth, K. E., Large, W. G., and Olson, J. G. 1989. The effective drag coefficient for evaluating wind stress over the oceans. Journal of Climate, 2: 1507–1516.

van Dongen-Vogels, V., Seymour, J. R., Middleton, J. F., Mitchell, J. G., and Seuront, L. 2011. Influence of local physical events on picophytoplankton spatial and temporal dynamics in South Australian continental shelf waters. Journal of Plankton Research, 33: 1825-1841.

van Dongen-Vogels, V., Seymour, J. R., Middleton, J. F., Mitchell, J. G., and Seuront, L. 2012. Shifts in picophytoplankton community structure influenced by changing upwelling conditions. Estuarine, Coastal and Shelf Science, 109: 81-90.

van Ruth, P. D., Ganf, G. G., and Ward, T. M. 2010a. Hot-spots of primary productivity: An Alternative interpretation to Conventional upwelling models. Estuarine, Coastal and Shelf Science, 90: 142-158.

van Ruth, P. D., Ganf, G. G., and Ward, T. M. 2010b. The influence of mixing on primary productivity: A unique application of classical critical depth theory. Progress in Oceanography, 85: 224-235.

Waldron, H. N., and Probyn, T. A. 1992. Nitrate supply and potential new production in the Benguela upwelling system. South African Journal of Marine Science, 12: 29-39.

3.2 Animal-borne instruments provide new observations of seasonal subsurface oceanographic features over the continental shelf of the Great Australian Bight (Bailleul, F., Richardson, L., van Ruth P.D., McMahon, C.R., Harcourt, R.G., Middleton, J., Ward, T., and Goldsworthy, S.D.)

3.2.1 Introduction

The vast majority of the worldwide commercial fish catch comes from coastal waters over continental shelves (e.g. Blanchard et al. 2012). Productivity in the most productive continental shelf regions is driven by significant nutrient enrichment, which is linked to a combination of wind, local topography and the global circulation of water masses (Huthnance 1995). Coastal upwelling that involves the movement of dense, cooler, and usually nutrient-rich water towards the surface, is a major feature of eastern boundary current systems off the west coasts of North and South America and northern and southern Africa. These regions support the world's most productive temperate fishing grounds, and abundant marine predator populations (Pauly and Christensen 1995, Kämpf and Chapman 2016). There are a number of smaller, less productive and well-known upwelling systems throughout the world that also support important fisheries and marine predator populations (e.g. Shetye et al. 1991). These smaller seasonal wind-driven upwelling systems, are comparatively poorly understood with respect to their physical, chemical and biological structure and function, and because of the limited sampling from conventional oceanographic observation systems. However, knowledge of the basic hydrographic information and the underlying mechanisms involved in their formation and functioning is critical for the sustainable management of these marine ecosystems, which have significant ecological and economic importance.

The shelf waters off southern Australia are influenced by various bathymetric and oceanographic conditions, and can be divided into three different sub-regions: the south eastern shelves; the eastern Great Australian Bight (GAB); and the central and western GAB (Fig. 3.2-1). The eastern GAB (GAB) region is the site of a seasonal upwelling system that supplies nutrients to a nutrient-depleted shelf, and is unique among upwelling systems as it is linked to the world's only northern boundary current, the Flinders Current (FC), which flows westward along the continental slope (hereafter referred to as the slope) off southern Australia (Middleton and Cirano 2002; Ward et al. 2006; Middleton and Bye 2007). Although the flow of the FC is quite weak in the eastern GAB, it is much stronger in the western GAB (~20 cm s^{-1}, Middleton and Bye 2007).

The south eastern shelves are influenced by enrichment from the Bonney Upwelling (Lewis 1981; Butler 2002; Pattiaratchi 2007), while the hydrodynamics of the central and western GAB region are dominated by year-round downwelling (Middleton and Bye 2007). Physical and biological oceanographic measurements in these sub-regions from conventional, vessel-based oceanographic observation methods are scant, and have limited the development of a better understanding of the region's oceanographic structure across space and time (e.g. McClatchie et al. 2006; Ward et al. 2006; Richardson et al. 2009; Van Ruth et al. 2010a, b). Other observation systems, including fixed moorings or autonomous platforms (e.g., gliders and other autonomous underwater vehicles) have been used to obtain measurements at particular locations or times (Hill et al. 2010), but even with these, many areas of Australia's southern shelves remain poorly sampled due to their remoteness and the costs of sampling. For the last 15 years, marine predators have been increasingly utilised as oceanographic sampling platforms, as they can gather detailed longitudinal oceanographic observations at fine temporal and spatial resolution and at relatively low cost, especially from

remote regions that are logistically difficult to access (Lydersen et al. 2004; McMahon and Harcourt 2014; Roquet et al. 2014; Hussey et al. 2015). While many studies using this approach have employed animals that inhabit oceanic habitats (Hussey et al. 2015), very few have focused on coastal shelves, except in Antarctic waters (Costa et al. 2008; Padman et al. 2010; Fedak 2013). As a result, most remote coastal shelves remain poorly sampled. However, as many large marine predators live in coastal waters, they could potentially provide suitable platforms from which to obtain the oceanographic observations needed to understand and manage these ecologically and economically important ecosystems.

The shelf waters of the GAB region support a uniquely diverse ecosystem (Shepherd and Edgar 2013). More than 1,200 algal species, 12 seagrass species, 6,000 invertebrate species, 350 fish species, 16 breeding seabird species and 33 marine mammal species have been recorded to date as either resident or migratory species in GAB waters (Edyvane 1999a, b). The latter three groups constitute the greatest density and biomass of apex predators in Australian coastal waters (Goldsworthy et al. 2013). In addition, the level of endemism of most of these species (80% on average, especially algae, fish and seagrass) is remarkable. By comparison, the Great Barrier Reef, considered by many as hyper-diverse, has low endemism and shares 80% of its fish, coral reefs and other marine organisms with other countries in the tropics (Phillips 2001). Moreover, the continental shelf of the GAB is part of the largest temperate “carbonate factory” in the world, containing living and skeletal fragments of bryozoan, molluscs, foraminifera and coralline algae made of calcium carbonate (James and Bone 2011). Understanding the physical dynamics of these carbonate hotspots is especially important in light of the current global carbon crisis. While the level of diversity and endemism in the GAB is nationally and internationally acknowledged, the region also supports significant commercial fisheries, aquaculture, and ecotourism sectors of regional socio-economic importance in Australia (Ward et al. 2006; Rogers et al. 2013). Consequently, the development of relevant management, conservation and sustainability strategies requires an understanding of the physical forcing processes in the region, and how they underpin the biological patterns and processes that drive the overall productivity of the ecosystem

The GAB is home to Australia’s largest population of Australian sea lions (*Neophoca cinerea*). As Australian sea lions are restricted to continental shelf waters and are benthic foragers, during dives they can collect oceanographic profiles of the entire water column. Moreover, as sea lions reside in these waters year-round, they can be utilised to collect longitudinal hydrographic information over wide spatial and temporal scales (i.e. over many months, across seasons and years) (Lowther et al. 2013). Being quite large and robust, adult male sea lions are of suitable size to regularly carry Conductivity-Temperature-Depth (CTD) biologging devices, and collect detailed bio-physical observations of the water column as they repeatedly traverse the continental shelf. As such, they have the potential to act as natural samplers and observers of local oceanographic change in the GAB, an area known to be affected by the circulation of diverse water masses influenced by the Indian, Southern and Pacific oceans.

Here we present new observations from the shelf waters off southern Australia, collected by Australian sea lions equipped with biologging devices that incorporate high accuracy temperature and salinity sensors (Fedak 2004). We highlight their applicability to better understand the regional oceanography of the central-western and eastern GAB, and south eastern shelves, including the spatial and temporal characteristics of an economically and ecologically important coastal upwelling system. The Great Australian Bight Research Program, through this project, funded the analysis of this dataset. Collection of the data was funded through the Animal Tracking Facility of the Australian Integrated Marine Observing System (IMOS).

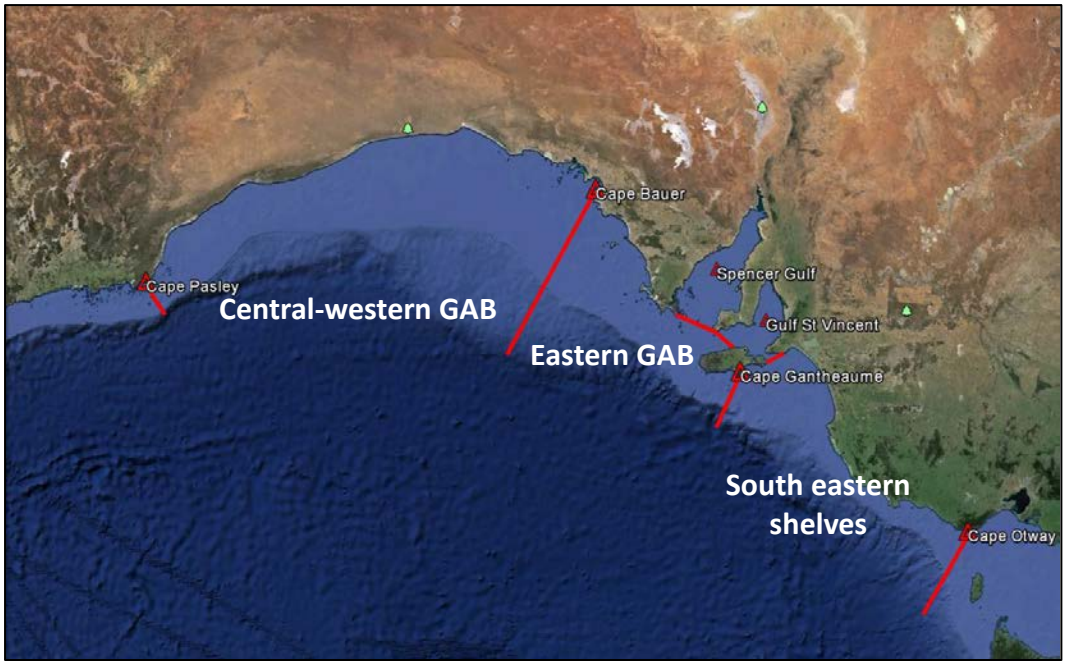

Figure 3.2-1 Map identifying three oceanographic sub-regions of the Great Australian Bight (GAB)

3.2.2 Methods

Instrumentation

A comprehensive technical description of the Conductivity-Temperature-Depth Satellite-Relay Data Logger (CTD-SRDL; Sea Mammal Research Unit Ltd, Scotland) used in this study can be found in Fedak et al. (2002) or Boehme et al. (2009). Briefly, the devices contain a Platform Terminal Transmitter (PTT) transmitting summarized data via the ARGOS satellite system in near real time when the animal is at the surface, and a miniaturised CTD (Valeport LTD, Totnes, UK) collecting ocean temperature and conductivity data as well as information on depths and duration of dives. CTD-SRDLs record TS profiles during the quasi-vertical ascent of seals. Unless tags are recovered and the comprehensive record can be downloaded, only the deepest profile in each 6 h time interval is retained and transmitted in a compressed form (20 data points per profile) through the ARGOS system (i.e., ≈ 4 profiles per day). The features of the different sensors (pressure transducer, temperature probe and conductivity sensor), such as the range of measurements and the accuracy, are available on the SMRU website (http://www.smru.st-and.ac.uk/Instrumentation/CTD). Instruments were calibrated after assembly (Boehme et al. 2009).

Animal handling and instrument attachment

From 2007, oceanographic data were collected using CTD-SRDLs deployed on 54 individual adult male Australian sea lions from 18 locations across most of their South Australian range, using the method described in Lowther et al. (2013). Males were initially sedated using zolazepam-tiletamine (300–350 mg Zoletil®, Virbac Ltd) delivered remotely by a powered tranquilizer gun (Paxarms MK24C Snap Projector gun, Paxarms New Zealand Ltd or Taipan 2000, Tranquil Arms Ltd). Once immobilized, animals were anaesthetized using isoflurane delivered through a portable gas anaesthesia machine (5% induction, 1–3% maintenance; Advanced Anaesthetic Specialists, New South Wales). A CTD-SRDL measuring 10.5 x 7 x 4 cm and weighing 545 g was attached to the pelage distal to the midpoint of

the back of each individual using two-part epoxy glue (Araldite K-268, Araldite 2017 Vantico, Basel, Switzerland or RS 850956 Epoxy Adhesive, RS Components, Australia). The Sensor typically remains on the animal for several months, and falls off upon moulting. Sensors are not buoyant, and are often lost at sea.

Vertical separation of the main water masses

Each individual temperature profile was investigated to identify, when present, the depth and thickness of the seasonal thermocline. Two different water layers were then defined: the surface mixed layer, corresponding to waters above the thermocline, and the deep water layer, below the thermocline. The absence of a thermocline indicated that the water column was well-mixed.

Properties of the main water masses

Identities and properties of three main water masses were defined after Richardson et al. (2009) and Richardson (2015) on the basis of temperature and salinity. Details are provided in Table 3.2-1. Slope water has temperatures and salinities of < 15°C and < 35.5 psu, respectively, and is present year-round at depths > 180 m. It is seasonally upwelled onto the shelf south of Eyre Peninsula or further east off Kangaroo Island and the Bonney Coast. It is then transported into the eastern GAB by westward coastal currents during summer (Richardson 2015). A mixed water mass, characterised by intermediate temperatures and salinities, is present at the surface along the coast and at depth in the central part of the study area (Richardson et al. 2009). This water is identified as Subtropical Surface Water (STSW), the most common surface water mass along the southern margin (James and Bone 2011; Richardson 2015). The Great Australian Bight Plume (GABP) has temperatures and salinities as high as 21 °C and 36.2 psu, respectively, and is formed from high surface heating and evaporation during summer. It is known to be present on the mid shelf and along the shelf edge in the western and central parts of the study area (Richardson et al. 2009).

Table 3.2-1 Properties of water masses defined on the basis of temperature and salinity, as outlined in Richardson et al. (2009) and Richardson (2015).

Water Mass	Temperature (°C)	Salinity (ppt)	Density (kg/m^3)
Slope water	<15.2	<35.5	26.0–26.5
Subtropical Surface Water (STSW)	15.4–20.0	35.5–35.9	25.5–26.0
GAB Plume (GABP)	17.4–21.0	35.9–36.2	25.0–25.5

3.2.3 Results

Information collected

From the 54 sea lions equipped, 46,836 dives were transmitted, covering from 10 m to a maximum of 244 m (69 ± 32 m) water depth and lasting for 5 ± 3 mins on average. From these 46,836 dives, over 20,000 temperature and salinity profiles were obtained across ~1,000 km of shelf, covering up to 10 months of the year, including the 4 – 6 months through the upwelling season (Fig. 3.2-2). All

the data recorded are stored and free to access in the IMOS Ocean Current web portal (see http://oceancurrent.imos.org.au/aatams.php).

Seasonal vertical stratification of the water column

In the three oceanographic sub-regions (south eastern shelves; eGAB; central and western GAB), the vertical stratification of the water column indicates that the deep layer is generally colder and denser than the surface layer during the summer months (December to February, Fig. 3.2-3). From March to May, the increase in the number of profiles with no clear seasonal thermocline indicates that vertical mixing processes are becoming more intense (Fig. 3.2-3). From June to August/September, the water column over the GAB shelf is well mixed from surface to bottom (Fig. 3.2-3).

Over the south eastern shelves, slope water can be observed from December to May, mixed waters being observed otherwise (Fig. 3.2-3A). In the eGAB, slope water is observed from December to April (Fig. 3.2-3B). In the central and western GAB, slope water is observed from February to April, while the GABP is observed from December to April (Fig. 3.2-3C). The incidence of cool, fresh slope water at depth, and the presence of warm, saline GABP water at the surface, enhances vertical stratification of the water column and leads to a strong thermocline during summer months.

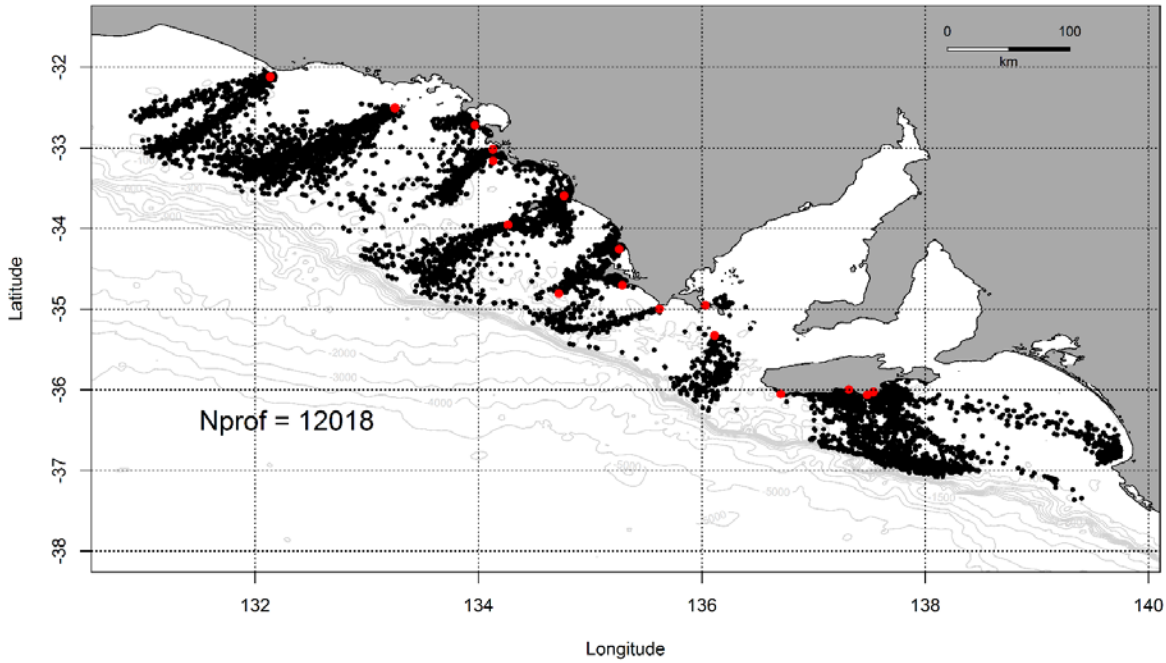

Figure 3.2-2 Location of the temperature and salinity profiles recorded by the sea lions over 8 years. Each black dot represents a profile (Nprof = total number of profiles). The red dots represent the different locations where CTD's have been deployed on sea lions

Spatio-temporal distribution of the main water masses in the GAB region

At depth (Fig. 3.2-4A), water originating from the slope is present south of the Eyre Peninsula in December. It then moves in a northwest direction along the coast, extending no further than Cape Bauer by March/April. After May, slope water is no longer observed in the GAB. Slope water is also

observed along the shelf edge, south of Kangaroo Island (KI), from December to May, with incursions over the continental shelf in March and April. From May/June, water originating from the slope is no longer observed south of KI. The GABP is present from December to May at the Head of Bight, along the coast to ~133 – 134°E and over the shelf to ~33 – 34°S. From June to December, the GABP is no longer observed in the central–western GAB.

At the surface, mixed waters are present over most of the shelf, and GABP waters are observed along the coast and on the mid shelf between 131 and 133°E (Fig. 3.2-4B). Water originating from the slope is only observed at the surface in March south/southeast of KI, which was likely sampled during a strong upwelling event.

As an example, figure 3.2-5 illustrates the seasonality in the circulation and the vertical stratification of the different water masses in the GAB region, as described in the sections above, over 8 months in 2010. The annual deployments conducted over the last 10 years on sea lions contribute to the observation of the inter-annual variation in these physical processes.

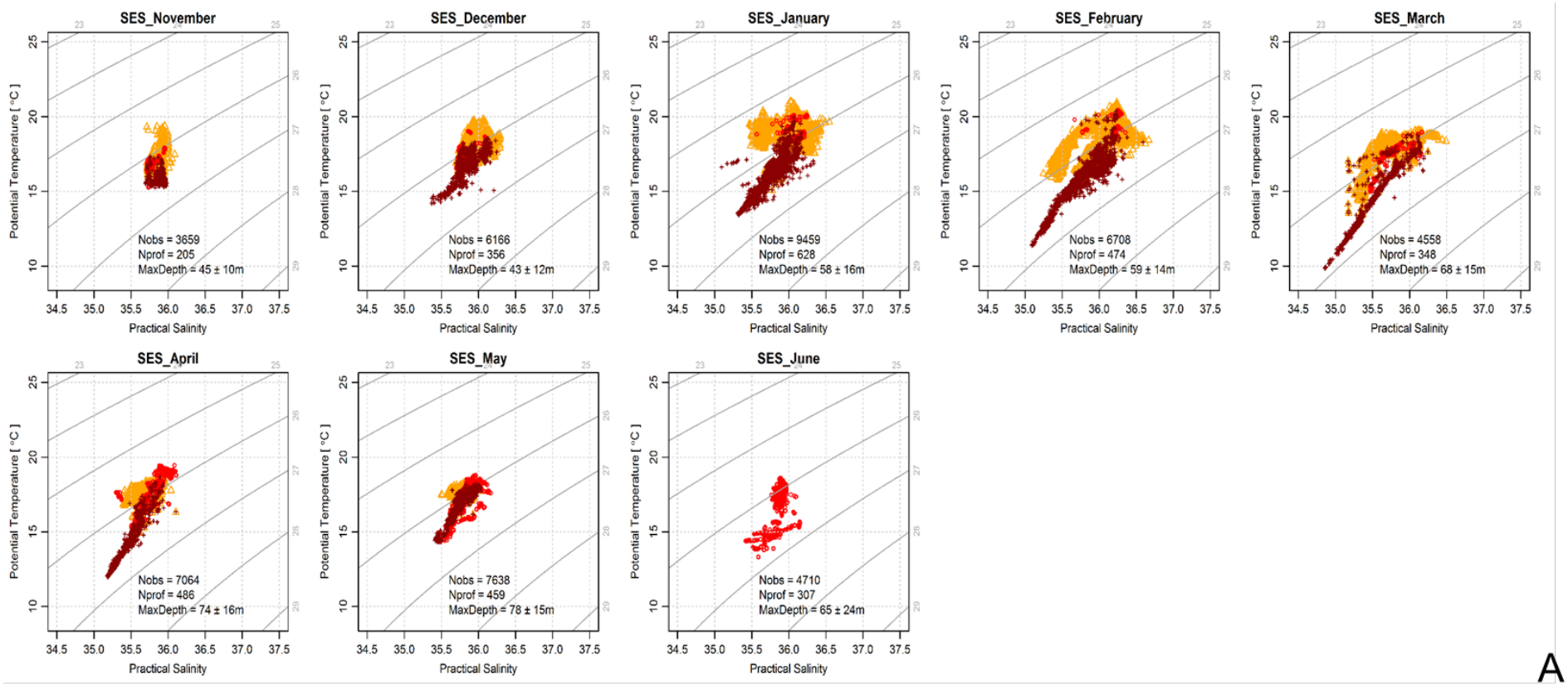

Figure 3.2-3 The monthly vertical stratification of the water column in the three oceanographic sub-regions (A) SES = South Eastern Shelves; (B) EGAB = Eastern Great Australian Bight; and (C) CWGAB = Central-Western Great Australian Bight. Each symbol represents an observation (Nobs = Total number of observations from Nprof = Total number of profiles; MaxDepth = mean maximum depth of all the profiles recorded ± sd. Orange triangles represent water masses at the surface (above the thermocline). Dark red crosses represent deep water masses (below the thermocline). Red opened circles represent mixed water masses (no thermocline).

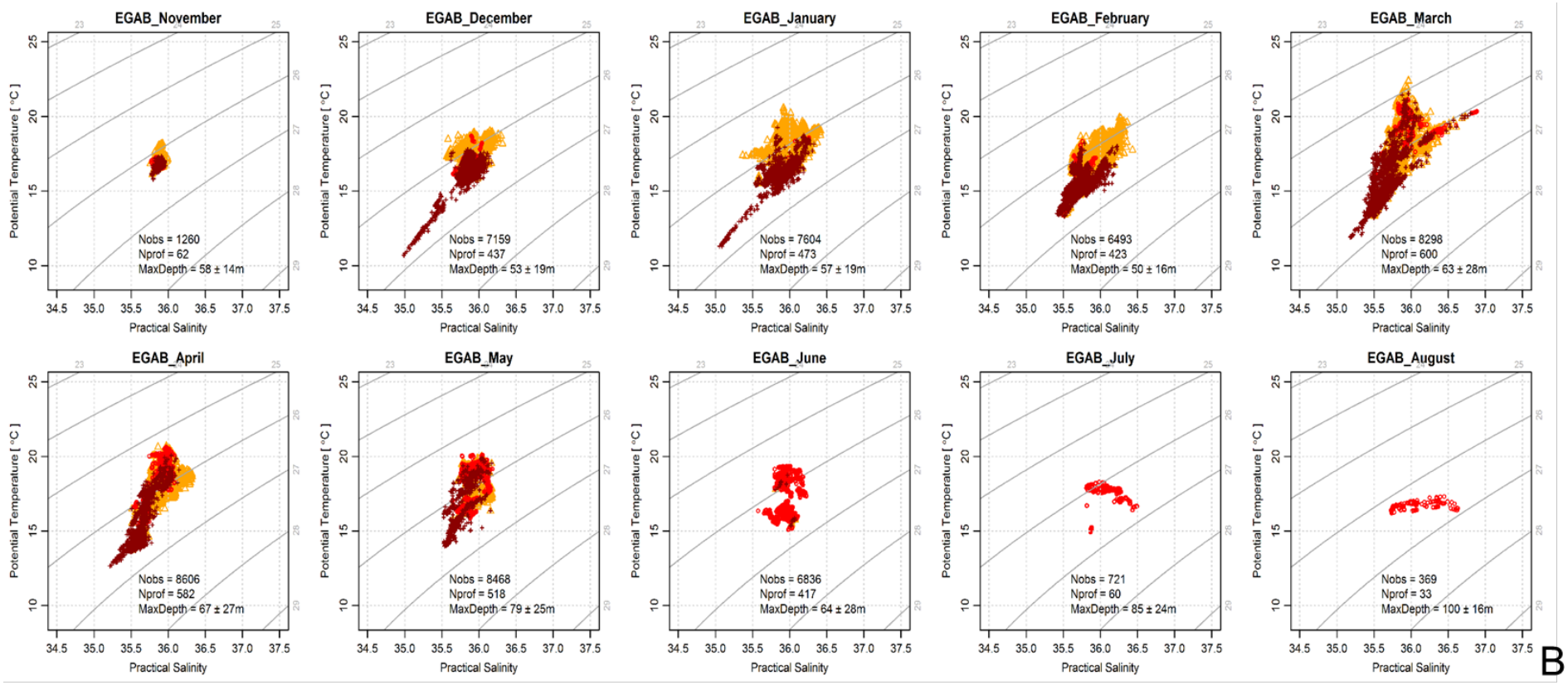

Fig. 3.2-3 continued.

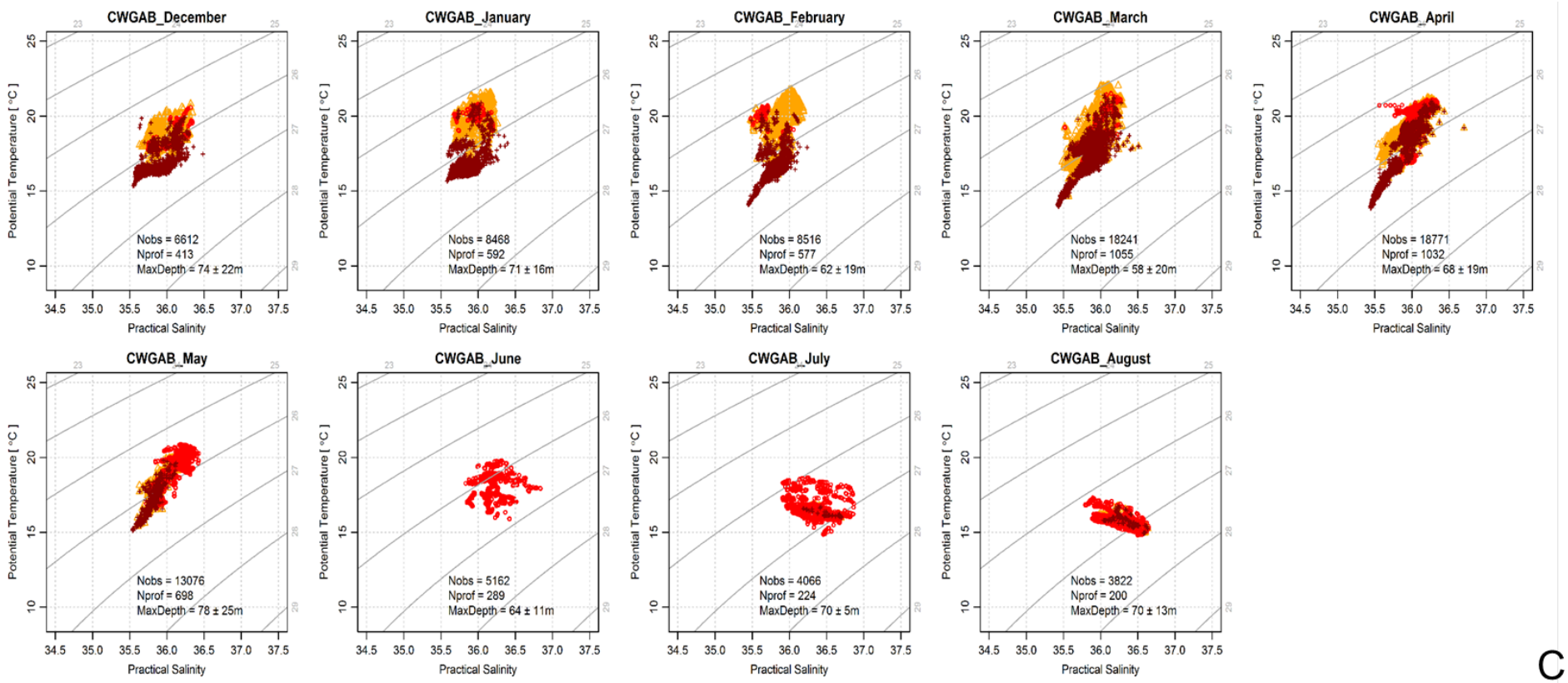

Fig. 3.2-3 continued.

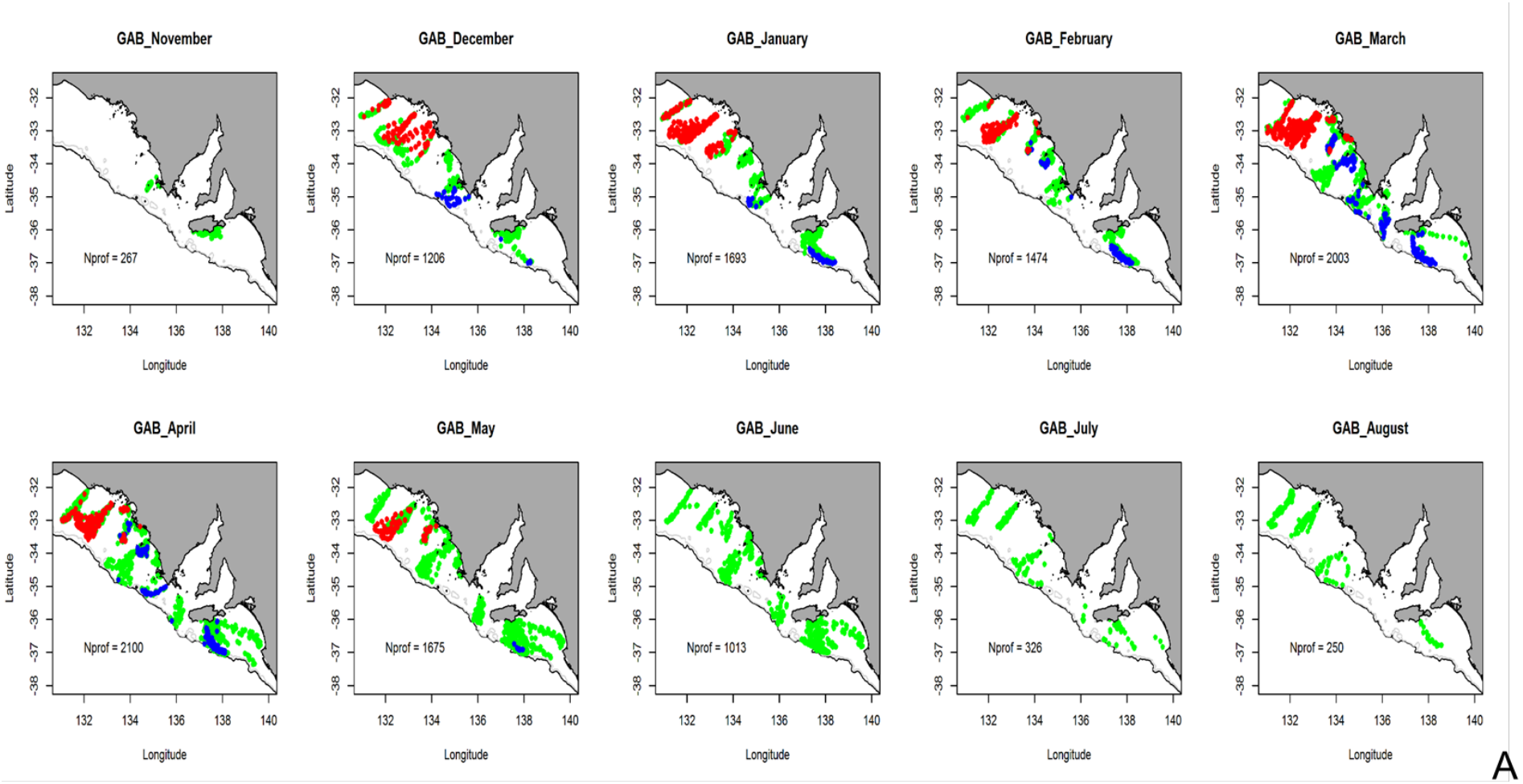

Figure 3.2-4 The monthly location of the main water masses (A) at the bottom (below the thermocline) (B) at the surface (above the thermocline). Each dot represents a profile. Blue dots = Slope water; Green dots = mixed water (STSW); Red dots = GABP (see text for details).

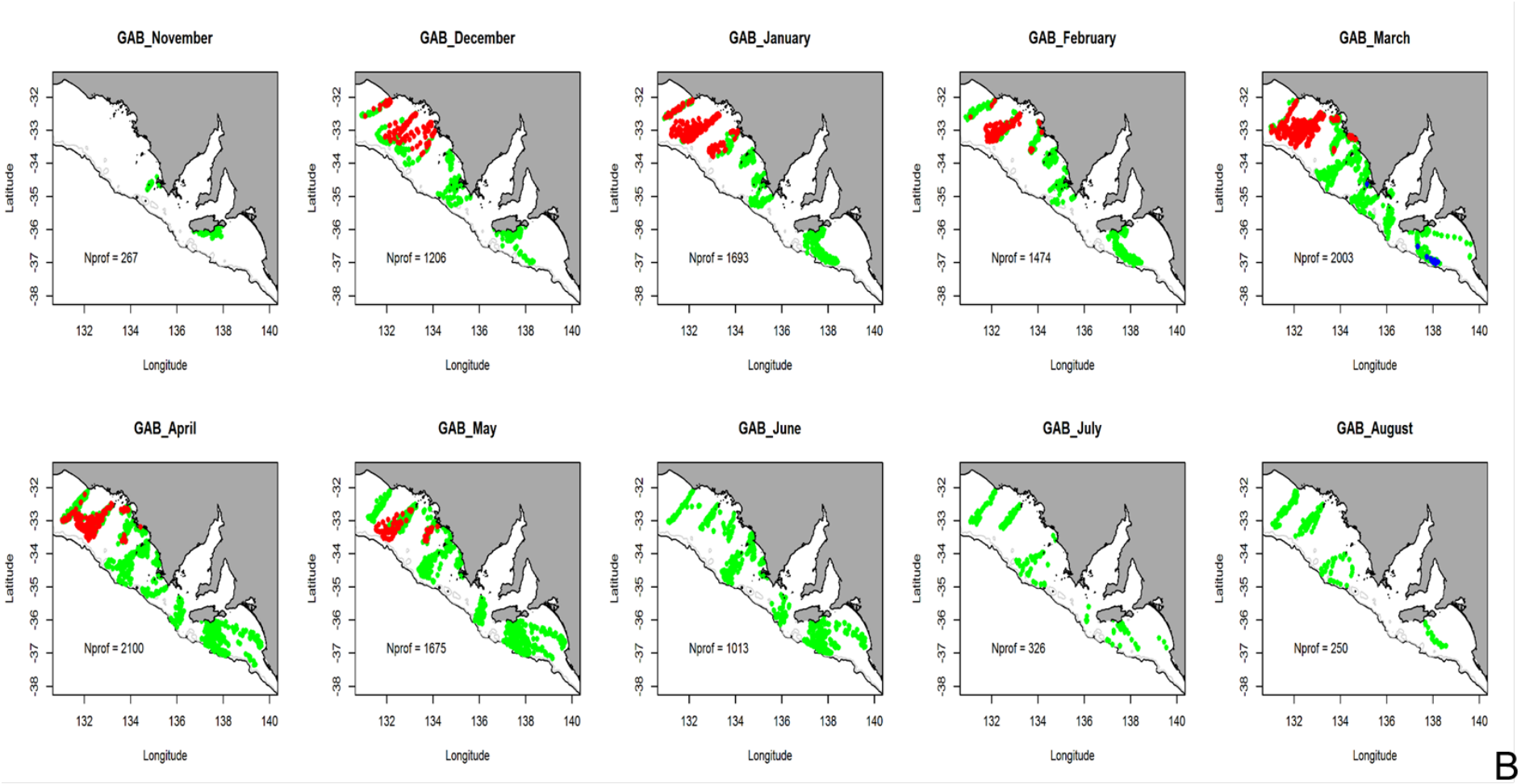

Fig. 3.2.4 continued

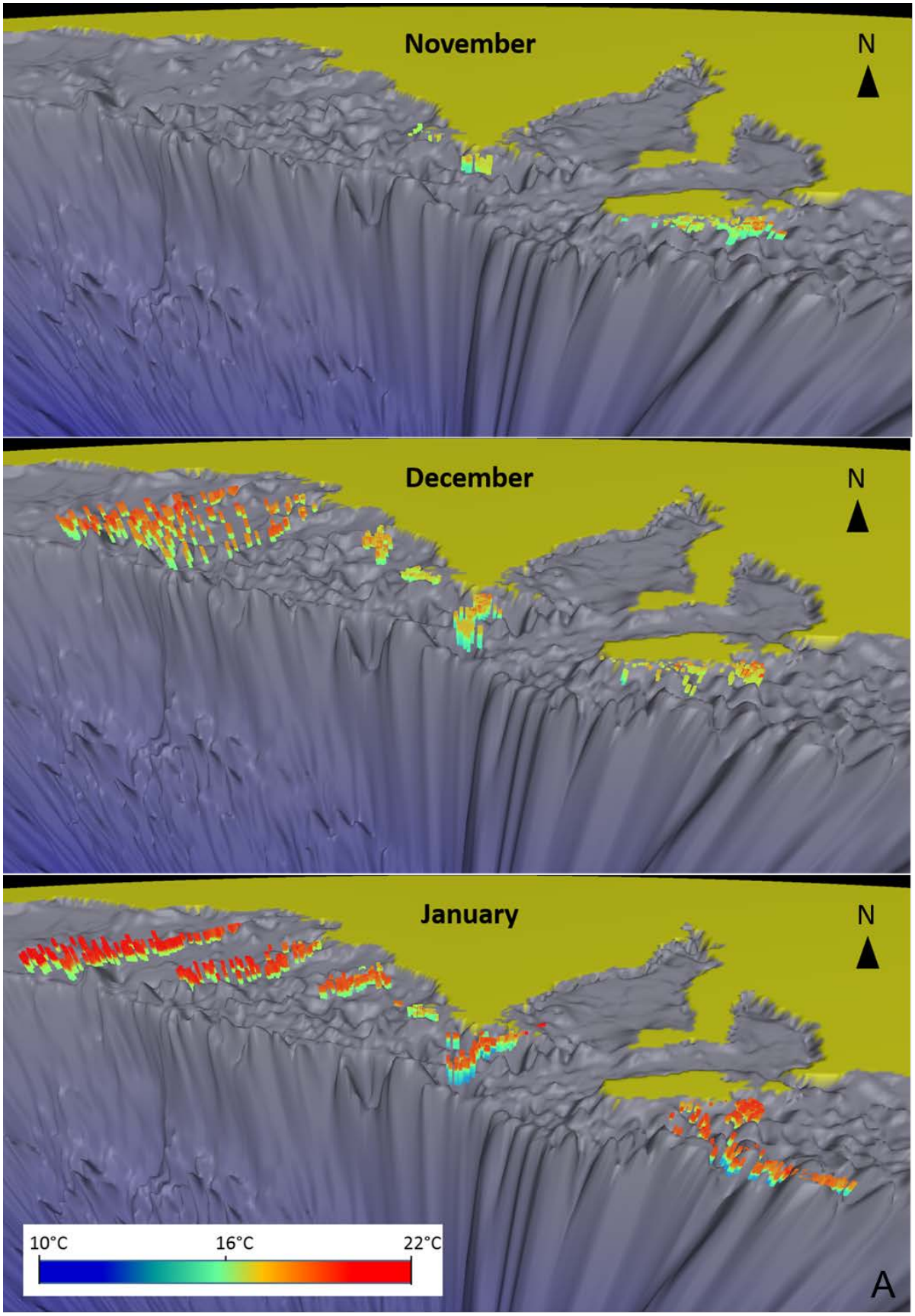

Figure 3.2-5 Monthly 3D representation of the temperature profiles recorded by 8 individuals from 7 different colonies in 2010. The vertical dimension has been exaggerated to better distinguish the contrasted water masses. The figure was made using MamVisAD software from the Sea Mammal Research Unit, University of St Andrews.

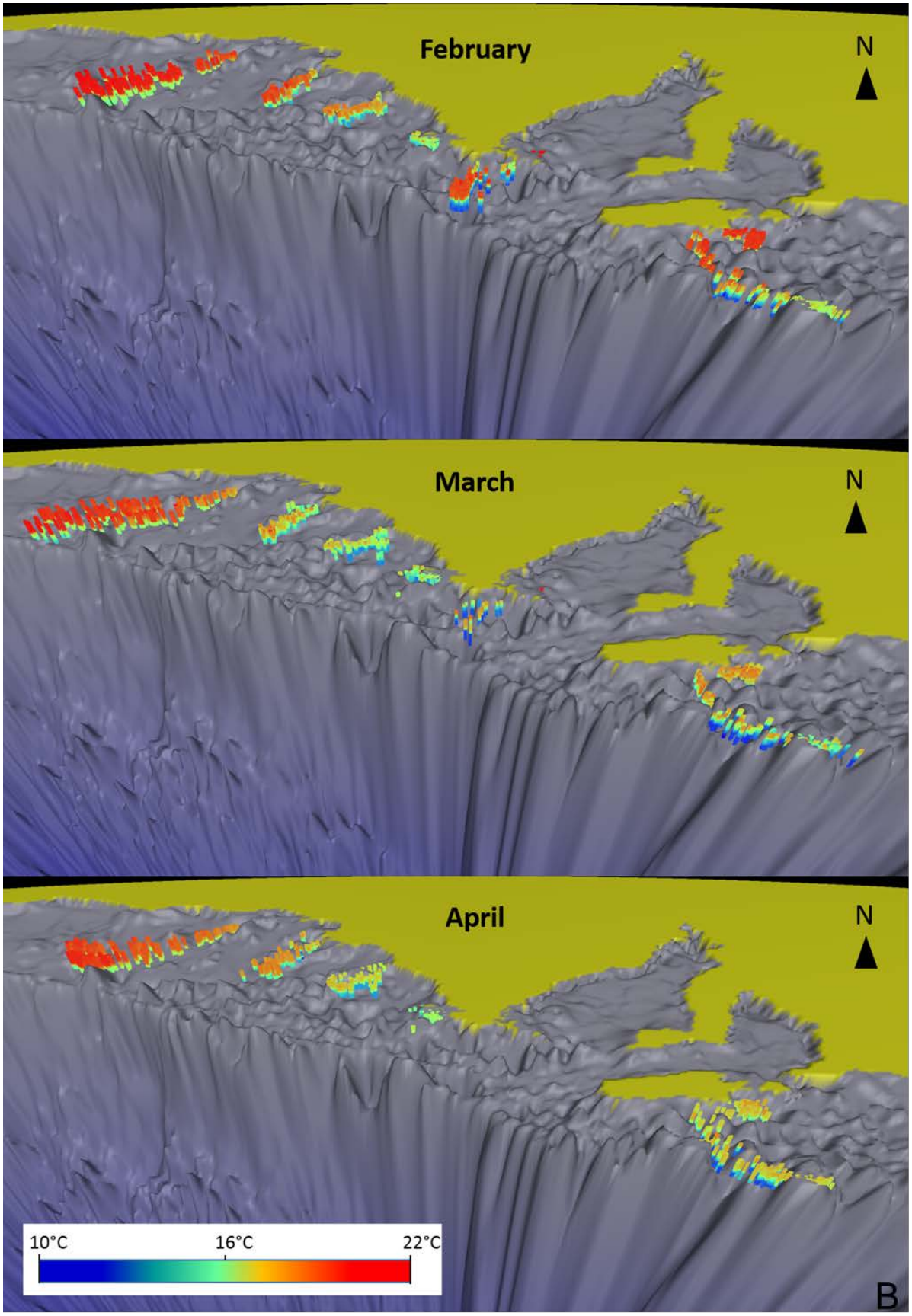

Fig.3.2-5 continued

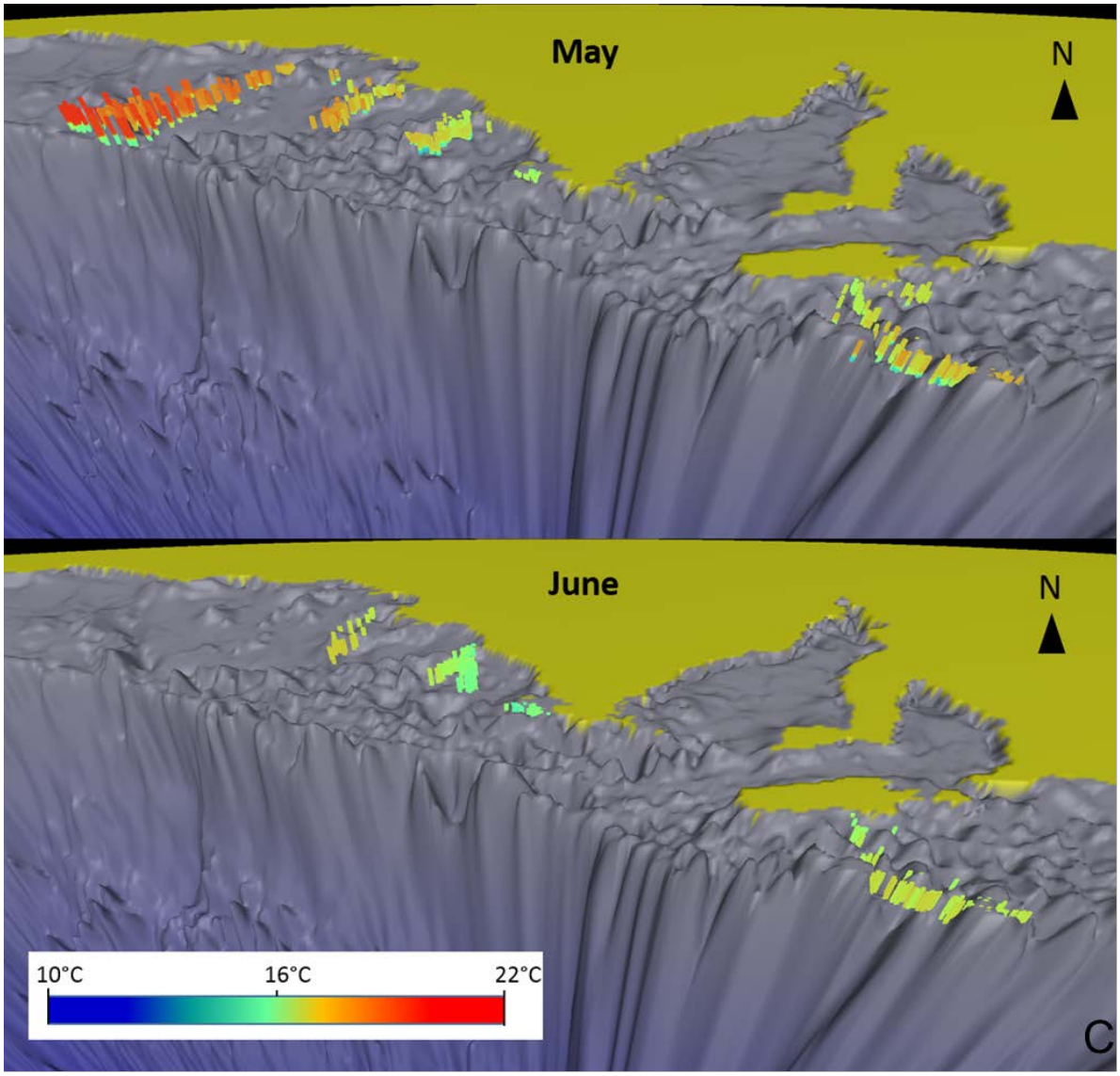

Fig.3.2-5 continued

3.2.4 Discussion

For decades, spatio-temporal variations in physical oceanographic conditions off Southern Australia have been investigated by oceanographers in order to describe and quantify variability in key physical and biological processes (e.g. Middleton & Cirano 2002; McClatchie et al. 2006; Ward et al. 2006; Middleton and Bye 2007; Richardson et al. 2009; Van Ruth et al. 2010a, b; Kämpf and Chapman 2016). Despite the wealth of information collected to date, highlighted for the eastern GAB in particular in chapter 3.1 of this report, there is still uncertainty around the mechanisms and dynamics of upwelling in the central and western GAB regions. Much of this uncertainty remains because of limited sub-surface observations, both spatially and temporally, for the regions. For example, clearly defining the spatial and temporal extent of upwelled water masses originating from the slope, and possibly sourcing water from the Flinders Current, is needed to better understand how the upwelling processes influence nutrient exchange and transport across the GAB region.

Australian sea lions equipped with CTD tags have provided observational capacity in a remote but ecologically and economically important coastal shelf region in southern Australia. Data from these deployments over the last 10 years have provided 1) a large number of spatial and temporal observations across 1,000 km of shelf, 2) the only source of near real-time, sub-surface observations in the GAB region, and 3) the only source of sub-surface data for some areas, especially the remote west where an observational gap exists. Longitudinal data collected continually over many months have provided a more detailed understanding of the spatial and temporal extent of the three main water masses influencing the continental shelf in the GAB region: 1) cool, fresh, nutrient-rich water upwelled from the continental slope, 2) warm, saline, nutrient-depleted GABP water, and 3) widespread Subtropical Surface Waters, and has also validated existing information about the seasonal nature of stratification and mixing processes in the water column. Based on these new data, the maximum spatial extent of upwelled water originating from the slope occurs over the GAB shelf during March and April. This is similar to the peak in upwelling observed off Kangaroo Island during February and March (Richardson 2015). These data also highlight the westward extent of upwelled water along the coast of the eastern GAB, which reaches as far as ~133.5°E, and the spatial and temporal extent of the warm and saline GABP in the central and eastern GAB (Fig. 3.2.3C, Fig. 3.2.4A).

Temperature and salinity remain the two primary variables required for water mass identification. Moreover, it should be noted that some CTD tags deployed from 2014 onwards included a fluorescence sensor and even more recently an irradiance sensor, which can provide a quantitative estimation of the primary production and its distribution through the different water masses (Bayle et al. 2015). Complementing these observations and analytical advancements, a recent study has shown that a dissolved oxygen sensor can be included in such tags (Bailleul et al. 2015). With further miniaturisation of tags and the capacity to add additional sensors easily, animal borne biologging has the potential to collect a range of new sensor data, in a cost-effective manner, that will further enhance oceanographic studies in the GAB region.

The oceanographically distinct sub-regions of Australia's southern shelves are characterised by different physical conditions, but are implicitly linked by nutrient enrichment processes that drive their productivity and ecosystem dynamics. Additional observations provided by animal borne biologging, simultaneously conducted in each of the sub-regions and on a broad temporal scale, will help to improve our understanding of boundary current and continental shelf processes. Moving forward, as satellite animal tracking data could provide the only source of near real-time subsurface observations in the region, they will assist in the development, calibration and validation of regional hydrodynamic and biogeochemical models. These data also complement those obtained from other observing systems, such as fixed moorings, Argo floats, gliders and satellites. The animal-borne biologging program in the GAB region has provided a valuable source of data and provides an example of an appropriate technology and platform to collect cost-effective observations from remote regions. Elsewhere, such an approach has proven to be of crucial importance to study biophysical interactions between marine predators and their environment and to examine and quantify globally significant hydrographic processes, such as dense water formation on the Antarctic continental shelf (e.g., Williams et al. 2016).

3.2.5 Summary and conclusions

This study represents the first use of oceanographic data collected by Australian sea lions to examine the water mass characteristics of Australia's southern shelves. This comprehensive dataset provides the only long time series in-situ data available in the central GAB and thus allowed us to

comprehensively examine spatial and temporal variation in the influence of upwelling and downwelling across this relatively poorly characterised region. The information presented here complements our findings for the data rich eastern GAB (chapter 3.1), and fills a key gap in our understanding of the drivers of productivity across the GAB. This study confirms our previous understanding that the influence of upwelling is restricted to the eastern GAB region during the November – April upwelling season, and suggests that different physical/biological mechanisms are underpinning productivity in the central GAB. The implications of this new knowledge for food web dynamics across the GAB will be explored further in project 2.2, particularly in the work detailed in sections 3 and 4.

References

Bailleul, F., Vacquie-Garcia, J., and Guinet, C. 2015. Dissolved oxygen sensor in animal-borne instruments: an innovation for monitoring the health of oceans and investigating the functioning of marine ecosystems. PloS one, 10(7): e0132681.

Blanchard, J. L., Jennings, S., Holmes, R., Harle, J., Merino, G., Allen, J. I., Dulvy, N. K., et al. 2012. Potential consequences of climate change for primary production and fish production in large marine ecosystems. Philosophical Transactions of the Royal Society of London B: Biological Sciences,, 367: 2979-2989.

Boehme, L., Lovell, P., Biuw, M., Roquet, F., Nicholson, J., Thorpe, S. E., Meredith, M. P., et al. 2009. Technical Note: Animal-borne CTD-Satellite Relay Data Loggers for real-time oceanographic data collection. Ocean Science. Ocean Science, 5: 685–695, doi: 610.5194/os-5195-5685-2009.

Butler, A., Althaus, F., Furlani, D., and Ridgway, K. 2002. Assessment of the conservation values of the Bonney upwelling area. Report to Environment Australia.

Costa, D. P., Klinck, J. M., Hofmann, E. E., Dinniman, M. S., and Burns, J. M. 2008. Upper ocean variability in west Antarctic Peninsula continental shelf waters as measured using instrumented seals. Deep Sea Research Part II: Topical Studies in Oceanography, 55 323-337.

Edyvane, K. S. 1999a. Conserving marine biodiversity in South Australia. Part 1. Background, status and review of approach to marine biodiversity conservation in South Australia. South Australian Research and Development Institute. 281 pp.

Edyvane, K. S. 1999b. Conserving Marine Biodiversity in South Australia. Part 2. Identification of Areas of High Conservation Value in South Australia. South Australian Research and Development Institute. 281 pp.

Fedak, M. 2004. Marine animals as platforms for oceanographic sampling: a" win/win" situation for biology and operational oceanography. Memoirs of National Institute of Polar Research, Special issue, 58: 133-147.

Fedak, M., Lovell, P., McConnell, B., and Hunter, C. 2002. Overcoming the Constraints of Long Range Radio Telemetry from Animals: Getting More Useful Data from Smaller Packages. Integrative and Comparative Biology, 42: 3–10. doi: 10.1093/icb/1042.1091.1093 PMID: 21708689.

Fedak, M. A. 2013. The impact of animal platforms on polar ocean observation. Deep Sea Research Part II: Topical Studies in Oceanography, 88:7-13.

Goldsworthy, S. D., Page, B., Rogers, P. J., Bulman, C., Wiebkin, A., McLeay, L. J., Einoder, L., et al. 2013. Trophodynamics of the eastern Great Australian Bight ecosystem: Ecological change associated with the growth of Australia's largest fishery. Ecological Modelling, 255: 38-57.

Hill, K., Moltmann, T., Proctor, R., and Allen, S. 2010. The Australian Integrated Marine Observing System: delivering data streams to address national and international research priorities. Marine Technology Society Journal, 44 65-72.

Hussey, N. E., Kessel, S. T., Aarestrup, K., Cooke, S. J., Cowley, P. D., Fisk, A. T., Harcourt, R. G., et al. 2015. Aquatic animal telemetry: A panoramic window into the underwater world. Science, 348.

Huthnance, J. M. 1995. Circulation, exchange and water masses at the ocean margin: the role of physical processes at the shelf edge. Progress in Oceanography, 35(4): 353-431.

James, N. P., and Bone, Y. 2011. Neritic Carbonate Sediments in a Temperate Realm,Southern Australia, Springer.

Kämpf, J., and Chapman, P. 2016. Upwelling Systems of the World: A Scientific Journey to the Most Productive Marine Ecosystems, Springer International Publishing Switzerland.

Lewis, R. K. 1981. Seasonal upwelling along the southeastern coastline of South Australia. Australian Journal of Marine and Freshwater Research, 32: 843–854.

Lowther, A. D., Harcourt, R. G., Page, B., and Goldsworthy, S. D. 2013. Steady as he goes: at-sea movement of adult male Australian sea lions in a changing marine environment. PlosOne: 10.1371/journal.pone.0074348.

Lydersen, C., Nøst, O. A., Kovacs, K. M., and Fedak, M. A. 2004. Temperature data from Norwegian and Russian waters of the northern Barents Sea collected by free-living ringed seals. Journal of Marine Systems, 46: 99-108.

McClatchie, S., Middleton, J. F., and Ward, T. M. 2006. Water mass analysis and alongshore variation in upwelling intensity in the eastern Great Australian Bight. Journal of Geophysical Research: Oceans, 111: doi:10.1029/2004JC002699.

McMahon, C. R., and Harcourt, R. 2014. Antarctica: Seals collect more Southern Ocean data. Nature, 513: 33-33.

Middleton, J. F., and Bye, J. A. T. 2007. A review of the shelf-slope circulation along Australia’s southern shelves: Cape Leeuwin to Portland. Progress in Oceanography, 75: 1-41.

Middleton, J. F., and Cirano, M. 2002. A northern boundary current along Australia's southern: The Flinders Current shelves. Journal of Geophysical Research: Oceans, 107: doi:10.1029/2000JC000701,002002.

Padman, L., Costa, D. P., Bolmer, S. T., Goebel, M. E., Huckstadt, L. A., Jenkins, A., McDonald, B. I., et al. 2010. Seals map bathymetry of the Antarctic continental shelf. Geophysical Research Letters, 37: L21601, doi:10.1029/2010GL044921.

Pattiaratchi, C. 2007. Understanding areas of high productivity within the south-west marine region. Report for the Commonwealth Government, Department for environment, water, heritage and the arts.

Pauly, D., and Christensen, V. 1995. Primary production required to sustain global fisheries. Nature, 374: 255-257.

Phillips, J. A. 2001. Marine macroalgal biodiversity hotspots: why is there high species richness and endemism in southern Australian marine benthic flora. Biodiversity and Conservation,, 10: 1555–1577.

Richardson, L. E. 2015. Water mass connectivity and mixing along the southern margin of Australia: hydrographic and stable isotope analyses. Australian National University, Canberra, 192pp.

Richardson, L. E., Kyser, T. K., James, N. P., and Bone, Y. 2009. Analysis of hydrographic and stable isotope data to determine water masses, circulation, and mixing in the eastern Great Australian Bight. Journal of Geophysical Research: Oceans: 114(C110).

Roquet, F., Williams, G., Hindell, M. A., Harcourt, R., McMahon, C., Guinet, C., Charrassin, J.-B., et al. 2014. A Southern Indian Ocean database of hydrographic profiles obtained with instrumented elephant seals. 1: 140028.

Bayle, S., Monestiez, P., Guinet, C., and Nerini, D. 2015. Moving toward finer scales in oceanography: predictive linear functional model of chlorophyll-a profile from light data. Progress in Oceanography: doi: 10.1016/j.pocean.2015.1002.1001.

Shepherd, S. 2013. Ecology of Australian temperate reefs: the unique South, CSIRO publishing.

Shetye, S. R., Shenoi, S. S. C., Gouveia, A. D., Michael, G. S., Sundar, D., and Nampoothiri, G. 1991. Wind-driven coastal upwelling along the western boundary of the Bay of Bengal during the southwest monsoon. Continental Shelf Research, 11: 1397-1408.

van Ruth, P. D., Ganf, G. G., and Ward, T. M. 2010a. Hot-spots of primary productivity: An alternative interpretation to conventional upwelling models. Estuarine, Coastal and Shelf Science, 90: 142-158.

van Ruth, P. D., Ganf, G. G., and Ward, T. M. 2010b. The influence of mixing on primary productivity: A unique application of classical critical depth theory. Progress in Oceanography, 85: 224-235.

Ward, T. M., McLeay, L. J., Dimmlich, W. F., Rogers, P. J., McClatchie, S. A. M., Matthews, R., Kämpf, J., et al. 2006. Pelagic ecology of a northern boundary current system: effects of upwelling on the production and distribution of sardine (*Sardinops sagax*), anchovy (*Engraulis australis*) and southern bluefin tuna (*Thunnus maccoyii*) in the Great Australian Bight. Fisheries Oceanography, 15: 191-207.

Ward, T. M., Smith, D. C., Lukatelich, R., Lewis, R., Begg, G. A., and Smith, R. 2014. Integrated approach to ecological and socio-economic research to support the oil and gas industry: The Great Australian Bight collaborative research science program. International Oil Spill Conference Proceedings, 2014: 2193-2205, American Petroleum Institute.

Williams, G. D., Herraiz-Borreguero, L., Roquet, F., Tamura, T., Ohshima, K. I., Fukamachi, Y., Fraser, A. D., et al. 2016. The suppression of Antarctic bottom water formation by melting ice shelves in Prydz Bay. Nature Communications, 7: 10.1038/NCOMMS12577.

4. VARIATION IN MICROBIAL AND PLANKTONIC ABUNDANCE, SIZE STRUCTURE AND COMMUNITY COMPOSITION

4.1 Scenario driven shifts in upwelling and downwelling drive food web dynamics in the eastern GAB (Patten, N.L., van Ruth P.D., Redondo Rodriguez, A. and Richardson, A.E.)

4.1.1 Introduction

The size structure and composition of planktonic communities has important implications for the flux of carbon through marine systems. Marine planktonic food webs are commonly divided into two types; either a microbial food web or a 'classical' food web. The former is typical in oligotrophic waters, where small pico- (< 2 µm) and nano- (2 – 20 µm) phytoplankton dominate the autotrophic biomass. As a result, nutrient regeneration rates are high, while sedimentation rates and overall carbon transfer to higher order organisms is low (Azam 1983, Stockner 1988). Classical food webs, where large phytoplankton (i.e. microphytoplankton (20 – 200 µm) dominate, commonly occur in nutrient rich waters (e.g. coastal upwelling areas). In this case, a large fraction of primary production is channelled thought a shortened chain, resulting in an increased efficiency of carbon transfer to higher trophic levels (Ryther 1969, Cushing 1989). Marine planktonic food webs are, however, more complex in nature than simple alternative food web states. Rather, a continuum of trophic pathways exist in most systems at most times, variations of which influence total system productivity (Legendre and Rassoulzadegan 1995). Furthermore, clear successional replacement of small phytoplankton by larger phytoplankton during periods of enrichment (Ryther 1969) does not always occur. In the Benguela upwelling system for example, phytoplankton biomass and production peaks in the stabilisation/relaxation period following upwelling. At that peak, large diatoms dominate the phytoplankton community, with (nano) flagellates also making an often significant contribution to biomass (Painting et al. 1993, Lamont et al. 2014). Similarly, in the Humboldt Current System, nanoplankton comprise a relatively (seasonally) stable and significant component of the planktonic community year round (Böttjer and Morales 2007), while large micro-phytoplankton blooms are frequent during the upwelling period (Anabalón et al. 2007). Small phytoplankton can also respond favorably to enrichment (Barber and Hiscock 2006). For example, enhanced picophytoplankton biomass and growth co-occurring with elevated diatom biomass is known for some upwelling influenced regions (e.g. Arabian Sea and California current system, Garrison et al. 2000, Linacre et al. 2010). It appears more common that only under extreme conditions do large phytoplankton (i.e. diatoms) outcompete smaller phytoplankton (Vargas et al. 2007, Linacre et al. 2010). However, under these 'extreme' enrichment conditions, enhanced protistan grazing rates on the smaller phytoplankton may suppress any observable biomass increase (Barber and Hiscock 2006).

Seasonal upwelling is a feature of the eastern Great Australian Bight (GAB) in southern Australia. Here, upwelling occurs in the austral spring through to early autumn (November to April) driven by favorable (south-easterly) winds, together with complex hydrodynamic and physical forces which are yet to be fully understood (Kämpf et al. 2004, McClatchie et al. 2006, Middleton and Bye 2007). In winter, south westerly winds dominate, suppressing any upwelling and resulting in a well-mixed water column. In the GAB, high autotrophic biomass (as Chlorophyll *a*) associated with upwelling coincides with enhanced zooplankton biomass (van Ruth and Ward 2009) and high densities of larval fish and fish eggs (Sardine; *Sardinops sagax*, and anchovy*; Engraulis australis*, Ward et al. 2006). However, little is known of the planktonic community structure that underpins this trophic pathway from primary to secondary producers. To date, focused studies in the eastern GAB have

characterised only the picoplankton and virus assemblages. During downwelling periods, *Prochlorococcus* (~0.6 µm) and *Synechococcus* (~0.9 µm) dominate the system, while in waters influenced by upwelling, picoeukaryote (~1 – 3 µm) abundances increase substantially (van Dongen-Vogels et al. 2011, 2012). Differences in community structure of bacteria and viruses occurred between two different water masses associated with an upwelling event (Paterson et al. 2013), but there is no information on how these groups respond to changing hydrographic conditions. Little is known about the community structure and composition of the nano- and micro-plankton communities in the eastern GAB. The GAB region supports some of Australia's largest and most productive fisheries (e.g. South Australian Sardine Fishery, Commonwealth Southern Bluefin Tuna Fishery), with high densities of pelagic fish (e.g. sardine and anchovy, Ward et al. 2005), and represents a 'hotspot' for migratory and resident apex predators (Goldsworthy et al. 2013, Rogers et al. 2015). To date, however, a holistic understanding of the planktonic organisms (or trophic pathways) that underpin these higher trophic orders is lacking.

van Ruth et al. (Chapter 3.1) proposed five scenarios under a conceptual model of upwelling and downwelling in the eastern GAB, developed using physical and chemical data. Briefly these are 1) winter-mixing, 2) preconditioning stages of the summer upwelling, 3) moderate upwelling conditions, when nutrient rich water reaches the shelf as a bottom layer and sits below the surface mixed layer, 4) strong upwelling, where nutrient rich water penetrates into the upper euphotic zone, and 5) suppression of upwelling which occurs in the late upwelling season and follows prior enrichment. van Ruth et al. (Chapter 3.1) proposed a microbial food web to dominate in the eastern GAB, except during upwelling events, where enrichment of the photic zone would support the growth of larger phytoplankton (i.e. a classical food web). In this study, we utilised a long-term data set for the region (~8 years), to test the conceptual model of van Ruth et al. (Chapter 3.1). We document changes in different groups of organisms at the base of the food web (from viruses, bacteria, pico-, nano-, and micro-plankton, through to meso-zooplankton) under five hydrographic scenarios which typically occur over the course of a year. These results represent the first cohesive look at the whole lower trophic food web in the eastern GAB, and highlight the efficient trophic transfer that occurs not only under strong upwelling conditions, but also at the commencement of the upwelling season due to hydrographic conditions not directly related to upwelling.

4.1.2 Methods

Hydrographic sampling, stratification index and wind stress

Sampling was conducted at the Kangaroo Island National Reference Station (NRSKAI) (35.50°S, 136.27°E) in the eastern GAB, in southern Australia (Fig. 4.1-1). This station is situated on the 100 m isobath, adjacent to Kangaroo Island and the large inverse estuary of Spencer Gulf, and is regularly monitored as part of the Australian Integrated Marine Observing System (IMOS; http://imos.org.au/). Sampling at NRSKAI began in February 2008 and has continued to the present. From February 2008 to April 2012, sampling was conducted monthly to quarterly, with increased sampling effort generally occurring during the austral spring/summer. Sampling frequency was then reduced to every six to ten months until January 2014. From January 2014 to May 2016, quarterly yearly sampling occurred. A summary of sampling dates are provided in Table 4.2-1, together with the measured biological and chemical parameters at each sampling depth which are outlined further below.

Temperature, salinity and *in vivo* fluorescence data were acquired with a SeaBird SBE 19plus Conductivity, Temperature, Depth recorder (CTD, Sea-Bird Scientific, Washington, US) equipped with an ECO FL fluorometer (WetLabs, Rhode Island, US).

An index for stratification, based on the potential energy anomaly (ϕ; J m^{-3}; Simpson & Bowers 1981), was calculated from each vertical CTD profile data from each sampling event:

$$\phi = \frac{1}{H} \int_{-H}^{0} gz(\rho - \overline{\rho})dz$$

where $\overline{\rho}$ is the depth-averaged density, $\overline{\rho} = \frac{1}{H} \int_{-H}^{0} \rho dz$, H is the water column depth, g is the gravitational acceleration and ρ is the density of seawater at depth z. High values of ϕ, indicate a more stratified and stable water column.

Wind data accessed from the Australian Bureau of Meteorology, were used to calculate three day averaged alongshore wind stress (τ)at an angle of 315°T according to:

$$\tau = \rho_a C_D U \mid U,$$

where ρ_a is the density of air (0.1 kg m^{-3}) and C_D is a drag coefficient from (Gill 1982). Positive values of τ correspond to upwelling (Middleton & Bye 2007).

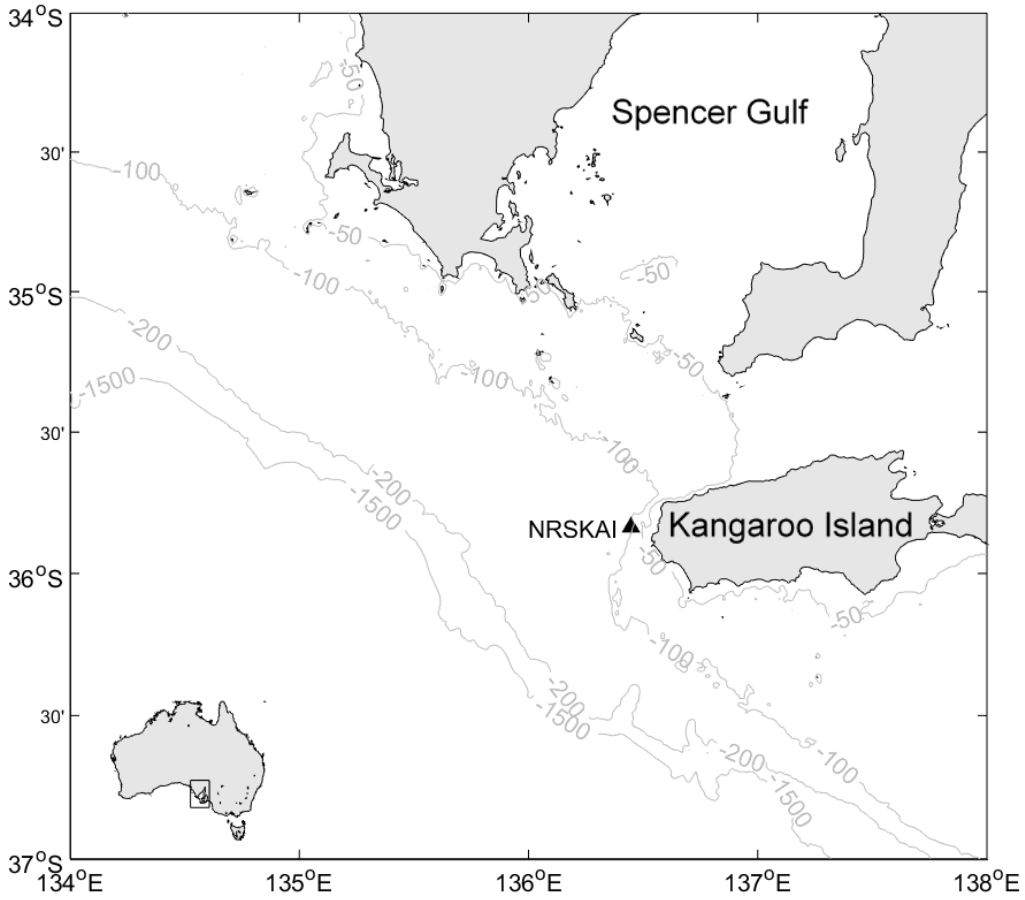

Figure 4.1-1 Location of the sampling station NRSKAI off Kangaroo Island in southern Australia (South Australia).

Table 4.1-1 Bio-chemical sampling overview at NRSKAI. Chlorophyll a [Chl a], Nut = dissolved nutrients [NO_x, NH_4, PO_4, SiO_2], Vir = virus, Bac = bacteria, Pico = picophytoplankton, Phyt = phytoplankton, Pig = pigments, Zoo Ab = Zooplankton abundance, Zoo B = Zooplankton Biomass. S = surface, SCM = sub-surface chlorophyll maxima, D = deep. ✳ = S only; ◇ = SCM only, ○ = S and SCM only; ✝ = SCM and D only; and • SCM and D only. For pigments; int = Integrated sample over upper 50 m, d = deep sample from pigment analysis.

Sampling event	Depths sampled (m)	Location in water column	Chl *a*	Nuts	Vir	Bac	Pico	Phyt	Pig	Zoo Ab	Zoo Bm
11-Feb-08	98	SCM	×	×	×	×	×	_	_	_	_
15-Mar-08	45	SCM	×	×	_	×	_	_	_	_	_
14-Apr-08	65	SCM	×	×	×	×	×	_	_	_	_
11-Aug-08	15, 75	S, SCM	×	×	×	×	×✳	_	_	_	_
19-Oct-08	15, 33, 105	S, SCM, D	×	_	×	×	×✳	_	_	_	_
11-Nov-08	15, 60,100	S, SCM, D	_	×	_	_	×○	_	_	_	_
14-Jan-09	15, 48, 100	S, SCM, D	×	×	_	_	×◇	_	_	_	_
5-Feb-09	15, 48, 102	S, SCM, D	×	×	×	×	×	_	_	_	_
7-Mar-09	15, 35, 75	S, SCM, D	×	×	×	×	×	_	_	_	_
2-Jun-09	15, 65, 105	S, SCM, D	_	×	×	×	×	_	_	_	_
7-Oct-09	15, 48, 97	S, SCM, D	_	×	×	×	×	_	_	_	_
15-Nov-09	15, 60, 100	S, SCM, D	×	×	×	×	×	_	_	×	×
14-Dec-09	15, 50, 100	S, SCM, D	×	×	×	×	×	×	×	×	×
12-Jan-10	15, 60, 100	S, SCM, D	×	×	×•	×•	×	_	_	×	×
15-Feb-10	15, 40, 103	S, SCM, D	×	×	×	×	×	_	_	_	_
15-Mar-10	15, 35, 105	S, SCM, D	×	×	×	×	×	_	_	_	_
19-Apr-10	15, 38, 105	S, SCM, D	×	×	×	×	×	_	×in	×	×
22-Jul-10	15, 25, 100	S, SCM, D	_	×	×	×	×	×✝	_	_	_
21-Nov-10	15, 25, 90	S, SCM, D	×	×	×	×	×	×	×	×	×
13-Dec-10	15, 45, 80	S, SCM, D	×	×	×	×	×	×	×	×	×
23-Jan-11	15, 46, 90	S, SCM, D	×	×	×	×	×	×	×	_	_
23-Feb-11	15, 20, 90	S, SCM, D	×	×	×	×	×	×	×in	×	×
20-Mar-11	15, 24, 90	S, SCM, D	×	×	_	_	_	×	×	×	×
28-Apr-11	15, 45, 100	S, SCM, D	×	×	×	×	×	×	×	×	×
18-Jul-11	15, 40, 95	S, SCM, D	×	×	×	×	×	×	×	×	×
26-Oct-11	15, 83, 100	S, SCM, D	×	×	×	×	×	×	×in	×	×
15-Nov-11	15, 50, 100	S, SCM, D	×	×	×	×	×	×	×in	×	×
20-Dec-11	15, 43, 100	S, SCM, D	×	×	×	×	×	×	×in	×	×
16-Jan-12	15, 35, 98	S, SCM, D	×	×	×	×	×	×	×	×	×
15-Feb-12	15, 60, 100	S, SCM, D	×	×	×	×	×	×	×	×	×
15-Apr-12	10, 45, 100	S, SCM, D	×	×	×	×	×	×	×	×	×
21-Feb-13	10, 59, 100	S, SCM, D	×	×	_	_	_	×	×	×	×
27-Aug-13	10, 30, 75	S, SCM, D	×	×	_	_	_	_	×	×	×
23-Jan-14	10, 30, 75	S, SCM, D	_	×	_	_	_	_	×in	×	×
14-Mar-14	10, 30, 50	S, SCM, D	×	×	_	_	_	_	×	×	×
7-May-14	5, 40, 50	S, SCM, D	×	×	×	×	×	×	×	×	×
13-Jul-14	5, 65, 75	S, SCM, D	×	×	×	×	×	×	×	×	×
29-Oct-14	5, 77, 87	S, SCM, D	×	×	×	×	×	×	×	×	×
1-Dec-14	10, 40, 75	S, SCM, D	×	×	_	_	_	_	×	×	×
25-Feb-15	5, 40, 50	S, SCM, D	×	×	×	×	×	×	×	×	×
9-Apr-15	5, 55, 65	S, SCM, D	×	×	×	×	×	×	×	×	×
9-Sep-15	5, 55, 65	S, SCM, D	×	×	×	×	×	×	×	×	×
17-Nov-15	5, 40, 50	S, SCM, D	×	×	×	×	×	×	×	×	×
24-Feb-16	5, 40, 50	S, SCM, D	×	×	×	×	×	×	×	×	×
26-May-16	5, 60, 70	S, SCM, D	×	×	×	×	×	×	×	×	×

Seawater sampling

Water samples were taken from the surface, at the subsurface chlorophyll fluorescence maximum (SCM), and in deep water. From February 2008 through to March 2014, the surface sample was taken at 10 – 15 m below the surface and the deep sample taken approximately 10 m from the bottom. After March 2014, surface samples were taken from 5 m below the surface and deep samples were taken 10 m below the SCM.

Dissolved nutrients

Samples for dissolved nutrients (nitrate + nitrite, NO_x), ammonium (NH_4), phosphate (PO_4) and silicate (SiO_2)) were filtered through 0.45 μm syringe filters and stored at -20 °C for nutrient analysis. Dissolved nutrient samples were analysed on a QuickChem QC8500 Automated Ion Analyser according to the Lachat QuickChem methods. Detection limits were 0.071 μM for NO_x and NH_4, 0.03 μM for PO_4 and 0.333 μM for SiO_2.

Bacteria and viruses

Triplicate bacteria and virus samples were fixed in glutaraldehyde (0.5% final concentration) in the dark for 15 minutes, quick frozen in liquid nitrogen and stored at -80 °C until analysis. Samples of bacteria and viruses were thawed at 37 °C, diluted 10 fold in Tris EDTA (pH = 8.0, Sigma-Aldrich), stained with SYBR I green (0.5 x 10-4 final concentration, Molecular Probes) in the dark at 80°C for 10 minutes and then 1.0 μm fluorescent beads (Polysciences) were added an internal standard (Brussaard 2004). Bacteria and viruses were analysed on a FACSCanto (Becton Dickenson, February 2008 – February 2013) or a FACSVerse (Becton Dickenson, May 2014 – May 2016) flow cytometer within a month of collection with acquisition run for 2 minutes. Bacteria and viruses were discriminated on the basis of green fluorescence, side-angle light scatter (SSC) and forward-angle light scatter (FSC) using WIN MDI 2.8 software (Joseph Trotter, February 2008 to February 2013) and FlowJo® flow cytometry analysis software (from May 2014 onwards). Bacteria and viruses were separated on plots of side scatter (SSC) and green (SYBR) fluorescence and SSC and red (Chlorophyll a (Chl *a*)) fluorescence. In deep samples, Prochlorococcus could clearly be discriminated from bacteria in SSC and red fluorescence plots (and SSC and green fluorescence), however in the surface and SCM, Prochlorococcus often coincided within the stained bacterial group. To correct for this, Prochlorococcus were included within the bacterial group for all three depths in the analysis. Bacteria counts were then corrected by subtracting total counts of Prochlorococcus (obtained from non-stained samples) from the stained bacterial group.

Picophytoplankton

Samples for picophytoplankton were fixed with paraformaldehyde (2% final concentration, February 2008 to February 2013) or glutaraldehyde (0.25% final concentration, May 2014 onwards), quick frozen in liquid nitrogen and stored at -80 °C until analysis. Picophytoplantkon samples were thawed at 37 °C, 1 μm beads (Polysciences) added as an internal reference and samples analysed on the same flow cytometer as above with acquisition run for 3 to 5 minutes. Different picophytoplanton groups were discriminated on the basis of red and orange autofluorescence of chlorophyll and the accessory pigment phycoerythrin and light scatter properties of side-angle light scatter and forward-angle light scatter, using the flow cytometry analysis software WIN MDI 2.8 software (Joseph Trotter, February 2008 to February 2013) or FlowJo® (May 2014 to May 2016).

Phytoplankton

Water samples (1 L) for phytoplankton taxonomy were preserved using Lugol's iodine solution. Phytoplankton (> 5 µm) were identified by Microalgal services (http://microalgal.com.au) using traditional taxonomic methods. Phytoplankton were identified to species level where possible. Phytoplankton data from the three discreet sampling depths began from July 2010 (Table 4.1-11).

Chlorophyll a and accessory pigments

From February 2008 through to April 2012, seawater (300 ml) was filtered through GF/C glass fibre filters. Filters were stored at -20 °C until analysis. Filters were extracted in methanol for 24 hours in the dark and chlorophyll *a* (Chl *a*) concentrations were determined using a Turner 450 fluorometer. From February 2013 onwards, seawater (4 L) was filtered through a stacked 5 µm mesh and pre-combusted GF/F (Whatman, nominal pore size 0.7 µm) glass fibre filters. Filters were stored in liquid nitrogen then transferred to -80 °C until analysis. Pigment concentrations were analysed via High Performance Liquid Chromoatography (HPLC) using an Agilent LC1260 HPLC with a photodiode array detector and a refrigerated autosampler, following extraction in HPLC grade acetone according to (Van Heukelem and Thomas 2001). For the fractionated samples, total Chl *a* was calculated as the sum of the concentrations of Chl *a*, divinyl Chl *a*, Chl *a* allomer and Chl *a* epimer in the < 5 um fraction + the >5 um fraction. For sampling dates in August 2013, March 2014 and December 2014, we used Chl *a* data (calculated as DV Chl *a* + Chl *a*) obtained through the Australian Ocean Data Network portal (https://portal.aodn.org.au/) for depths of 40 m and 100 m at NRSKAI. These depths were close to those sampled for the SCM and deep samples (see Table 4.1-1). The use of a GFC filter (nominal pore size 1.2 µm) versus a GFF (nominal pore size 0.7 µm) for Chl *a* samples collected prior to February 2013 may have resulted in under estimations of Chl *a* at some times (van Dongen-Vogels et al. 2011; i.e. when *Prochlorococcus* and *Synechococcus* made up a large fraction of the autotrophic community).

Only a short-term data set (~ 2 years; 10 sampling events) was available for size fractionated accessory pigments (above), with sampling most commonly (50 %) occurring during 'winter-mixing'. Therefore, in order to gain insight into pigment distributions under the assigned five scenarios and with adequate representation within each scenario, we accessed pigment data through the Australian Ocean Data network portal (https://portal.aodn.org.au/). These data were obtained from NRSKAI on the same day and were available from July 2011 onwards (Table 4.1-1). Methods for collecting and analysing phytoplankton pigment samples are described in detail in Thompson et al. (2015). For each sampling date, we used pigment data from a 50 m integrated sample, and for discreet sampling depths of 40 m and 100 m. While these depths do not always align with those outlined in Table 4.1-1, we believe the integrated, 40 m and 100 m depths are representative of our surface, SCM and deep samples, respectively (Table 4.1-1). Bio-marker pigments were then used to infer dominant algal classes and functional groups following Jeffrey et al. (1997) (Table 4.1-2). Pigment data provided additional information on the autotrophic community, particularly on the small nanophytoplankton, which would otherwise be missed with flow cytometry (i.e. cells <2 µm) and phytoplankton identification via microscopy (i.e. cells >5 µm).

The size structure of the phytoplankton community was further investigated according to the approach of Vidussi et al. (2001) and Uitz et al. (2008), with three phytoplankton size classes estimated; pico (<2 µm); nano (2 – 20 µm) and micro (>20 µm). The fractions of these three pigment based size classes relative to the total algal biomass were calculated as:

$$\text{micro} = (1.41 \times \text{Fuco} + 1.41 \times \text{Peri})/\text{wDP} \quad (1)$$

nano = (0.60 × Allo + 0.35 ×19But + 1.27 × 19Hex)/ wDP (2)

pico = (0.86 ×Zea+1.01×(Chl *b* – DV Chl *b*)/wDP (3)

Where wDP is the weighted sum of the concentration of the seven pigments:

wDP = 1.41×Fuco + 1.41×Peri + 0.60 ×Allo + 0.35 × 19But + 1.27 × 19Hex +

0.86 × Zea + 1.01 × (Chl *b* – DV Chl *b*) (4)

Table 4.1-2 Contribution of major taxonomically significant pigments in algal classes. The nine pigments used in calculations for picoplankton, nanoplankton and microplankton are in bold.

Pigment	Abbreviation	Taxa
Chlorophyll *a*	**Chl *a***	All photosynthetic algae
Divinyl Chl *a*	**DV chl *a***	Prochlorophytes (*Prochlorococcus* spp.)
Chlorophyll b	**Chl *b***	Dominant in green algae (e.g. chlorophytes, euglenophytes, prasinophytes)
Zeaxanthin	**Zea**	Cyanobacteria (e.g. *Synechococcus*); also prochlorophytes (*Prochlorococcus*)
19'hexanoyloxyfucoxanthin	**19Hex**	Prymnesiophytes; some dinoflagellates with endosymbionts
19'butanoloxylfucoxanthin	**19But**	Chrysophytes; some prymnesiophytes and some dinoflagellates with endosymbionts
Alloxanthin	**Allo**	Cryptophytes; also some dinoflagellates with endosymbionts
Peridinin	**Peri**	photosynthetic dinoflagellates, except those containing endosymbionts of other algal classes
Fucoxanthin	**Fuco**	Diatoms; also Prymesiophytes, Chrysophytes and some dinoflagellates with endosymbionts
Prasinoxanthin	Pras	Prasinophytes

Zooplankton

NRSKAI zooplankton data were accessed from the Australian Ocean Data Network portal (https://portal.aodn.org.au/). Zooplankton were collected using a 100 µm mesh drop net with 60 cm mouth diameter, falling at 1 m^{-1} s^{-1}, sampling on the way down. The net was deployed to 10 m above the bottom. Samples were fixed in formalin and subsequently identified to lowest taxonomic grouping (commonly species level). Zooplankton dry biomass was also determined from frozen samples.

Assigning sampling dates to scenarios of enrichment and absence of enrichment

At NRSKAI, for the period 2008 – 2012, temperature has been shown to explain 50% of the variation in NO_x (van Ruth et al. Chapter 3.1). Using nitrate (NO_3) data from a 7 year (February 2009 to May 2016) time series of high resolution samples (taken every 10 – 25 m from surface to bottom) obtained from the Australian Ocean Data Network portal (https://portal.aodn.org.au/), a similar linear relationship was found (y = -0.79x +13.98, r^2 = 0.50; P <0.001; Fig. 4.1-2). When the winter mixing period (May – October) was removed, a stronger relationship occurred (y = -0.89x +15.87, r^2 = 0.59; P <0.001; Fig. 4.1-2). Upwelling in the eastern GAB region has previously been defined to occur when temperatures fall below 15 - 16 °C (McClatchie et al. 2006, Middleton and Bye 2007, van Ruth et al. 2010a, b, van Dongen-Vogels et al. 2011). Based on these previous works and the relationship between temperature and NO_3 for our study (Fig. 4.1-2) we used a temperature threshold of <15.5

°C to indicate the presence (≤15.5 °C) and/or absence (>15.5 °C) of upwelled water and to subsequently categorise the sampling events into one of the five scenarios (see below).

We used seawater temperature at three depths in the water column to categorise the sampling events: at ~100 m depth, representing near bottom, at 40 m depth (mid-water column) and at ~5 m depth, representing the surface. Each sampling event is categorised into one of the five scenarios based on timing and temperatures for the three depths in the water column (Table 4.1-3). For the majority of sampling events, we used *in situ* temperature at the specified depth obtained from the CTD profiles. For those sampling events were the CTD did not provide a temperature value for the bottom or mid-water depths (Table 4.1-4, Fig. 4.1-3,) we used temperature data from a deployed mooring at the same location, where temperature was recorded at ~40 m and ~100 m depth using a CTD or a temperature sensor on an acoustic Doppler current profiler. In the absence of surface temperature data from the CTD, we used daily satellite sea surface temperature (SST) derived from the Moderate Resolution Imaging Spectrophotometer (MODIS) onboard the Aqua satellite at 1 km resolution, available from the Australian Ocean Data Network portal (https://portal.aodn.org.au/) . If the MODIS SST was not available for the sampling day, SST was inferred using a linear interpolation (Table 4.1-4, Fig. 4.1-3).

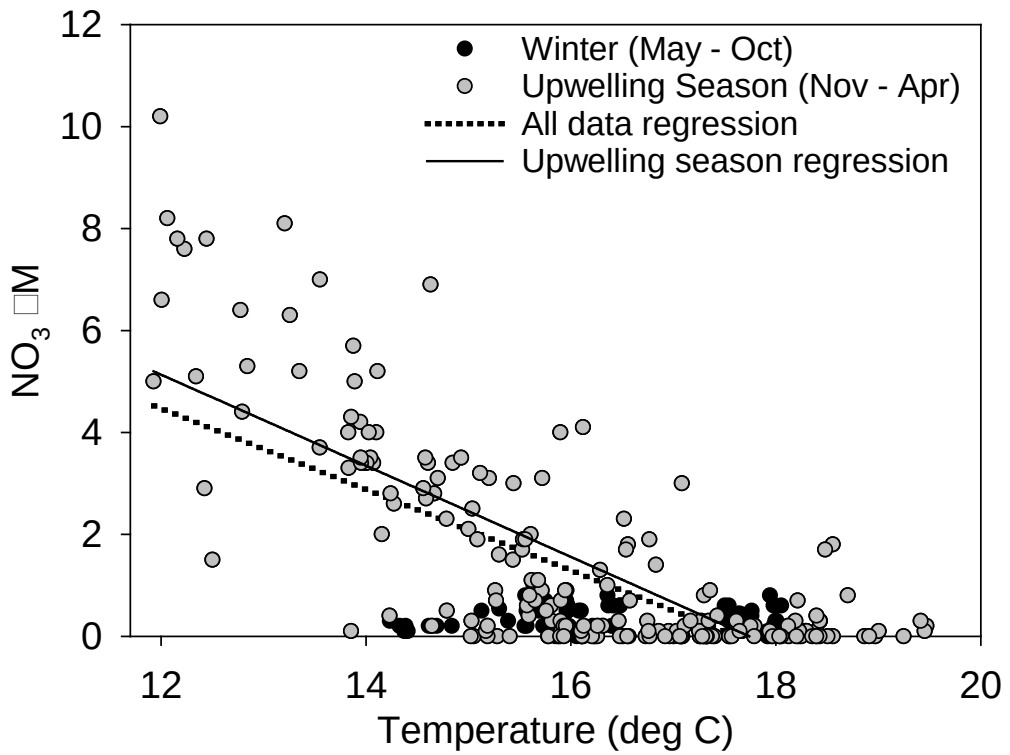

Figure 4.1-2 Temperature versus NO_3 for water samples taken at 10 to 25 m intervals from the surface to the near bottom (~100 m) at NRSKAI from February 2009 to May 2016 as part of the IMOS sampling program.

Table 4.1-3 Definition of scenarios based on timing period and/or sea water temperatures at 5 m, 40 m and 100 m in the water column.

Scenario	Period	Temperature at 5 m (°C)	Temperature at 40 m (°C)	Temperature at 100 m (°C)
Winter-mixing*	May - Oct	Not defined	Not defined	Not defined
Preconditioning	Nov - Dec	> 15.5	> 15.5	> 15.5
Moderate upwelling	Nov - April	> 15.5	> 15.5	< 15.5
Strong upwelling	Nov - April	< 15.5 or > 15.5	< 15.5	< 15.5
Suppression	Jan - April	> 15.5	> 15.5	> 15.5

** water temperatures as low as 15.0 °C can occur during winter-mixing but this is due to surface cooling and mixing conditions and not upwelling.*

Data analysis

Dissolved nutrient and Chl *a* data are reported as means ± standard error (SE) for each depth within each scenario. Results for plankton groups are reported by averaging over the three depths (mean ± standard error (SE)) of the water column. Exceptions to this were made on occasions in the Results section for moderate and strong upwelling and suppression scenarios, when distinct differences occurred in some plankton groups between depths.

Statistical analyses were performed in Primer Version 6 (PRIMER-E, Plymouth, UK). Dissolved nutrient data were $\log_{(x+1)}$ transformed and normalised and a principal component analysis performed to identify the main patterns between scenarios and depths. Euclidian distance similarity matrices were also computed for each of the dissolved nutrient parameters in order to formally test any differences between scenarios and/or depths (see below).

Biological data were either $\log_{(x+1)}$ transformed (virus, bacteria, picophytoplankton) or forth root transformed (phytoplankton, zooplankton, pigments). Gower similarity matrices were applied for bacteria, virus and picophytoplankton and Bray Curtis similarity matrices for phytoplankton, zooplankton, and pigments. For phytoplankton and copepods, where taxa were identified to the lowest taxonomic resolution, differences in community composition were visualized in two-dimensional space by applying non-metric multi-dimensional scaling ordination (nMDS) plots coupled with a cluster analysis.

Differences between scenarios and depths were formally tested for the different chemical and biological parameters using a PERmutational Multivariate Analysis of VAriance (PERMANOVA), which relies on the analysis of similarities between samples (Anderson et al. 2008). P-values for the PERMANOVA were obtained for each term of the model, using 9999 permutations, with Type III (partial) sum of squares and unrestricted permutation of raw data, testing the factors of scenario (winter-mixing, preconditioning, moderate upwelling, strong upwelling and suppression) and depth in the water column (three depths for all data sets except for zooplankton which were sampled from the entire water column). P values <0.05 were considered statistically significant.

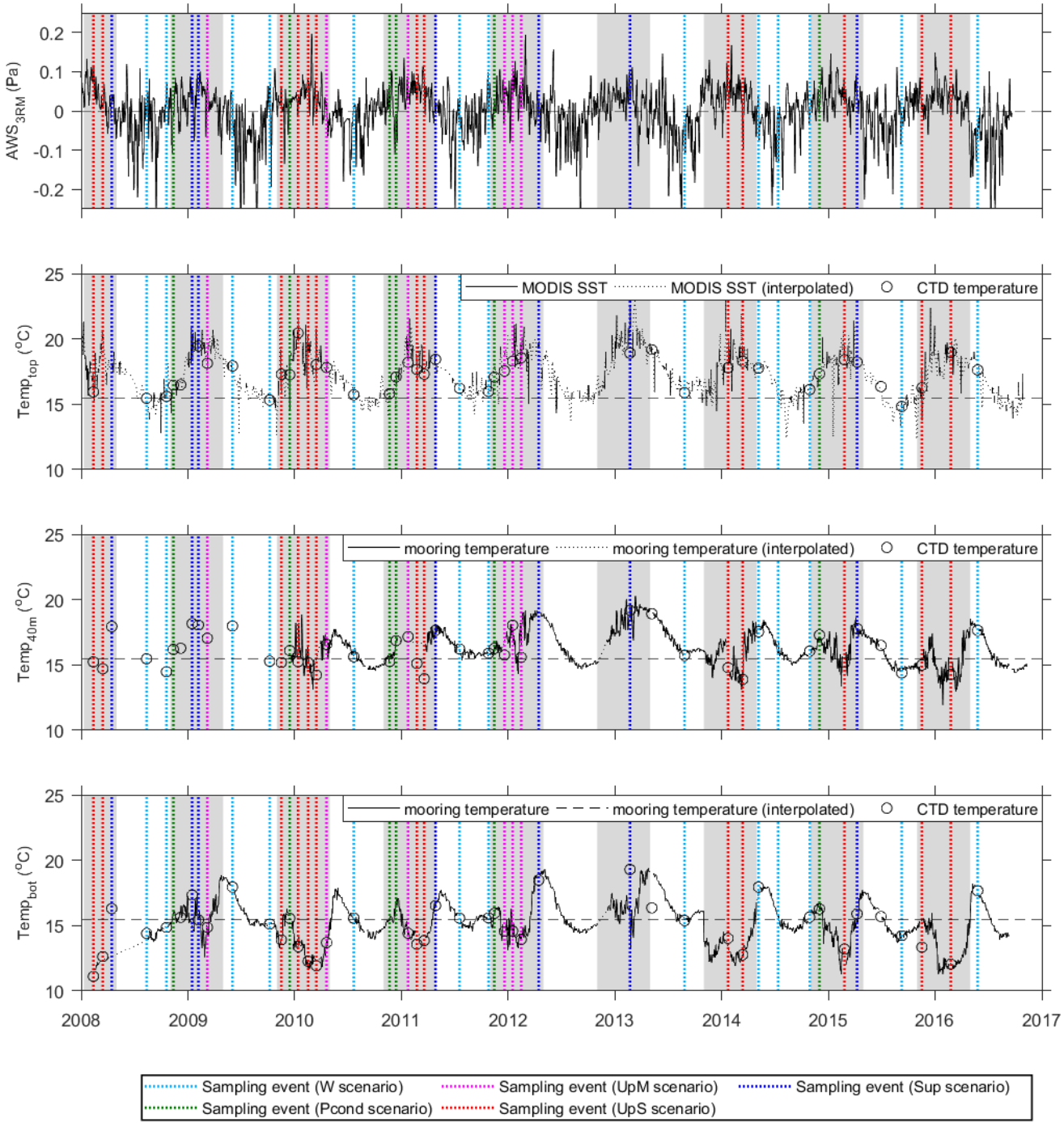

Figure 4.1-3 Alongshore Wind stress (AWS) (A) and water column seawater temperatures at the surface (B), at 40 m depth (C) and at ~ 100 m depths (D) from 2008 through to mid-2016. For (A) positive values reflect upwelling favourable winds and negative values reflect downwelling favourable winds. The upwelling season (November to April) is shaded grey. Dashed lines represent sampling events assigned to winter-mixing (W; aqua), preconditioning (Pcond; green), moderate upwelling (UpM: magenta), strong upwelling (UpS; red) and suppression (Sup; blue). Also see Table 4.1-4 for sampling dates and corresponding measures.

Table 4.1-4 Summary of sampling events and their corresponding: potential energy anomaly (ϕ); along shore wind stress (AWS); bottom (~100 m depth) temperature from: CTD profile (T_B CTD), mooring (T_B mooring) and mooring-interpolated (T_B int); 40 m depth temperature from: CTD profile (T_{40m} CTD), mooring (T_{40m} mooring) and mooring-interpolated (T_{40m} int); surface (~ 5 m) temperature from CTD profile (T_S CTD); MODIS SST (T_S satellite); MODIS SST-interpolated (T_S int); and the assigned scenarios (W = winter-mixing; Pcond = preconditioning; Up_M = moderate upwelling, Up_S = Strong upwelling and Sup = Suppression).

Sampling event	ϕ	AWS	T_B CTD	T_B mooring	T_B int	T_{40m} CTD	T_{40m} mooring	T_{40m} int	T_S CTD	T_S satellite	T_S int	Assigned scenario
11-Feb-08	55	8.365	11.12	-	-	15.23	-	-	15.94	16.71	16.71	Up_S
15-Mar-08	-	2.179	12.63	-	12.35	14.71	-	-	-	-	19.96	UP_S
14-Apr-08	63	2.273	16.31	-	12.65	17.94	-	-	-	17.83	17.83	Sup
11-Aug-08	74	0.944	14.40	-	13.84	15.47	-	-	15.46	14.89	14.89	W
19-Oct-08	85	5.006	14.86	-	14.91	14.48	-	-	15.60	15.61	15.61	W
11-Nov-08	64	0.015	-	15.92	15.92	16.19	-	-	16.46	-	16.24	Pcond
14-Jan-09	47	2.660	17.34	-	15.04	18.16	-	-	-	-	18.90	Sup
5-Feb-09	137	4.644	15.44	15.45	15.45	18.05	-	-	19.47	-	20.03	Sup
7-Mar-09	92	5.067	14.87	14.89	14.89	17.05	-	-	18.13	17.56	17.56	Up_M
2-Jun-09	64	1.756	17.96	-	17.89	17.98	-	-	17.92	-	17.79	W
7-Oct-09	55	6.408	15.12	-	15.12	15.29	-	-	15.32	15.24	15.24	W
15-Nov-09	74	5.069	13.91	13.89	13.89	15.19	-	-	17.30	17.55	17.55	Up_S
14-Dec-09	94	2.541	15.55	-	15.41	16.10	-	-	17.26	18.59	18.59	Pcond
12-Jan-10	131	-0.666	13.39	13.47	13.47	15.24	16.25	16.25	20.45	-	20.32	Up_S
15-Feb-10	122	7.214	12.27	11.97	11.97	15.17	16.41	16.41	-	19.15	19.15	Up_S
15-Mar-10	144	-0.728	11.93	-	12.45	14.23	-	15.31	18.04	20.82	20.82	Up_S
19-Apr-10	108	1.698	13.70	13.62	13.62	16.57	17.12	17.12	17.81	-	17.65	Up_M
22-Jul-10	64	1.251	15.57	15.52	15.52	15.64	16.00	16.00	15.73	-	16.19	W
21-Nov-10	50	4.302	-	15.38	15.38	15.26	15.43	15.43	15.81	15.57	15.57	Pcond
13-Dec-10	43	-0.881	-	16.71	16.71	16.86	16.88	16.88	17.09	-	15.59	Pcond
23-Jan-11	97	4.557	14.42	14.35	14.35	17.17	-	16.76	18.21	19.76	19.76	Up_M
23-Feb-11	82	5.840	13.58	-	14.40	15.11	-	16.69	17.67	17.97	17.97	Up_S
20-Mar-11	82	8.216	13.86	-	14.13	13.94	-	16.62	17.30	-	17.44	Up_S
28-Apr-11	54	-0.413	16.54	16.50	16.50	17.65	18.12	18.12	18.43	-	18.04	Sup
18-Jul-11	64	0.534	15.57	-	15.58	16.23	-	16.15	16.23	-	16.21	W
26-Oct-11	67	3.992	15.59	15.53	15.53	15.90	15.87	15.87	15.98	-	15.89	W
15-Nov-11	81	1.237	15.93	15.90	15.90	16.26	16.48	16.48	17.08	-	17.81	Pcond
20-Dec-11	87	3.983	14.56	-	14.83	15.76	-	16.84	17.55	-	18.73	Up_M
16-Jan-12	107	3.036	14.58	14.51	14.51	18.03	17.88	17.88	18.29	19.56	19.56	Up_M
15-Feb-12	105	0.963	13.95	13.83	13.83	15.59	16.43	16.43	18.56	-	19.12	Up_M
15-Apr-12	-	0.182	18.48	-	18.79	-	-	19.08	-	-	19.25	Sup

Table 4.1-4 continued.

Sampling event	ϕ	AWS	T_B CTD	T_B mooring	T_B int	T_{40m} CTD	T_{40m} mooring	T_{40m} int	T_S CTD	T_S satellite	T_S int	Assigned scenario
21-Feb-13	79	6.697	19.29	16.38	16.38	19.17	19.42	19.42	18.92	-	21.42	Sup
27-Aug-13	60	-3.347	15.39	-	15.60	15.73	-	15.82	15.88	-	16.82	W
23-Jan-14	84	4.969	14.03	-	13.34	14.79	-	15.29	17.79	-	18.49	UP_S
14-Mar-14	119	-2.809	12.77	12.75	12.75	13.89	14.56	14.56	18.29	18.35	18.35	UP_S
7-May-14	56	2.966	17.94	-	17.34	17.54	-	17.75	17.76	18.02	18.02	W
13-Jul-14	46	-0.104		15.70	15.70	-	15.95	15.95	-	-	15.60	W
29-Oct-14	59	-1.327	15.65	-	15.78	16.05	-	15.84	16.12	-	15.81	W
1-Dec-14	80	-0.228	16.29	16.32	16.32	17.28	17.14	17.14	17.33	17.60	17.60	Pcond
25-Feb-15	96	4.723	13.21	-	12.54	15.19	-	15.45	18.40	19.44	19.44	UP_S
9-Apr-15	78	4.533	15.90	15.38	15.38	17.79	17.60	17.60	18.22	-	15.58	Sup
9-Sep-15	52	-0.144	14.23	14.17	14.17	14.39	14.58	14.58	14.84	14.71	14.71	W
17-Nov-15	54	0.286	13.35	-	15.40	15.00	-	15.16	16.26	17.83	17.83	UP_S
24-Feb-16	150	-2.435	12.06	-	12.09	14.27	-	15.43	18.97	-	19.11	UP_S
26-May-16	35	-7.022	17.67	-	17.55	17.65	-	17.78	17.63	17.45	17.45	W

4.1.3 Results

Hydrographic conditions

Scenarios of moderate and strong upwelling were most likely to occur in the late upwelling season (Table 4.1-4). Specifically, moderate upwelling occurred in January through April in five of the six sampling events, while strong upwelling occurred in January, February and March in eleven of the thirteen sampling events (Table 4.1-4). Cold water (<15.5 °C) didn't reached the surface for any sampling event during the study period (Table 4.1-4). Relatively high ϕ, indicative of stratification, occurred during moderate and strong upwelling (99 ± 3 J m^{-3} and 99 ± 10 J m^{-3}, respectively), while ϕ values more similar to those during winter and preconditioning occurred during suppression (76 ± 13 J m^{-3}), indicating a less stable water column and/or breakdown of stratification (Table 4.1-4).

Water column chemical and biological parameters

Highest average NO_x concentrations occurred in deep water during moderate and strong upwelling (3.54 ± 0.97 µM and 5.42 ± 0.73 µM respectively, Fig. 4.1-4), exceeding those in deep water during winter-mixing, preconditioning, and suppression (all $P < 0.01$). Lowest NO_x concentrations (0.16 ± 0.05 µM) occurred in surface waters during strong upwelling, differing only to surface waters during winter-mixing ($P < 0.05$). PO_4 followed the overall trend of NO_x (Fig. 4.1-4B) with significantly higher concentrations occurring in deep water during moderate and strong upwelling compared to other scenarios. Highest SiO_2 concentrations occurred in deep water during strong upwelling (1.94 ± 0.30 µM). In addition, surface SiO_2 concentrations during winter-mixing (1.11 µM ± 0.07 µM) were ~2 times higher than in surface waters for any other scenarios (all $P < 0.03$). NH_4 concentrations were highest during strong upwelling for all depths (all $P < 0.03$).

Separation of deep water from SCM and surface water was evident in the PCA plot, with moderate and strong upwelling scenarios further separating from other scenarios (Fig. 4.1-5). PC1 accounted for 48.1% (driven predominantly by NO_x, SiO_2 and PO_4) and PC2 (NH_4) accounted for (24.9%) (Fig. 4.1-5).

Surface waters were potentially N limited for all scenarios (NO_x: PO_4; averaging <12:1) except during suppression when waters tended towards potential P limitation (NO_x: PO_4; averaging >17:1). Potential P limitation persisted at the SCM and in deep water during suppression, concomitant with potential Si limitation at these depths (NO_x: SiO_2 >1:1).

Chlorophyll a

Highest (1.73 ± 0.87 µg L^{-1}) and most variable Chl *a* concentrations (ranging from 0.20 to 10.34 µg L^{-1}, occurred during strong upwelling in the SCM, with relatively high average Chl *a* also occurring in the SCM during moderate upwelling (0.54 ± 0.22 µg L^{-1}) (Fig. 4.1-6). Chl *a* in the SCM was statistically higher than surface waters but not deep water for all scenarios ($P = 0.011$), with Chl *a* concentrations during strong upwelling significantly higher than for any other scenario (all $P < 0.05$).

The high Chl *a* of 10.34 µg L^{-1} occurred on only one occasion (March 2010 in the SCM) coinciding with the highest recorded NO_x concentration in deep water (9.68 µM). In fact, Chl *a* greater than 1 µg L^{-1} occurred only during nine of the 45 sampling events (under moderate and strong upwelling events only) most commonly in the SCM (for seven sampling events), and once for in each of the surface (April 2010) and deep water (February 2015).

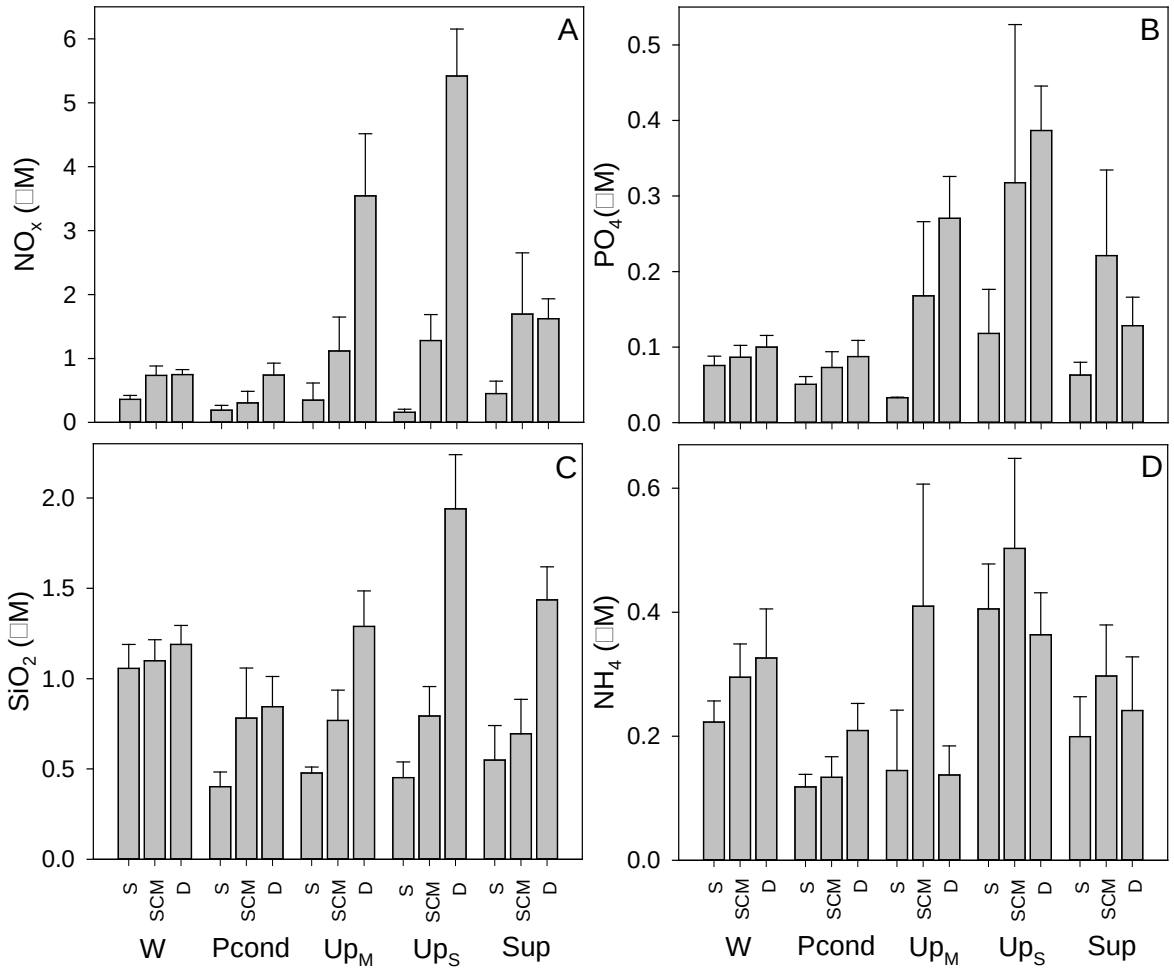

Figure 4.1-4 Plots of dissolved nutrient concentrations: (A) NO_x (NO_2 + NO_3), (B) PO_4, (C) SiO_2 and (D) NH_4 for surface (S), subsurface chlorophyll maxima (SCM) and deep samples (D) under different scenarios of upwelling and downwelling in the eGAB; W = Winter-mixing, Pcond = Preconditioning, UpM = moderate upwelling, UpS = strong upwelling and Sup = Suppression. Values represent means ± SE.

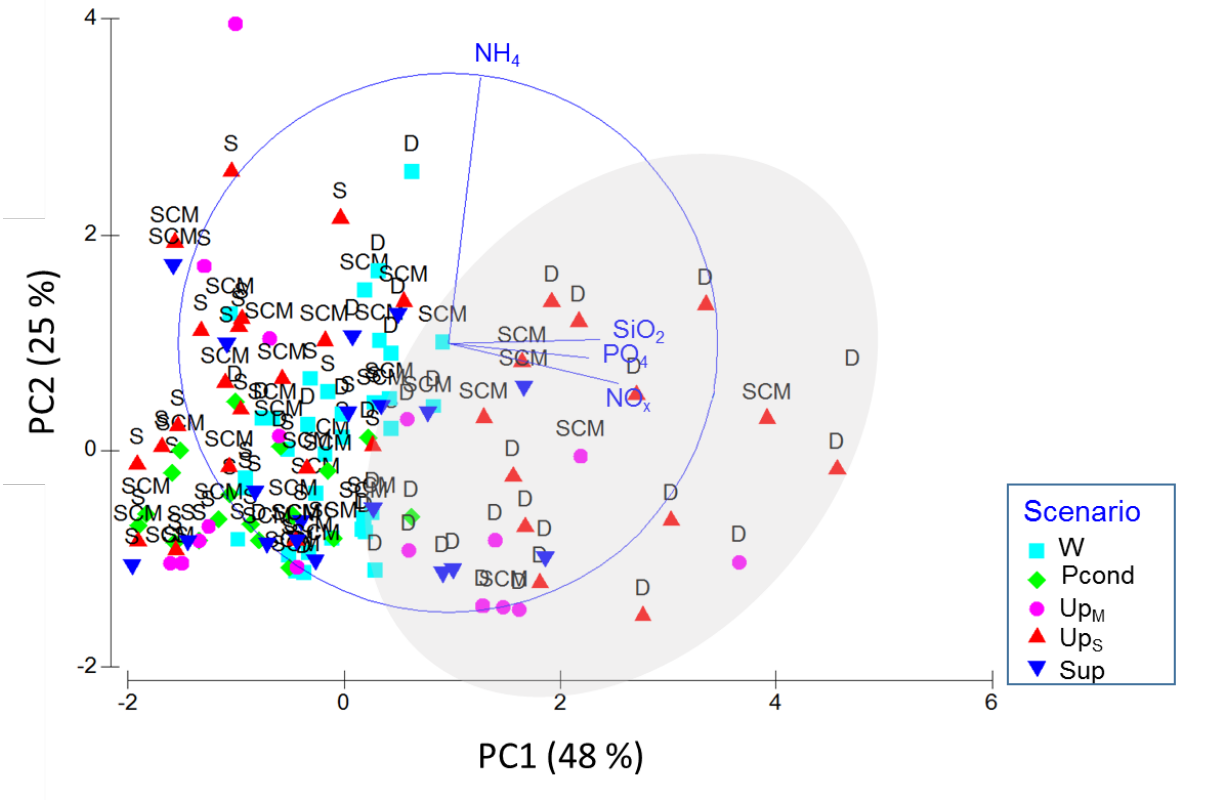

Figure 4.1-5 Principal component analysis (PCA) of dissolved nutrient concentrations [NH_4, NO_x [NO_2 + NO_3], PO_4 and SiO_2]. W = Winter-mixing, Pcond = Preconditioning, UpM = moderate upwelling, UpS = strong upwelling and Sup = Suppression. S = surface, SCM = subsurface chlorophyll maximum and D = deep water. The grey shaded area highlights the majority of deep water samples.

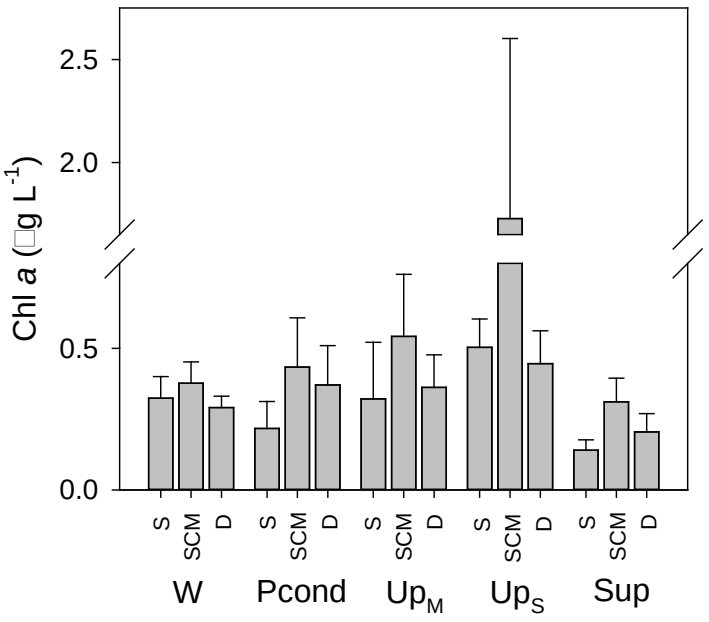

Figure 4.1-6 Figure 4.1-6 Plots of Chlorophyll a (Chl a) for surface (S), subsurface chlorophyll maxima (SCM) and deep samples (D) under different scenarios of upwelling and downwelling in the eGAB; W = Winter-mixing, Pcond = Preconditioning, UpM = moderate upwelling, UpS = strong upwelling and Sup = Suppression (see Methods for a summary). Values represent means ± SE.

Bacteria and viruses

Overall, bacterial abundances exhibited a 3-fold difference between scenarios and depths (Fig. 4.1-7A). Lowest water column averaged bacterial abundances occurred during winter-mixing ($4.18 \pm 0.26 \times 10^8$ cells L^{-1}), and highest average abundances during preconditioning ($10.2 \pm 6.52 \times 10^8$ cells L^{-1}), however statistical differences only occurred between winter-mixing compared with preconditioning and moderate upwelling. Viruses exhibited a 6.3-fold variation between scenarios (and depths), ranging between $7.74 \pm 1.20 \times 10^8$ cells L^{-1} (moderate upwelling in deep water) and $48.5 \pm 15.5 \times 10^8$ cells L^{-1} (during strong upwelling at the surface, Fig. 4.1-7B). Virus abundances during moderate upwelling were significantly lower than for all other scenarios ($P < 0.01$) and with no difference between depth ($P = 0.08$). Virus to bacteria ratios (data not shown) (VBR) were lowest during preconditioning and moderate upwelling (3.00 ± 0.18 and 3.66 ± 0.24, respectively) and highest during strong upwelling (11.3 ± 3.43).

Picophytoplankton

Highest *Prochlorococcus* abundances occurred during moderate upwelling (in the SCM) and in surface waters during suppression (both averaging ~ 43.5×10^6 cells L^{-1}) (Fig.4.1-8A). Highest average water column concentrations of *Synechococcus* and picoeukaryotes ($31.9 \pm 6.15 \times 10^6$ cells L^1, $12.2 \pm 2.83 \times 10^6$ cells L^{-1} respectively) occurred under strong upwelling (Fig. 4.1-8B – C). Shifts in the picophytoplankton community occurred under different scenarios. For example, *Synechococcus* was the dominant picophytoplankton group under all scenarios (42 – 61%) except during suppression, where *Prochlorococcus* dominated (50 ± 4.3%). Picoeukaryotes contributed overall similarly to picophytoplankton community composition for all scenarios (22 – 28%) but with the highest contribution during moderate upwelling in deep water (48 ± 8.5%). Under moderate upwelling, all three picophytoplankton groups were proportionally most similar.

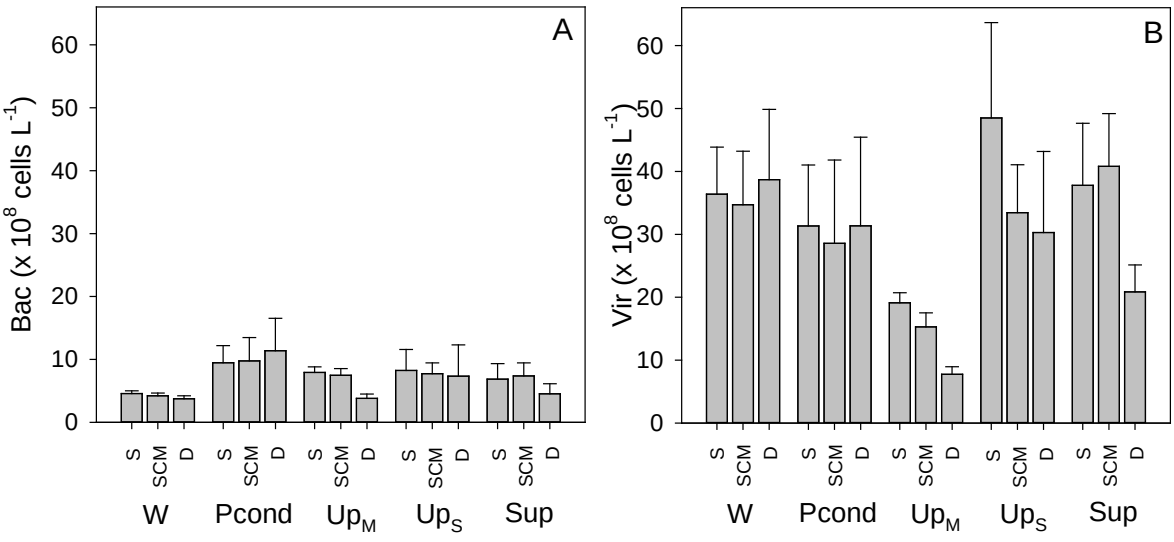

Figure 4.1-7 Bacteria (Bac) (A) and virus (Vir) abundances (x 10^8 cells L^{-1}) for surface (S), subsurface chlorophyll maxima (SCM) and deep samples (D) under different scenarios of upwelling and downwelling in the eastern GAB; W = Winter-mixing, Pcond = Preconditioning, UpM = moderate upwelling, UpS = strong upwelling and Sup = Suppression (see Methods for a summary). Values represent means ± SE.

Phytoplankton

Highest total phytoplankton abundances occurred during preconditioning (278 ± 100 × 10^3 cells L^{-1}), with similarly high numbers of diatoms and flagellates occurring at this time (Fig. 4.1-8D – E). Despite slightly lower diatom abundances occurring during strong upwelling compared to preconditioning (Fig. 4.1-8F), diatoms were the dominant group at this time (44 ± 6.9%). Lowest phytoplankton abundances occurred during moderate upwelling and suppression, with the community dominated by flagellates during moderate upwelling and by dinoflagellates during suppression. During winter-mixing, flagellates and dinoflagellates co-dominated phytoplankton counts. Of the broad phytoplankton groups, dinoflagellates showed the lowest variability in abundances between scenarios (6.4 – 43 ×10^3 cells L^{-1}) (Fig. 4.1-8E). The diatom to dinoflagellate ratio was highest during strong upwelling (averaging 6.6 ± 4.0) and lowest (<1:1) during winter-mixing and suppression. Despite the markedly higher abundance of flagellates occurring during pre-conditioning (Fig. 4.1-8D), the proportion of flagellates in the community was similar across all scenarios (32 – 45%).

The centric diatoms *Cyclotella* spp. and the pennate diatom *Cylindrotheca closterium* were present in the eastern GAB during the majority of sampling events, comprising on average, 7 – 31% and 7 – 29%, respectively, of the diatom community, and with highest average combined contributions occurring during suppression (51%) and lowest during strong upwelling (21%). In addition to *Cyclotella* spp. and *C. closterium, Nitzschia* spp. was also dominant in winter-mixing (17 ± 3.7%), *Chaetoceros* spp. and *Leptocylindricus danicus* together making up on average 33% of the community during preconditioning, *Chaetoceros* spp., *Leptocylindricus danicus* and *Dactyliosolen phukutensis* making up on average 35% of the community during moderate upwelling, and *Chaetoceros* spp., *Naviculoid* spp. and *Nitzschia* spp. dominant members (with a combined average of 28%) during suppression. During strong upwelling, *Guinardia striata* was commonly present, comprising 18 ± 9.2% of the diatom community (compared with 0.6 – 6.5% during other scenarios) and with *Nitzschia* spp. (12 ± 4.5%) and *Chaetoceros* spp. (10.6 ± 3.7%) in addition to *C. closterium*, also dominant at this time.

The dinoflagellates *Gymnodinioid* group. *Gryrodinium* spp. and *Heterocapsa rotunda* were the most abundant dinoflagellates present in the water column for the majority of sampling events, making up on average 34 – 48%, 20 – 30% and 11 – 24% of the dinoflagellate community, respectively, with no clear differences between any of the scenarios. While comprising only a small fraction of the dinoflagellate community in terms of abundance, other dinoflagellates that showed shifts relative to the different scenarios were *Katodinium glaucum and Karlodinium* spp., both of which represented 2.4 ± 1.5% and 1.8 ± 1.0% of the community during strong upwelling but 0.0 – 0.9% for other scenarios, while *Oxytoxum scolopax* represented ~3% of the community during winter-mixing and suppression but was low to absent during preconditioning. *Scrippsiella* spp. averaged 1.6% and 2.9% during moderate and strong upwelling and was low to absent during winter and suppression.

Highest abundances of flagellates occurring during preconditioning were driven by the Cryptophytes, *Hemiselmis* spp. and to a lesser extent *Pelagioselmis prolonga,* with these taxa present in relatively high abundances for most sampling events. The Prymnesiophyte, *Chrysochromulina* spp. was also present in relatively high abundances at all times but particularly during preconditioning.

At the lowest phytoplankton taxonomic level (genus/species), there appeared separation between each of the scenarios in an MDS ordination plots (Fig. 4.1-9A). PERMANOVA confirmed these results, with significant differences occurring between all scenarios (all $P < 0.05$), except preconditioning and strong upwelling ($P = 0.09$) and with no differences between depths ($P > 0.05$).

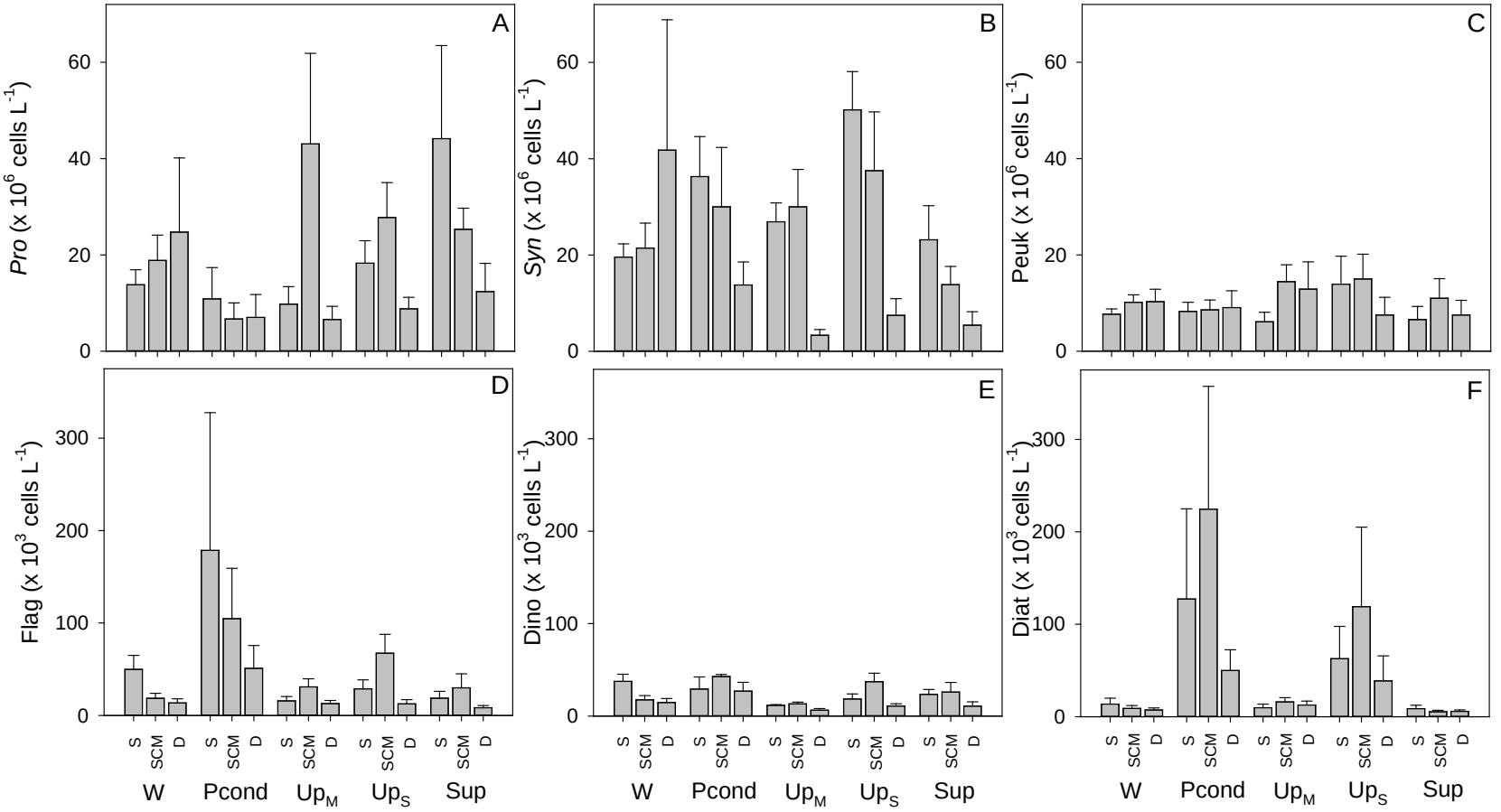

Figure 4.1-8 Picophytoplankton abundances (x 10^6 cells L^{-1}) determined via flow cytometry (A – C) and phytoplankton abundances (x 10^3 cells L^{-1}) determined via microscopy for surface (D – F) for surface (S), subsurface chlorophyll maxima (SCM) and deep samples (D) under different scenarios of upwelling and downwelling in the eastern GAB; W = Winter-mixing, Pcond = Preconditioning, UpM = moderate upwelling, UpS = strong upwelling and Sup = Suppression. Pro = Prochlorococcus, Syn = Synechococcus, Peuk = picoeukaryotes, Flag = flagellates, Dino = dinoflagellates and Diat = diatoms. Values represent means ± SE.

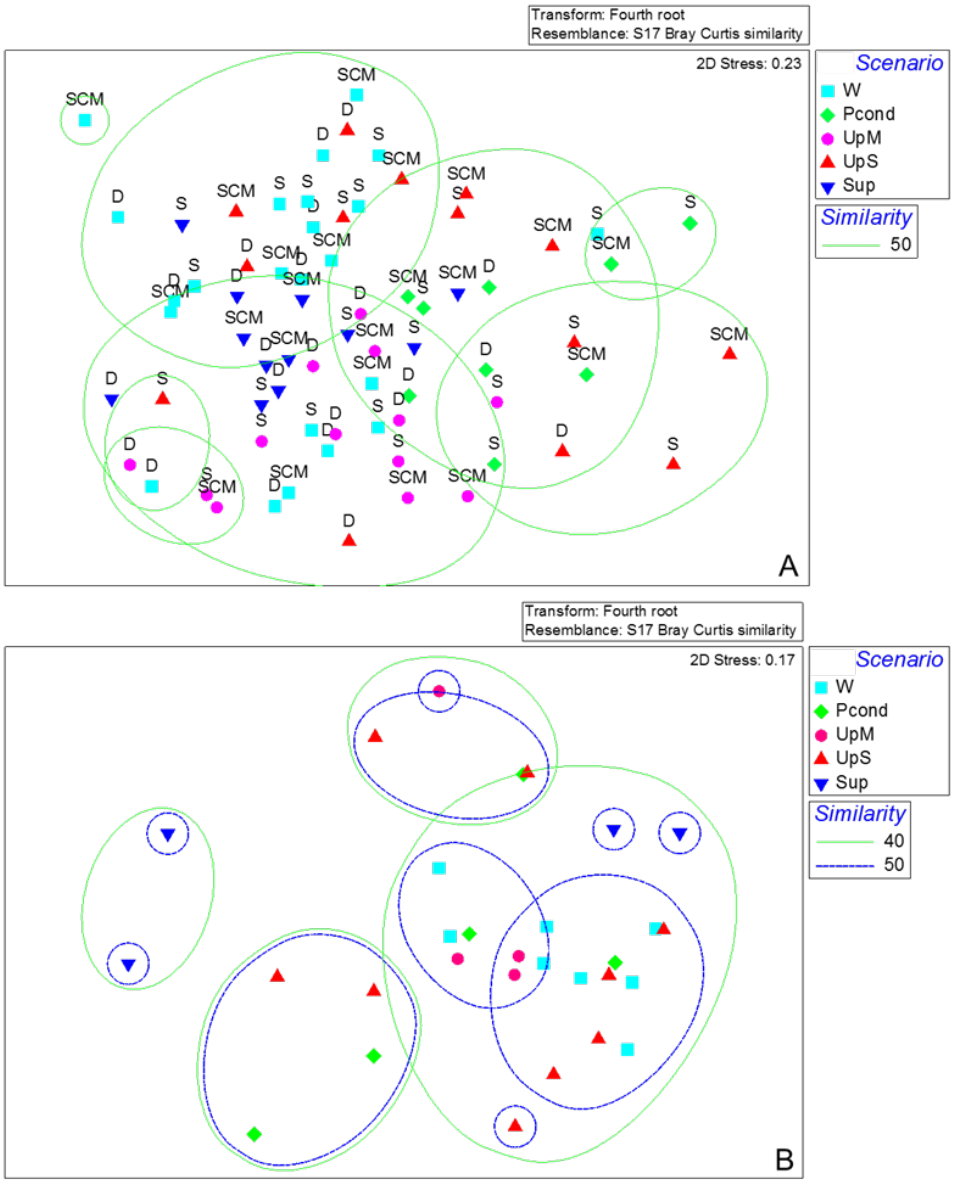

Figure 4.1-9 Multidimensional scaling (MDS) ordination coupled with a cluster analysis of (A) Phytoplankton and (B) Copepod to lowest taxonomic resolution, overlaid with cluster analysis. W = Winter-mixing, Pcond = Preconditioning, UpM = moderate upwelling, UpS = strong upwelling and Sup = Suppression.

Pigments

To compare between scenarios, nine major accessory pigments (Table 4.1-2) were normalised to Chl *a* (Fig. 4.1-10). During winter-mixing and preconditioning, 19Hex, Fuco and Chl *b* were dominant pigments, with similar ratios of between 0.10 and 0.18, averaged across the water column, occurring for each. During moderate upwelling, DV Chl *a* (0.15 $\pm$ 0.032) and Zea (0.16 $\pm$ 0.038) together with Fuco (0.20 $\pm$ 0.041) and Chl *b* (0.13 $\pm$ 0.016) were the dominant pigments. Fuco was the major accessory pigment during strong upwelling (0.24 $\pm$ 0.028) despite highest diatom abundances (microscopy counts) occurring under preconditioning. 19But, 19Hex and Chl *b* (0.16 $\pm$ 0.012, 0.15 $\pm$ 0.028, 0.12 $\pm$ 0.013, respectively) also present in relatively high concentrations during strong upwelling. During suppression, DV Chl *a* was the dominant pigment, and with 19But, 19Hex and Chl *b* the other dominant pigments. The biomarkers Peri, Allo and Pras were low to absent, but with highest concentrations for Peri and Pras occurring under strong upwelling at 40 m depth (Fig. 4.1-10G-I).

Shifts in the dominant suite of pigments between scenarios were reflected in the estimates of the proportions of picophytoplankton, nanophytoplankton and microphytoplankton (Fig. 4.1-11). Nanoplankton were proportionally dominant under winter (36 $\pm$ 1.8%) and suppression (42 $\pm$ 2.6%). The slightly lower proportions of nanophytoplankton during moderate (23 $\pm$ 2.3%) and strong upwelling (32 $\pm$ 2.5%) coincided with increases in the contribution of microphytoplankton, averaging 37 $\pm$ 6.9% and 50 $\pm$ 4.3% respectively. The contribution of picophytoplankton was similar for all scenarios (averaging 28% to 33%) except during strong upwelling when the overall contribution was lowest (17 $\pm$ 2.5%) (Fig. 4.1-11).

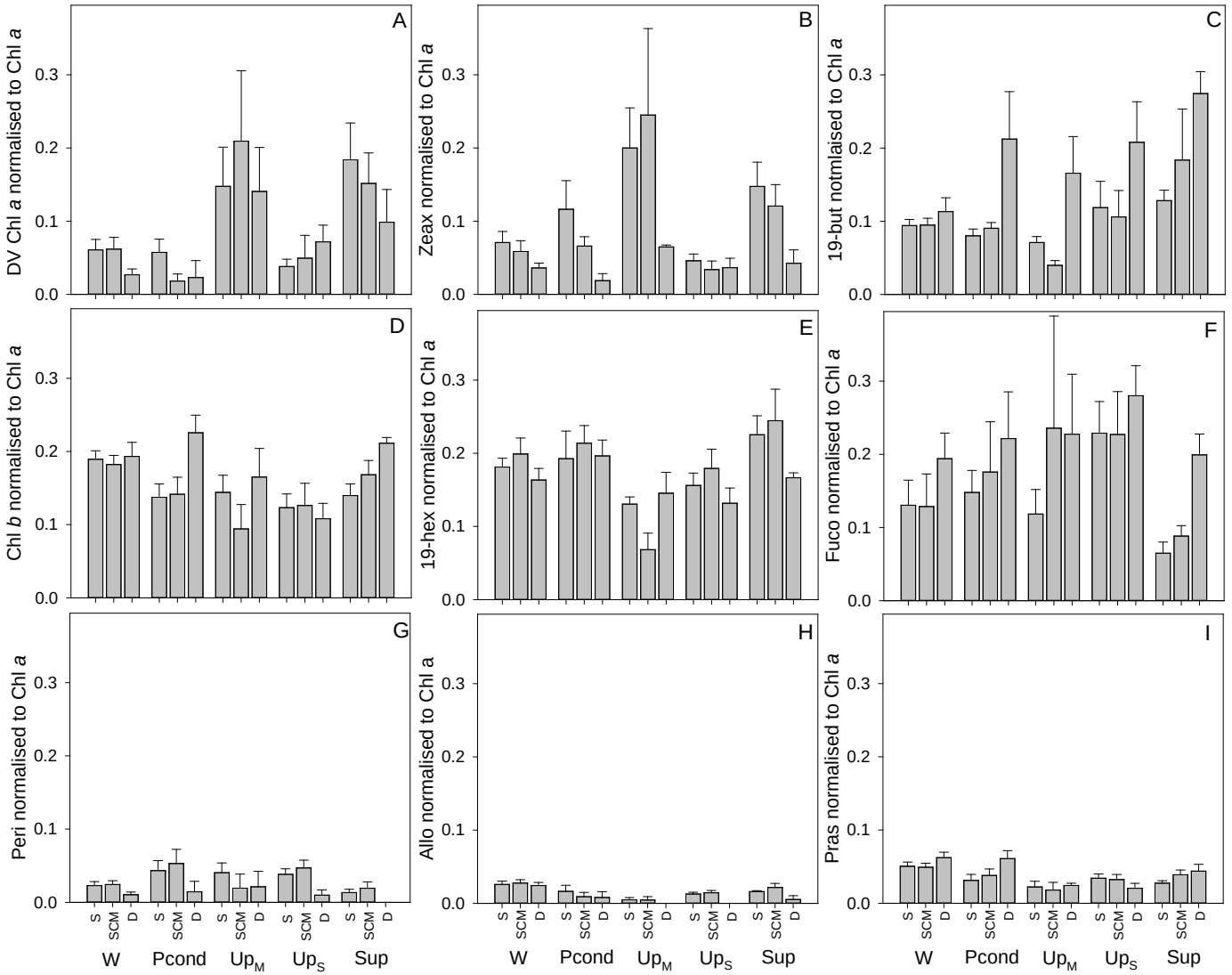

Figure 4.1-10 Pigments of dominant algal classes normalised to Chl a for surface (S), subsurface chlorophyll maxima (SCM) and deep samples (D) under different scenarios of upwelling and downwelling in the eastern GAB; W = Winter-mixing, Pcond = Preconditioning, UpM = moderate upwelling, UpS = strong upwelling and Sup = Suppression. See Table 4.1-3 for full names of pigments. Values represent means ±SE.

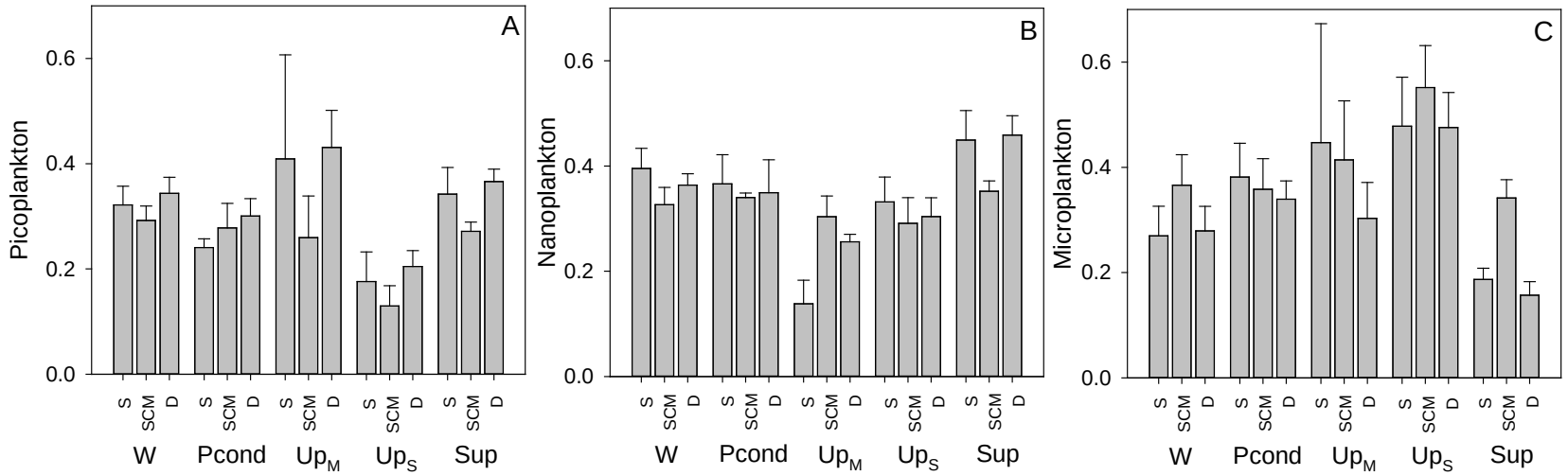

Figure 4.1-11 Proportions of three phytoplankton size classes (A) Picophytoplankton, (B) Nanophytoplankton and (C) Microphytoplankton) as estimated from pigments according to Uitz et al. (2008) for surface (S), subsurface chlorophyll maxima (SCM) and deep samples (D) under different Scenarios of upwelling and downwelling in the eastern GAB; W = Winter-mixing, Pcond = Preconditioning, UpM = moderate upwelling, UpS = strong upwelling and Sup = Suppression. Values represent means ± SE.

Zooplankton

Zooplankton biomass was similar during winter-mixing (23.3 ± 18.4 mg m^{-3}) and strong upwelling (22.2 ± 12.0 mg m^{-3}) and lowest during moderate upwelling (1.6 ± 0.7 mg m^{-3}) and suppression (1.7 ± 0.9 mg m^{-3}, Fig. 4.1-12A). Winter-mixing was, however, associated with the highest variation (% coefficient of variation = 650), driven by one sampling period, where biomass was an order of magnitude higher than for any other sampling period in that scenario (May 2014, zooplankton biomass = 151 mg m^{-3}). Median values of biomass during strong upwelling (9.7 mg m^{-3}) were 2.1 times higher than median winter-mixing biomass and 7.0 times higher than during suppression.

The pattern for zooplankton abundance differed slightly to biomass, with similarly high average zooplankton abundance occurring under winter mixing (2085 ± 690 individuals m^{-3}), preconditioning (1722 ± 948 individuals m^{-3}) and strong upwelling (2047 ± 870 individuals m^{-3}, Fig. 4.1-12B). In agreement with results for biomass, lowest zooplankton abundances occurred under suppression (280 ± 186 individuals m^{-3}) and with moderate upwelling zooplankton abundance more similar to suppression (595 ± 151 individuals m^{-3}, Fig. 4.1-12B). Copepods dominated the zooplankton community (59 – 88%), and thus followed the overall zooplankton trend. Juveniles dominated the copepod community during winter-mixing, preconditioning and strong upwelling, with nauplii the next dominant life stage. Highest proportions of adult copepods occurred during moderate upwelling and suppression (47 ± 13.4% and 53.8 ± 11.8%). During suppression, nauplii were low, comprising 5 ± 2.0% of the copepod community, compared with 13 – 23% for other scenarios.

Further examination of copepod community composition indicated that *Euterpina acutifrons*, *Oithona* spp. and *Oncaea* spp. were present in all samples, while *Microsetella novegica* and *Paracalanus indicus* were detected in the majority of sampling events. *Oithona* spp. was the dominant taxa for all scenarios except for moderate upwelling when *M. norvegica* dominated the copepod community. However, for any scenario, the most abundant copepod taxa on average were, never the same. For example, after the dominant copepod taxa, the next two to three most abundant taxa were *M. norvegica and Oncaea* spp. during *winter mixing, Oncaea* spp. and *E. acutifrons* and *M. norvegica* during preconditioning, *Oncaea* spp. and *Oithona* spp. during moderate upwelling*, M. norvegica, E. actufirons and Oncaea* spp. during strong upwelling and *M. gracilis* and *M. norvegica* during suppression. Together the three most abundant copepod taxa for each of the scenarios comprised on average, 48 – 57% of identifiable copepod community.

Other notable differences in the copepod community were the relatively high proportion of *Microsetella* spp. during preconditioning (comprising on average 10.1% of the copepod community compared to less than 1.0 to 4.0% for any other scenario). *Diothona rigida* made up on average 3.2% of the copepod community in winter-mixing but less than 0.8% for other scenarios. While commonly detected, *P. indicus* comprised at most 3.9% of the copepod community (during suppression).

The overall community structure for zooplankton taxa other than copepods also showed clear differences between scenarios (Fig. 4.1-12). For example, the predatory dinoflagellate, *Noctiluca scintilans*, which was better detected in zooplankton samples than phytoplankton, exhibited highest abundances and proportionally highest numbers during preconditioning but with a secondary abundance peak occurring during strong upwelling (Fig. 4.1-12D). Appendicularians and bivalves followed a similar trend to each other, with their abundances and proportions highest during winter-mixing and preconditioning. During moderate and strong upwelling, Thaliaceans and Cladocerans were dominant members of the zooplankton community, together with highest average abundances of larval echinoderms (Fig. 4.1-12D). Despite low overall abundances occurring during suppression, Thaliaceans and echinoderms numerically comprised more than 50% of the other zooplankton taxa.

At the lowest taxonomic resolution for copepods, separation of the copepod community was difficult to visualise in two dimensional space in MDS plots (Fig. 4.1-9B). PERMANOVA however revealed significant differences between some scenarios (P <0.001) with suppression different to both winter-mixing and strong upwelling (P <0.05).

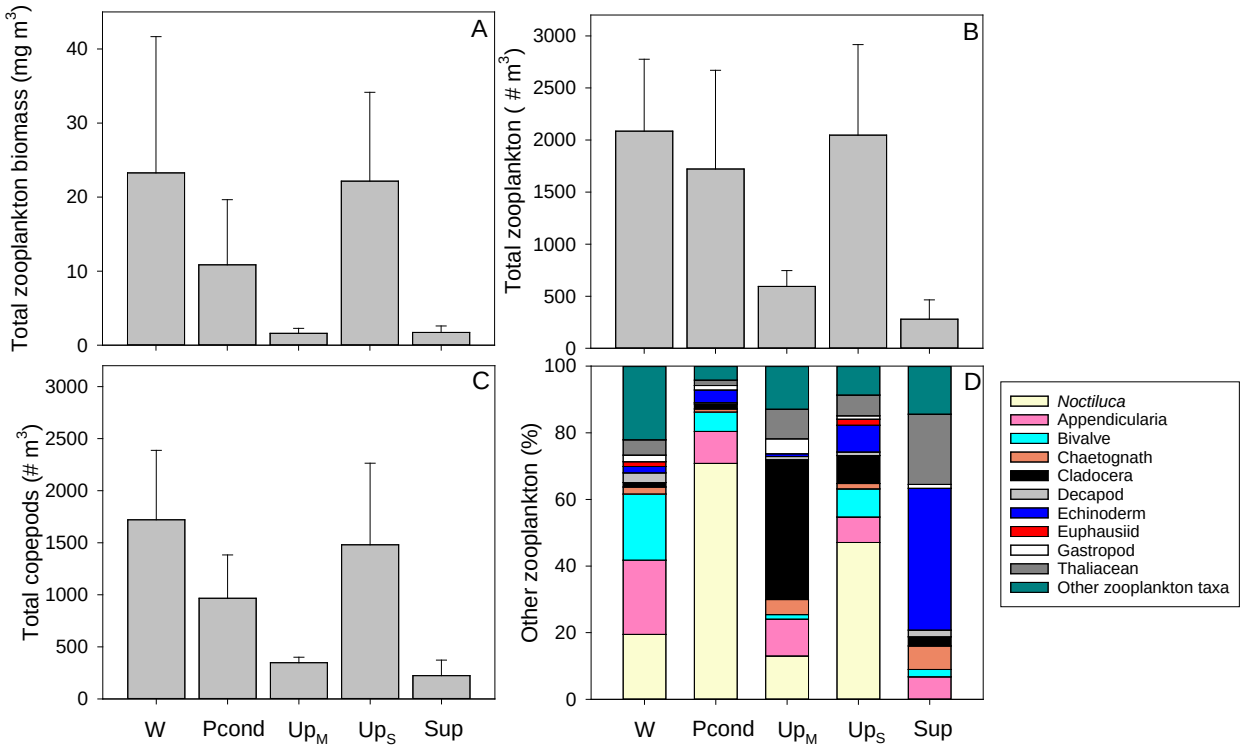

Figure 4.1-12 Zooplankton biomass (A), Total zooplankton abundance (B), Total copepod abundance (C) and the percent (%) contributions of other zooplankton taxa (copepods not included) (D) under different scenarios of upwelling and downwelling in the eGAB; W = Winter-mixing, Pcond = Preconditioning, UpM = moderate upwelling, UpS = strong upwelling and Sup = Suppression (see Methods for a summary). Values represent means ± SE.

4.1.4 Discussion

Understanding the way that shifts in community composition at the base of the food web influence higher trophic levels is inherently difficult given the different time scales of responses to nutrient enrichment (i.e. picoplankton: ~hours to days; nanoplankton: ~1 – 3 days; microplankton: ~3 – 7 days; zooplankton; days to weeks). Indeed, in most systems, plankton are typically under sampled in space and time, making clear relationships between the lower food web (viruses, bacteria, phytoplankton) and higher trophic order organisms (i.e. zooplankton, small pelagic fish) difficult to unravel. Here we utilised an ~8 year time series to characterize, for the first time, the community composition of the lower food web (viruses, bacteria, phytoplankton through to mesozooplankton) in the eastern GAB. We assigned each sampling event to one of five scenarios related to the known hydrographic conditions occurring in the eastern GAB, to capture the responses of organisms at the base of the food web over a spectrum of sizes and trophic modes (see chapter 3.1). The timing of sampling events reflected various time scales within each of the scenarios (e.g. during the strong upwelling scenario - hours to days after upwelling), likely contributing to the high degree of

variability within scenarios. Below we document the oceanographic conditions and subsequent plankton community composition and size structure which characterised each of the scenarios in the eastern GAB.

Oceanographic conditions and timing of upwelling and overall trends

Moderate and strong upwelling were on the majority of occasions confined to the later part of the upwelling season (January to March predominantly). During moderate and strong upwelling scenarios, the water column was well stratified, with nitrate limitation occurring in surface waters and peaks in phytoplankton biomass below the surface mixed layer. Subsurface peaks in Chl *a* biomass have been reported previously for the eastern (Kämpf et al. 2004, van Ruth et al. 2010a, b, van Dongen-Vogels et al. 2011, 2012, Paterson et al. 2013) and central GAB (SARDI unpublished, Kloser et al. 2017). The presence of enhanced phytoplankton biomass below the surface mixed layer (as a 'deep chlorophyll maxima'; here as the 'SCM') is typical of oligotrophic waters of the subtropical gyre systems (Cullen 1982), the Mediterranean (Siokou-Frangou et al. 2010), and waters off Australia's east (Hallegraeff and Jeffrey 1993) and west coasts (Hanson et al. 2007). This sub-surface phytoplankton biomass accumulates in spring and summer due to photoacclimation processes together with erosion of the nutricline (Mignot et al. 2014). The fact that a large proportion of phytoplankton biomass in the GAB occurs below surface waters that are sampled via satellites suggests that modelled values of primary productivity using remote sensed surface Chl *a* may be under estimates (van Ruth et al. 2010a, b), and that the timing of surface phytoplankton blooms described by Cetina-Heredia et al. (2016) do not reflect the timing of significantly enhanced (compared to surface) phytoplankton biomass that accumulates below the surface in response to nutrient enrichment via upwelling.

At times of moderate and strong upwelling, highest average NO_x (5.4 µM) and SiO_2 (1.9 µM) occurring in deep water were of an order of magnitude lower than the nutrient rich water of other upwelling regions (e.g. Benguela upwelling system, Californian Current System and Humboldt Current System), but were similarly scaled to the Canary Current System (Mann and Lazier 2006) and to those upwelling centers off the east and west coasts of Australia (Hallegraeff and Reid 1986, Hanson et al. 2005). Concentrations of SiO_2 in surface waters (and the lower water column) averaged close to 1 µM during winter-mixing, without clear elevation of NO_x, suggesting an additional SiO_2 source(s) in the eastern GAB, not linked to upwelled water (e.g. groundwater intrusions and or benthic resuspension). A similar finding was also shown in the central GAB, with enhanced SiO_2 relative to NO_x occurring between the shelf and the upper slope (Kloser et al. 2017).Van Ruth et al. (2010a) reported SiO_2 concentration as high as 29.4 µM in near-coastal surface waters in the GAB, further west of station NRSKAI. These concentrations far exceed those measured in upwelled water, further supporting the hypothesis of an external source of SiO_2. NH_4 concentrations were variable but highest overall during strong upwelling, suggestive of active remineralisation processes in response to nitrate enrichment.

Winter-mixing

During winter-mixing, Chl *a* averaged 0.33 µg L^{-1}, with nanoplankton dominating the autotrophic biomass, followed by picoplankton and then microphytoplankton. Of the phytoplankton >5 µm, when broadly categorised, dinoflagellates and flagellates dominated and diatom numbers were low. The pigment aligned to autotrophic dinoflagellates, Peridinin (Peri) was however low (Peri: Chl *a* ~0.02) indicating a large fraction of dinoflagellates present either contained endosymbionts of other algal classes (Jeffrey 1997) and or, that the dinoflagellates were dominated by mixotrophic and or heterotrophic species (Stoecker 1999). A similar finding was also shown in the central GAB, with enhanced SiO_2 relative to NO_x occurring between the shelf and the upper slope (Kloser et al. 2017). Heterotrophy is common in dinoflagellates with the dominant taxa occurring here (Gymnodinioid group, *Gryrodinium* spp. and *Heterocapsa rotunda*) known to a feed on a diverse range of plankton

from bacteria, through to diatoms as well as on other dinoflagellates (reviewed in (Jeong et al. 2010). Thompson et al. (2015) also highlighted the abundant dinoflagellate community in eastern GAB shelf waters compared to other national reference stations around Australia, noting the presence of large dinoflagellates (by biovolume; in the genus *Noctiluca*, *Ceratium*, *Gryodinium* and *Protoperdinium*) in the region.

Accessory pigments Chl *b* and 19Hex were dominant during winter-mixing, indicating Chlorophytes and Prasinophytes (from Chl *b*), and Prymesiophytes (from 19Hex) were dominant phytoplankton groups. In the microalgal counts, Chlorophytes were low to absent, while Prasinophytes and Prymnesiophytes made similar contributions to total counts (~10% each). The mismatch between Chlorophyte counts and their indicator pigment (Chl *b*) point to the presence of small (i.e. <5 µm) Prasinophytes in the GAB, which were likely missed with microscopy and which may, or may not fall within the flow cytometrically detected picoeukarotes. Prasinophytes within the pico-size range (<3 µm; e.g. *Ostreococcus* spp., *Bathycoccus* spp. and *Micromonas* spp.) are ubiquitous components within the picoplankton in other coastal and ocean regions (Not et al. 2004, Not et al. 2008). In shelf to offshore waters of the eastern and central GAB, Chl *b* comprised approximately 10 – 20% of Chl *a* less than 5 µm in size (Kloser et al. 2017) indicating pico- and or small nano-sized Prasinophytes and or Chlorophytes may represent a significant and ubiquitous community in eastern GAB waters. Chryptophytes dominated the flagellate community from microalgal counts, yet their representative pigment, Alloxanthin was low (Allo:Chl *a* ~0.03). Reasons for the mismatch are unclear, but in other systems, the reverse is commonly found (Wright et al. 1996).

The picophytoplankton community was dominated by *Synechococcus*, followed by *Prochlorococcus*, with the lowest numerical contribution from picoeukaryotes. *Synechococcus* have a wide global distribution from tropical to polar seas and low to high nutrient waters. Abundances of *Synechococcus* occurring during winter-mixing (and overall for all scenarios) reflected those predicted by Flombaum et al. (2013) in their global model. While close to the limits of its distribution (Partensky et al. 1999a), *Prochlorococcus* is commonly detected at relatively high abundances in GAB waters year round, including winter, but can also be low to absent during this time (van Dongen-Vogels et al. 2011). van Dongen-Vogels et al. (2011) pondered the origins of *Prochlorococcus* populations in the GAB, questioning whether they were resident populations, or originated in tropical waters on the east and west coasts of Australia, possibly transported to the GAB via dominant ocean currents. While these questions are difficult to resolve, we suggest that the overall consistent abundances of *Prochlorococcus* across all scenarios might indicate the former.

The occurrence of lowest bacterial abundances during winter-mixing may result from lower substrate availability for growth, reduced metabolism from lower water temperatures (Pomeroy and Wiebe 2001), or high grazing pressure (Vargas et al. 2007). The low variation noted here in bacterial abundances between scenarios and depths (maximum ~3-fold) is similar to that occurring spatially in the GAB (Kloser et al. 2017) and for other coastal regions worldwide (~2-fold) over various spatial and temporal scales (Calvo-Díaz and Morán 2006, Linacre et al. 2010). Virus abundances did not follow those of bacteria, with higher variation occurring between scenarios and depths (varying up to 6-fold between scenarios) and with virus abundances during winter-mixing similarly scaled to those for all other scenarios, except moderate upwelling. Bacteria are generally considered the major host of viruses in marine systems (Fuhrman 1999). The disparity between viruses and bacteria might reflect different phases of infection and subsequent release from host cells, or different infection strategies under different scenarios (lysogenic vs lytic infections, (Weinbauer and Suttle 1996, Knowles et al. 2016). In addition to bacteria, other planktonic groups including picophytoplankton and nanoplankton are infected by viruses in marine systems (Brussaard et al. 1999, Baudoux et al. 2008) and may represent suitable hosts in GAB waters.

Zooplankton biomass and abundances were on average, high during winter, and comparable to those during preconditioning and strong upwelling, but driven predominantly, by high abundances for one sampling event (May 2014). The occurrence of low bottom water temperatures in the later part of the upwelling season in 2014 (Fig. 4.1-3) may have been a key driver for enhanced primary production and subsequently, this occurrence of high zooplankton biomass in May. *Oithona* spp. dominated the copepod community (and for all scenarios), with *M. novegica* and *Oncaea* spp. the next two dominant taxa. These taxa show different feeding strategies and preferences for prey in other systems. For example, *Oithona* spp. feed preferentially on heterotrophic protists rather than phytoplankton, while *Oncaea* spp. are associated and feed upon marine snow attached particles (Turner 2004). *M. novegica*, a smaller copepod species (<0.5 mm) that is widely distributed in tropical and temperate waters, is also often associated with marine snow aggregates (Alldredge 1972), though nano-sized phytoplankton also represent their major food source (Uye et al. 2002). The occurrence of highest numbers of appendicularia and bivalves in winter also reflects the dominant plankton community size available as a food source, given larvae of these taxa can efficiently feed on pico- and nano-sized organisms (Gallager et al. 1994, Gorsky et al. 1999).

Preconditioning

The highest abundances of flagellates and diatoms occurred during preconditioning, with similar contributions to overall Chl *a* biomass by microphytoplankton and nanophytoplakton. We propose that the elevated abundances of diatoms and flagellates that occur during preconditioning are somewhat analogous to the spring blooms observed in other temperate regions, including the east coast of Australia (Hallegraeff and Reid 1986, Hallegraeff and Jeffrey 1993), though on a much smaller scale, and likely highly ephemeral in nature. Spring diatom blooms develop in temperate regions in the transition period between winter and spring (Hallegraeff and Reid 1986, Hallegraeff and Jeffrey 1993), in response to increased irradiance and at the onset of temperature stratification (Sverdrup 1953). They are associated with high Chl *a* biomass concomitant with diatom dominance, and with the succession of nanoflagellates following the peak bloom (Lochte et al. 1993, Sieracki et al. 1993). While in this study, Chl *a* was slightly higher than during winter-mixing (and suppression), Chl *a* did not match those relatively higher concentrations during strong upwelling, nor were they on the order of Chl *a* values seen in surface waters of other temperate systems during the spring blooms (i.e. > 2 µg L^{-1} off eastern Australia (Hallegraeff and Reid 1986, Hallegraeff and Jeffrey 1993), or the North Atlantic (Sieracki et al. 1993, Daniels et al. 2015)). The dominant diatom during preconditioning, was the pennate diatom *C. closterium*, and the centric diatoms *Chaetoceros* spp. and *L. danicus.* While cell measurement were not undertaken, these diatom taxa are all representative of relatively smaller diatom species; and may even fall within the nanoplankton size range (2 – 20 µm, Hallegraeff et al. 2010). For example, *C. closterium* is typically a smaller (often nano-) sized pennate diatom, exploiting a half benthic, half planktonic existence (Round 1981). It is plausible that C*. closetrium* were seeded from the preceding winter mixing (where they represented a dominant component of the diatom community). Due to their large surface area to volume ratios, these diatoms could then utilize the modest levels of SiO_2 (~1 µM) and NO_x present following winter-mixing, together with increased irradiances and reduced mixing. Smaller diatoms (i.e <10 µM) have been shown to dominate the early stages of a spring bloom in the North Atlantic, with the seed population either sustained in the upper water column over winter, or arising from benthic resting stages that are mixed into the water column in spring (Daniels et al. 2015). The high numbers of flagellates may represent the succession observed following the demise of spring blooms elsewhere (Lochte et al. 1993, Sieracki et al. 1993), or may represent the planktonic community during the preconditioning period when nutrient availability is overall lower for a particular sampling event. Pigment data supported the high observed abundances of Prymnesiophytes, with the dominance of the pigment 19Hex (19Hex:Chl *a* ~0.20), however, as found for the winter-mixing, Cryptophyte abundances were not reflected in high concentrations of their biomarker pigment Allo (i.e. Allo:Chl *a* ~0.01).

Synechococcus was the dominant picophytoplankton group, with abundances similar to those found in the winter scenario. However, picophytoplankton community composition during preconditioning differed to that observed during winter, with picoeukaryotes comprising a greater numerical fraction of the picophytoplankton community than *Prochlorococcus*. In other systems, *Synechococcus* has been shown to peak just prior to diatom blooms (Larsen et al. 2004, Tai and Palenik 2009). The shift to a *Synechococcus* and picoeukaryote dominated picophytoplankton community can result in more efficient trophic transfer, since these groups have more carbon per cell than *Prochlorococcus.* High grazing rates on *Synechococcus* and picoeukaryotes (but also *Prochlorococcus*) by nano- and micro-plankton have been shown in other coastal systems (Worden and Binder 2003, Christaki et al. 2005, Linacre et al. 2010) as well as in the GAB (van Ruth et al., Project 2.2, Chapter 4.2). Bacterial abundances were highest during preconditioning, possibly in response to the diatom and flagellate bloom at this time. While viral abundances were similar to those occurring during the winter-mixing scenario, viruses have been shown to be important agents in the demise of flagellates following a spring bloom (Larsen et al. 2004). The Prymnesiophyte *Chrysochromulina* spp., which dominates during this scenario, is also known to be subject to viral infection (Suttle and Chan 1995).

Dominant dinoflagellate taxa during preconditioning (*Gymnodinioid* group, *Gryrodinium* spp. and *H. rotunda*) were the same as those for winter-mixing. The high abundances of the predatory dinoflagellate *N. scintilans* observed during preconditioning matches the known biology and distributions of the species on the east coast of Australia (spring/late summer blooms; Murray and Suthers 1999, Dela-Cruz et al. 2002), with high abundances often coinciding with enhanced phytoplankton abundances (Dela-Cruz et al. 2008). *N. scintilins* feed on a variety of prey from bacteria and phytoplankton through to micro- and mesozooplankton (Kirchner et al. 1996, Quevedo et al. 1999, Fonda Umani et al. 2004). Recently, high growth rates of *N. scintilins* were shown on a mixed diet of diatoms and chlorophytes (Zhang et al. 2016). It is possible then that the high diatom and flagellate abundances occurring during preconditioning in the GAB fuel significant growth of *Noctiluca* at this time.

The overall high zooplankton abundances (dominated as for all scenarios by copepods), coupled with moderate average zooplankton biomass (relative to winter-mixing and strong upwelling and enhanced phytoplankton abundances), suggests efficient trophic transfer from the autotrophic to the heterotrophic community. This may result from direct feeding of copepods on diatoms (Cushing 1989), or grazing of diatoms and nanoflagellates by dinoflagellates or other nanoflagellates (Calbet and Landry 2004, Calbet 2008, Worden et al. 2015).

Moderate upwelling

During moderate upwelling, picophytoplankton and microphytoplankton dominated phytoplankton biomass, with proportionally similar abundances of flagellates and diatoms exceeding dinoflagellates. *L. danicus*, one of the dominant diatom species found during this scenario, are known to bloom in response to upwelling on the east coast of Australia (Hallegraeff and Reid 1986, Armbrecht et al. 2014, 2015). Fuco concentrations were similar to those measured during preconditioning, when diatom counts were highest. While considered a biomarker for diatoms, Fuco is also present in other algal classes (e.g. Prymesiophytes, raphidophytes, some dinoflagellates; Jeffrey 1997) and caution should be taken when interpreting pigment signatures which overlap different algal classes.

Following winter-mixing and preconditioning, *Synechococcus* continued to numerically dominate the picophytoplankton (reaching ~35 $\times$ 10^6 cells L^{-1} at the surface and SCM), with highest Zea concentration and relative proportion (to Chl *a*, ~0.20) also occurring at the surface and SCM. The concurrence of relatively high abundances of diatoms with *Synechococcus,* associated with increased

nutrient availability and sufficient irradiances, have also been reported for the Arabian Sea (Tarran et al. 1999, Ahmed et al. 2016). The contribution of *Prochlorococcus*, particularly at the SCM and in deep water, significantly increased (~2 fold) from the preconditioning scenario. Differences in the distributions of *Synechococcus* (i.e. shallower) and *Prochlorococcus* (i.e. deeper) within the water column which have been observed here, have been previously documented in oceanic waters (Partensky et al. 1999). While elevated abundances of *Prochlorococcus* under upwelling conditions have been shown to occur in the GAB (van Dongen-Vogels et al. 2011, Paterson et al. 2013), and in open ocean upwelling systems (Taylor et al. 2011), this is inconsistent with the conventional thinking of the global distributions of *Prochlorococcus*, where highest abundances should occur under nutrient deplete conditions at low latitudes (Partensky et al. 1999). It has recently been recognised, however, that links between water column nutrient status and *Prochlorococcus* are likely more complex than previously thought (Flombaum et al. 2013). The relatively low to high abundances occurring from preconditioning to moderate upwelling may further indicate ecotype replacement of *Prochlorococcus* under different hydrographic regimes (Martiny et al. 2009, Scanlan et al. 2009).

Despite overall lower flagellate abundances during moderate upwelling, compared with preconditioning, flagellate abundances exceeded dinoflagellate abundances. A similar broad scale community occurs during upwelling in the Benguela upwelling system, with diatoms exceeding flagellates and with flagellates then exceeding dinoflagellates (Lamont et al. 2014). Despite lowest dinoflagellate abundances occurring at this time, the Gymnodinoid group remained the dominant dinoflagellate (as for all scenarios), with *H. rotunda* then followed by *Gyrodinium* spp. as the next two dominant groups. As observed during winter-mixing and preconditioning, the pigment Peri (indicative of autotrophic dinoflagellates) was low, indicating again the possible importance of heterotrophy in the GAB (also see Kloser et al. 2017). Bacterial abundances were comparable to the high abundances occurring during preconditioning, but lowest virus abundances occurred at this time. Reduced viral activity due to enrichment from upwelled water, and/or, the switch from lytic to lysogenic infections, may explain these low virus abundances. Alternatively, the coincidence of low viral abundances with low nanoflagellates abundances might indicate nanoflagellates are significant hosts for viruses during moderate upwelling.

Zooplankton biomass and abundance were low at this time, and similar to that during suppression. The copepod community composition was however more similar to that in winter, with the top three dominant taxa being *M. norvegica*, *Oncaea* spp. and *Oithona* spp. One way to explain these low abundances may be due to significant grazing on copepods or their eggs. For example, the high abundance of *N. scintilins* during preconditioning may have exerted significant grazing pressure on the copepod community, and their eggs, at that time, as shown in other systems (Quevedo et al. 1999), essentially clearing the water column of this cohort. The time lag then for uptake of 'new' upwelled nutrients by phytoplankton (during moderate upwelling), and the subsequent time lag of copepod reproduction and growth, may have been captured through the comparison of preconditioning versus moderate upwelling scenarios.

Cladocerans and Thaliaceans were the only two groups to exhibit near highest abundances during moderate upwelling. Cladocerans have short generation times (days) compared to copepods (weeks), with reproduction occurring via pathogenesis under favorable conditions (Egloff et al. 1997). Highest abundances are commonly noted in spring and summer in other systems, when sea surface temperatures have increased, promoting stratification of the water column (Egloff et al. 1997), and abundance peaks are closely coupled to peaks in phytoplankton biomass (Bode and Alvarez-Ossorio 2004, Atienza et al. 2008). Cladocerans feed on a range of prey, but preferentially feed on plankton in the greater than 2.5 µm and less than ~100 µM size range (Katechakis and Stibor 2004). Thaliaceans also exhibit high population growth under favourable conditions, feeding on small colloids through to large phytoplankton, but are very efficient filter feeders of picoplankton

(Sommer & Stibor 2002). Thaliaceans may thus represent a shortened pathway between picoplankton and higher metazoans (Sommer and Stibor 2002).

Strong upwelling

Microplankton dominated the phytoplankton biomass during strong upwelling, but abundances were lower than during preconditioning, particularly at the surface and SCM. Assuming diatoms (and not dinoflagellates – discussed below) were the major group contributing to the higher Chl *a* biomass during strong upwelling, then either those diatoms present were of relatively larger size, or they had more Chl *a* per cell than those communities associated with the preconditioning scenario. *G. striata* was a dominant diatom during strong upwelling, with low concentrations observed during other scenarios. While not a typical blooming species (compared with *L. danicus* for example, (Carstensen et al. 2015), *G. striata* is a larger (>200 µm wide), weakly silicified diatom (Hallegraeff et al. 2010) which has been observed to be abundant during upwelling conditions in other regions (Gómez et al. 2007, Siokou-Frangou et al. 2010, Loick-Wilde et al. 2017). On the east coast of Australia, however, this species has been associated with downwelling conditions (Armbrecht et al. 2014). Diatoms are rapidly able to take up and store nitrate (Lomas and Glibert 2000) and have been shown to dominate the phytoplankton community when silicate concentrations are greater than 2 µM (Egge and Aksnes 1992). Average concentrations of SiO_2 exceeding 2 µM were observed in deep water during strong upwelling, with SiO_2 concentrations approximately half of that at the SCM at the same time. In addition to silicate, iron can be a limiting factor for diatom growth, even in coastal upwelling systems (Hutchins and Bruland 1998). It is not known whether iron limits diatom growth in the GAB.

The autotrophic dinoflagellate pigment Peri, while relatively low overall, was highest during strong upwelling (Peri: Chl *a* up to 0.05 in the SCM), suggesting a small contribution by autotropic dinoflagellates to microplankton biomass (i.e. Fuco:Chl *a* ratio of ~0.24). This was matched by highest average dinoflagellate counts in the SCM during strong upwelling. The same dominant dinoflagellate taxa (Gymnodinoid group, *Gyrodinium* spp. and *H. rotunda*) occurred at this time. A second peak in *N. scintilins* was also observed at this time, matching distributional trends on the east coast of Australia (Murray and Suthers 1999, Dela-Cruz et al. 2002). Significant grazing rates (i.e. averaging 60% of primary production) by the microzooplankton (<200 µm) community are well known for both low and high productivity systems (Calbet and Landry 2004), resulting in loss of primary production though respiration, but also trophic transfer via metazoan consumption on the microzooplankton community (Calbet 2008). However, this view does not match traditional thinking, whereby diatoms are directly consumed by mesozooplankton (Ryther 1969, Cushing 1989). The relatively high numbers of dinoflagellates occurring in the GAB, and the likelihood that a large fraction of these are mixotrophic and or heterotrophic, suggests a significant trophic pathway occurs through dinoflagellates in GAB waters.

Zooplankton abundances that were similarly high during strong upwelling and preconditioning were not matched by similar zooplankton biomass between scenarios. The higher biomass during strong upwelling compared to preconditioning suggests overall larger zooplankton during upwelling compared to preconditioning. Coincident with highest zooplankton biomass were highest Chl *a* concentrations, highest proportions of microphytoplankton and highest dinoflagellate counts for any scenario. These results point to efficient trophic transfer from the autotropic community to higher trophic levels in the GAB during strong upwelling conditions. These results also support previous findings which show high numbers of zooplankton (van Ruth and Ward 2009) and abundant sardine and anchovy eggs and larvae (Ward et al. 2006), with high Chl *a* during the late upwelling season. While their prey items are not well known in the GAB region, in other regions (e.g Adriatic Sea, Mediterranean Sea, Benguela and Humboldt current systems) copepod nauplii and copepodites represent major prey items for anchovy and sardine larvae (Tudela and Palomera 1995), while

sardine adults and larvae also feed directly on phytoplankton, and in particular dinoflagellates (Van Der Lingen 2002, Espinoza et al. 2009). The role of dinoflagellates as primary consumers, should not be overlooked in the GAB, given their important role in other regions. In the Southern Californian Bight for example, Anchovy larvae were stimulated to feed when the abundances of the dominant dinoflagellate (*Gymnodinium splendens*) reached densities of $\sim 20 - 30 \times 10^3$ cells L^{-1} (Lasker 1975). In that study, anchovy larvae did not feed when diatoms were the dominant phytoplankton. Densities of *Gymnodinium splendens* in the Southern Californian Bight are well matched to those encountered in the GAB from the *Gymnodinoid* group alone, and it is therefore plausible that the abundant dinoflagellate community may be a direct food source for anchovies and/or sardines in the region, especially during strong upwelling.

High abundances of all picophytoplankton groups occurred during strong upwelling, with the numerical contribution of each picophytoplankton group matching most closely in the SCM at this time. While abundances themselves were not highest, the numerical contribution of flagellates, dinoflagellates and diatoms to total abundances also matched most closely at this time. These results support recent studies which found that all plankton groups respond positively to enrichment, resulting in an 'add on' effect rather than the replacement of small to large cells (Barber and Hiscock 2006, Linacre et al. 2010, Romagnan et al. 2015). However, the overall contributions of the larger cells to total biomass are greater at this time.

Bacterial and viral abundances were also high during strong upwelling, indicating the presence of a functioning microbial food web under enriched conditions. At this time, bacteria likely utilise a combination of released photosynthates from phytoplankton (Morán et al. 2002), released dissolved organic matter from protozoans and metazoans (sloppy feeding, leakage from fecal pellets, excretion, Nagata 2000), and direct metabolism of nitrate and phosphate from upwelled waters (Gregoracci et al. 2015). Grazing of bacteria by nanoflagellates would serve as an intermediate step for possible trophic transfer to higher organisms but some energy loss would also occur via respiration (Calbet and Landry 2004, Calbet 2008). In other upwelling systems, more than 80 % of bacterial production can be removed via grazing (Vargas et al. 2007, Linacre et al. 2010). Viral lysis would also influence the dissolve organic matter pools through transfer of bacterial biomass back into dissolved and colloidal forms for subsequent uptake within the microbial food web (Wilhelm & Suttle 1999). Viral lysis would also influence the dissolve organic matter pools through transfer of bacterial biomass back into dissolved and colloidal forms for subsequent uptake within the microbial food web (Wilhelm and Suttle 1999). Viruses play additional roles in planktonic food webs, for example, by positively enhancing *Synechococcus* growth rates (Weinbauer et al. 2011) and influencing large scale ecosystem functioning (Weitz et al. 2015). The roles of viral lysis and grazing in lower trophic ecosystem dynamics in the GAB should be a focus of future work.

Suppression

During suppression, there was significant partitioning of the water column in terms of plankton community composition. For example, surface waters showed lowest Chl *a* and dominated by picophytoplankton (e.g. *Prochlorococcus*); nanoplankton and picoplankton were found in similar abundances in the SCM, while in deep water, nanoplankton and microphytoplankton exceeded picophytoplankton. These results suggest there are important niches for the plankton community within the water column, with a dominant microbial food web occurring in surface waters, and a multivorous food web in the lower water column. Some seeding of nutrients and planktonic communities may occur from deeper water during this time, with mixing of the water column following an upwelling event (van Ruth et al. 2010a, b, van Ruth et al. Chapter 3.1). With the proposed microbial and multivorous food webs dominating in different parts of the water column during suppression, it is then likely that there would be lower transfer of biomass to higher trophic levels compared with strong upwelling under a more 'classical food web'. Zooplankton biomass and

abundances were indeed lowest at this time, with the proportion of copepod nauplii lower than for any other scenario. Alternatively, high levels of grazing directly on the mesozooplakton community from higher trophic orders (i.e. larval fish) may have suppressed zooplankton biomass and abundances. We have no measure of biomass of higher trophic levels coinciding with timing and location of sampling from this data set. However, with the occurrence of generally high numbers of sardine and anchovy adults and larvae during late summer in the GAB (Ward et al. 2006), and given their important mid-trophic level position in upwelling systems (Cury et al. 2000), there could exist strong grazing pressure on both the phytoplankton and zooplankton by sardine and anchovy adults and larvae.

Food web structure and trophic transfer in the eastern GAB

Over a back drop of highly variable hydrographic conditions, nanoplankton represent a relatively stable component of lower planktonic food web in eastern GAB waters. This feature has been reported in other upwelling (Böttjer and Morales 2007) and ocean systems (Li 2002). The importance of picoplankton in the eastern GAB should also not be neglected. *Synechococcus* and *Prochlorococcus* show high and variable abundances across very different hydrographic regimes. In contrast, picoeukaryotes and bacteria and viruses show less variation, exhibiting more of a stable backdrop, in line with nanoplankton. Together these results support a growing body of evidence that the microbial food web is a persistent feature of the GAB, and that rather than these small cells being replaced when nutrient rich water enters the system, that growth and biomass buildup of larger phytoplankton occur over the top of the existing microbial food web. These results are consistent with this pattern in other regions of the global ocean (Barber and Hiscock 2006, Linacre et al. 2010, Romagnan et al. 2015).

The typically portrayed, classic trophic pathway from diatoms to mesozooplankton (Ryther 1969, Cushing 1989) is likely to occur in the eastern GAB when nutrient rich waters enter the euphotic zone (i.e. during strong upwelling), but not in isolation of a diatom to dinoflagellate to mesozooplankton pathway. This latter pathway might represent a more typical trophic pathway in GAB waters except under those (relatively) 'extreme' upwelling conditions. During preconditioning, the mechanism for higher numbers of phytoplankton (diatoms, flagellates, and *Synechococcus*), and subsequent enhanced zooplankton abundance and (to a lesser extent) biomass, does not seem to be associated with upwelling. Rather, these increases appear to be due to changes in hydrographical conditions in the GAB related to the onset of upwelling, and physiological responses of the phytoplankton community. However, while rare, the occurrence of upwelled water reaching the photic zone during pre-conditioning (on two occasions during the study) also highlights the potential for interactive physical mechanisms (upwelling and the onset of stratification) and physiological processes (responses to increased irradiance) to occur (i.e. upwelling on top of the spring bloom). This preconditioning scenario then not only 'primes' the system with an enriched layer of bottom water for subsequent enhanced biomass and production during upwelling (SARDI unpublished), but also starts the trophic transfer from autotrophs to higher trophic levels in the early spring and summer.

4.1.5 Summary and conclusions

The results of this study represent the first holistic view of the lower trophic food web in the eastern GAB, and highlight the efficient trophic transfer that occurs not only under strong upwelling conditions, but also at the commencement of the upwelling season due to hydrographic conditions not directly related to upwelling. The key features of the lower food web for each scenario are shown in Table 4.1-5. In summary, during winter-mixing, small phytoplankton dominated, with high numbers of viruses but low numbers of bacteria, suggesting small autotrophic phytoplankton are dominant hosts of viruses at this time. Zooplankton biomass and abundance was on average high

(but variable) with the community dominated by copepod and zooplankton taxa known to preferentially feed on small pico- and nanoplankton (e.g. Appendicularia, bivalves). During preconditioning, moderate phytoplankton biomass was present, with nano- and micro-phytoplankton comprising the bulk of the autotrophic community. Peaks in diatoms and flagellates (and bacteria) during preconditioning likely occur in response to the winter to spring transition, where irradiance and stratification of the water column increases. Coincident high abundances and biomass of zooplankton indicate strong trophic transfer from primary to secondary producers at this time. *Noctiluca* was a dominant zooplankton member at this time, likely exerting strong influence on the plankton communities. During moderate upwelling, picophytoplankton and microphytoplankotn contributed similarly to moderate levels of Chl *a* biomass, with viruses the lowest of any scenario. Zooplankton abundances and biomass were overall low, and proposed to result from significant grazing on copepods and their eggs during preconditioning, with enrichment of the upper euphotic zone not yet occurring. The highest autotrophic biomass, occurred during strong upwelling, dominated by microplankton (specifically diatoms). Abundances of viruses and bacteria were moderate to high indicating strong microbial processes continue under enriched conditions. High zooplankton biomass, with dominant taxa (Cladocera, Thaliaceans) known to respond to enriched waters and enhanced microphytoplankton biomass, suggests strong trophic transfer from primary producers to secondary consumers. The dominance of smaller picophytoplankton during suppression occurred together with moderate to high numbers of bacteria and viruses. Coincident low zooplankton biomass and abundance at this time indicate a food web more reliant on microbial recycling processes following uptake of nutrient rich water during the strong upwelling scenario.

In line with our novel findings of scenario driven shifts in plankton community structure in this seasonally driven upwelling system, a number of gaps in our understanding have been identified. Currently lacking are rate measurements (e.g. micro/meso-grazing and viral lysis) as well as *in situ* rates of production. First estimates of microzooplankton grazing on the picoplankton component indicate picophytoplankton and bacteria represent potentially important food sources for higher trophic levels, particularly in nutrient depleted waters of the central GAB (Kloser et al. 2017). Given the proposed importance of the nanoplankton, enumeration of the autotrophic and heterotrophic nanoplankton would also provide critical information on trophic pathways through this important group. We believe this current work provides a strong foundation for further building on our understanding for the lower food web structure and function and their links to higher trophic levels in this ecologically and economically important region.

Table 4.1-5 Quantitative summary of microbial and planktonic abundances, biomass, composition and size structure during the different Scenarios

Organism size	Group	Measure	W_{mix}	P_{cond}	Up_M	Up_S	Supp
Femto	**Virus**	**Abundance**	High	High	Low	High	High
Pico	**Bacteria**	**Abundance**	Low	High	Medium	Medium	Medium
Pico	**Picophyt**	**%** #	*Syn* > *Pro* > Peuk	*Syn* > Peuk > *Pro*	*Syn* > *Pro* ~ Peuk	*Syn* > *Pro* > Peuk	*Pro* > *Syn* > Peuk
Nano/Micro	**Phyto**	**%** #	Flag ~ Dino > Diat	Flag ~ Diat > Dino	Flag > Diat > Dino	Diat > Flag ~ Dino	Dino > Flag > Diat
Pico/Nano/Micro	**Phyto**	**Biomass**	Medium	Medium	Medium	High	Low
		% *	Nano > Pico > Micro	Micro ~ Nano > Pico	Pico ~ Micro > Nano	Micro > Nano > Pico	Nano > Pico > Micro
Micro/Meso	**Zoo**	**Abundance**	High	High	Medium	High	Low
		Biomass	High	Medium	Low	High	Low

Femto = Femtoplankton (< 0.2 µm); Pico = Picoplankton (0.2 – 2 µm); Nano = Nanoplankton (2 – 20 µm); Micro = Microplankton (20 – 200 µm) and Meso = Mesoplankton (0.2 – 20 mm).
Picophyt = picophytoplankton; Phyto = Phytoplankton; Zoo = Zooplankton.

 # Based on abundances.

** Based on pigment biomass and using the approach of (Vidussi et al. 2001) and (Uitz et al. 2008) with three phytoplankton size classes estimated; pico (< 2 µm); nano (2 – 20 µm) and micro (> 20 µm) (see Equations 1, 2, 3 and 4 from Chapter 4.1).*

Scores of High, Medium, and Low are relative to the range of values for that measure across the study location and duarion.

References

Ahmed, A., Kurian, S., Gauns, M., Chndrasekhararao, A. V., Mulla, A., Naik, B., Naik, H., et al. 2016. Spatial variability in phytoplankton community structure along the eastern Arabian Sea during the onset of south-west monsoon. Continental Shelf Research, 119: 30-39.

Alldredge, A. L. 1972. Abandoned Larvacean Houses: A Unique Food Source in the Pelagic Environment. Science, 177: 885-887.

Anabalón, V., Morales, C. E., Escribano, R., and Angélica Varas, M. 2007. The contribution of nano- and micro-planktonic assemblages in the surface layer (0–30 m) under different hydrographic conditions in the upwelling area off Concepción, central Chile. Progress in Oceanography, 75: 396-414.

Anderson, M. J., Gorley, R. N., and Clarke, K. N. 2008. PERMANOVA+ for PRIMER; a guide to software and statistical methods, PRIMER-E, Plymouth, UK.

Armbrecht, L. H., Roughan, M., Rossi, V., Schaeffer, A., Davies, P. L., Waite, A. M., and Armand, L. K. 2014. Phytoplankton composition under contrasting oceanographic conditions: Upwelling and downwelling (Eastern Australia). Continental Shelf Research, 75: 54-67.

Armbrecht, L. H., Thompson, P. A., Wright, S. W., Schaeffer, A., Roughan, M., Henderiks, J., and Armand, L. K. 2015. Comparison of the cross-shelf phytoplankton distribution of two oceanographically distinct regions off Australia. Journal of Marine Systems, 148: 26-38.

Azam, F. 1983. The ecological role of water-column microbes in the sea. Marine Ecology Progress Series, 10: 257-263.

Barber, R., and Hiscock, M. 2006. A rising tide lifts all phytoplankton: Growth response of other phytoplankton taxa in diatom-dominated blooms. Global Biogeochemical Cycles, 20.

Baudoux, A. C., Veldhuis, M. J. W., Noordeloos, A. A. M., van Noort, G., and Brussaard, C. P. D. 2008. Estimates of virus- vs. grazing induced mortality of picophytoplankton in the North Sea during summer. Aquatic Microbial Ecology, 52: 69-82.

Bode, A., and Alvarez-Ossorio, M. T. 2004. Taxonomic versus trophic structure of mesozooplankton: a seasonal study of species succession and stable carbon and nitrogen isotopes in a coastal upwelling ecosystem. ICES Journal of Marine Science, 61: 563-571.

Böttjer, D., and Morales, C. E. 2007. Nanoplanktonic assemblages in the upwelling area off Concepción (∼36°S), central Chile: Abundance, biomass, and grazing potential during the annual cycle. Progress in Oceanography, 75: 415-434.

Brussaard, C. P. D. 2004. Optimization of procedures for counting viruses by flow cytometry. Applied and Environmental Microbiology, 70: 1506-1513.

Brussaard, C. P. D., Thyrhaug, R., Marie, D., and Bratback, G. 1999. Flow cytometric analysis of viral infection in two marine phytoplankton species, *Micromonas pusilla* (Prasinophyceae) and *Phaeocystis pouchetti* (Prymnesiophaceae). Journal of Phycology, 35: 941-948.

Calbet, A. 2008. The trophic roles of microzooplankton in marine systems. ICES Journal of Marine Science: Journal du Conseil, 65: 325-331.

Calbet, A., and Landry, M., R. 2004. Phytoplankton growth, microzooplankton grazing, and carbon cycling in marine systems. Limnology and Oceanography, 49: 51-57.

Calvo-Díaz, A., and Morán, X. A. G. 2006. Seasonal dynamics of picoplankton in shelf waters of the southern Bay of Biscay. Aquatic Microbial Ecology, 42: 159-174.

Carstensen, J., Klais, R., and Cloern, J. E. 2015. Phytoplankton blooms in estuarine and coastal waters: Seasonal patterns and key species. Estuarine, Coastal and Shelf Science, 162: 98-109.

Cetina-Heredia, P., van Sebille, E., Matear, R., and Roughan, M. 2016. Lagrangian characterization of nitrate supply and episodes of extreme phytoplankton blooms in the Great Australian Bight. Biogeosciences Discuss., 2016: 1-15.

Christaki, U., Vázquez-Domínguez, E., Courties, C., and Lebaron, P. 2005. Grazing impact of different heterotrophic nanoflagellates on eukaryotic (*Ostreococcus tauri*) and prokaryotic picoautotrophs (*Prochlorococcus* and *Synechococcus*). Environmental Microbiology, 7: 1200-1210.

Cullen, J. J. 1982. The Deep Chlorophyll Maximum: Comparing Vertical Profiles of Chlorophyll a. Canadian Journal of Fisheries and Aquatic Sciences, 39: 791-803.

Cury, P., Bakun, A., Crawford, R. J., Jarre, A., Quinones, R. A., Shannon, L. J., and Verheye, H. M. 2000. Small pelagics in upwelling systems: patterns of interaction and structural changes in "wasp-waist" ecosystems. ICES Journal of Marine Science: Journal du Conseil, 57: 603-618.

Cushing, D. 1989. A difference in structure between ecosystems in strongly straified waters and those that are only weakly stratified Journal of Plankton Research, 11: 1-13.

Daniels, C. J., Poulton, A. J., Esposito, M., Paulsen, M. L., Bellerby, R., St. John, M., and Martin, A. P. 2015. Phytoplankton dynamics in contrasting early stage North Atlantic spring blooms: composition, succession, and potential drivers. Biogeosciences Discussions, 12: 93-133.

Dela-Cruz, J., Ajani, P., Lee, R., Pritchard, T., and Suthers, I. 2002. Temporal abundance patterns of the red tide dinoflagellate *Noctiluca scintillans* along the southeast coast of Australia. Marine Ecology Progress Series, 236: 75-88.

Dela-Cruz, J., Middleton, J. H., and Suthers, I. M. 2008. The influence of upwelling, coastal currents and water temperature on the distribution of the red tide dinoflagellate, *Noctiluca scintillans*, along the east coast of Australia. Hydrobiologia, 598: 59-75.

Egge, J., and Aksnes, D. 1992. Silicate as regulating nutrient in phytoplankton competition. Marine ecology progress series. Oldendorf, 83: 281-289.

Flombaum, P., Gallegos, J. L., Gordillo, R. A., Rincón, J., Zabala, L. L., Jiao, N., Karl, D. M., et al. 2013. Present and future global distributions of the marine Cyanobacteria *Prochlorococcus* and *Synechococcus*. Proceedings of the National Academy of Sciences, 110: 9824-9829.

Fonda Umani, S., Beran, A., Parlato, S., Virgilio, D., Zollet, T., De Olazabal, A., Lazzarini, B., et al. 2004. *Noctiluca scintillans* (Macartney) in the Northern Adriatic Sea: long-term dynamics, relationships with temperature and eutrophication, and role in the food web. Journal of Plankton Research, 26: 545-561.

Gallager, S. M., Waterbury, J. B., and Stoecker, D. K. 1994. Efficient grazing and utilization of the marine cyanobacterium *Synechococcus sp*. by larvae of the bivalve *Mercenaria mercenaria*. Marine Biology, 119: 251-259.

Garrison, D. L., Gowing, M. M., Hughes, M. P., Campbell, L., Caron, D. A., Dennett, M. R., Shalapyonok, A., et al. 2000. Microbial food web structure in the Arabian Sea: a US JGOFS study. Deep Sea Research Part II: Topical Studies in Oceanography, 47: 1387-1422.

Gill, A. E. 1982. Atmosphere-Ocean Dynamics, Academic press, London. 662 pp.

Goldsworthy, S. D., Page, B., Rogers, P. J., Bulman, C., Wiebkin, A., McLeay, L. J., Einoder, L., et al. 2013. Trophodynamics of the eastern Great Australian Bight ecosystem: Ecological change associated with the growth of Australia's largest fishery. Ecological Modelling, 255: 38-57.

Gómez, F., Claustre, H., Raimbault, P., and Souissi, S. 2007. Two High-Nutrient Low-Chlorophyll phytoplankton assemblages: the tropical central Pacific and the offshore Perú-Chile Current. Biogeosciences, 4: 1101-1113.

Gorsky, G., Chretiennot-Dinet, M. J., Blanchot, J., and Palazzoli, I. 1999. Picoplankton and nanoplankton aggregation by appendicularians: Fecal pellet contents of *Megalocercus huxleyi* in the equatorial Pacific. Journal of Geophysical Research-Oceans, 104: 3381-3390.

Gregoracci, G. B., Soares, A. C. d. S., Miranda, M. D., Coutinho, R., and Thompson, F. L. 2015. Insights into the Microbial and Viral Dynamics of a Coastal Downwelling-Upwelling Transition. PLOS ONE, 10: e0137090.

Hallegraeff, G., and Jeffrey, S. 1993. Annually recurrent diatom blooms in spring along the New South Wales coast of Australia. Marine and Freshwater Research, 44: 325-334.

Hallegraeff, G., and Reid, D. 1986. Phytoplankton species successions and their hydrological environment at a coastal station off Sydney. Marine and Freshwater Research, 37: 361-377.

Hallegraeff, G. M., Bolch, C. J. S., Hill, D. R. A., Jameson, I., LeRoi, J.-M., McMinn, A., Murray, S., et al. 2010. Algae of Australia: Phytoplankton of temperate coastal waters, CSIRO Publishing, Melbourne.

Hanson, C. E., Pattiaratchi, C. B., and Waite, A. M. 2005. Sporadic upwelling on a downwelling coast: Phytoplankton responses to spatially variable nutrient dynamics off the Gascoyne region of Western Australia. Continental Shelf Research, 25: 1561-1582.

Hanson, C. E., Pesant, S., Waite, A. M., and Pattiaratchi, C. B. 2007. Assessing the magnitude and significance of deep chlorophyll maxima of the coastal eastern Indian Ocean. Deep Sea Research Part II: Topical Studies in Oceanography, 54: 884-901.

Hutchins, D. A., and Bruland, K. W. 1998. Iron-limited diatom growth and Si:N uptake ratios in a coastal upwelling regime. Nature, 393: 561-564.

Jeffrey, S. W. 1997. Application of pigment methods to oceanography. *In* Phytoplankton pigments in oceanography: guidelines to modern methods, pp. 127-166. Ed. by S. W. Jeffrey, R. F. C. Mantoura, and S. W. Wright. UNESCO, Paris.

Jeong, H. J., Yoo, Y. D., Kim, J. S., Seong, K. A., Kang, N. S., and Kim, T. H. 2010. Growth, feeding and ecological roles of the mixotrophic and heterotrophic dinoflagellates in marine planktonic food webs. Ocean Science Journal, 45: 65-91.

Kämpf, J., Doubell, M., Griffin, D., Matthews, R., L., and Ward, T. M. 2004. Evidence of a large seasonal coastal upwelling system along the southern shelf of Australia. Geophysical Research Letters, 31.

Katechakis, A., and Stibor, H. 2004. Feeding selectivities of the marine cladocerans *Penilia avirostris*, *Podon intermedius* and *Evadne nordmanni*. Marine Biology, 145: 529-539.

Kirchner, M., Sahling, G., Uhlig, G., Gunkel, W., and Klings, K. W. 1996. Does the red tide-forming dinoflagellate *Noctiluca scintillans* feed on bacteria? Sarsia, 81: 45-55.

Kloser R, van Ruth P.D, Doubell M, Downie R, Flynn A, Gershwin L, Patten N, Revill A, Richardson A.E, Ryan T.E and Sutton C.A (2017). Characterise spatial variability of offshore/slope plankton and micronekton communities. Final Report GABRP Project 2.2. Great Australian Bight Research Program, GABRP Research Report Series Number 22, 301pp.

Knowles, B., Silveira, C. B., Bailey, B. A., Barott, K., Cantu, V. A., Cobián-Güemes, A. G., Coutinho, F. H., et al. 2016. Lytic to temperate switching of viral communities. Nature, 531: 466-470.

Lamont, T., Barlow, R. G., and Kyewalyanga, M. S. 2014. Physical drivers of phytoplankton production in the southern Benguela upwelling system. Deep-Sea Research Part I-Oceanographic Research Papers, 90: 1-16.

Larsen, A., Fonnes Flaten, G. A., Sandaa, R., Castberg, T., Thyrhaug, R., Erga, S. R., Jacquet, S., et al. 2004. Spring phytoplankton bloom dynamics in Norwegian coastal waters: Microbial community succession and diversity. Limnology and Oceanography, 49: 180-190.

Lasker, R. 1975. Field criteria for the survival of anchovy larvae: the relation between isnhore chlorophyll maximum layers and successful first feeding. Fisheries Bulletin US, 73: 847-855.

Legendre, L., and Rassoulzadegan, F. 1995. Plankton and nutrient dynamics in marine waters. Ophelia, 41: 153-172.

Li, W. K. W., Head, E. J. H., and Glen Harrison, W. 2004. Macroecological limits of heterotrophic bacterial abundance in the ocean. Deep Sea Research Part I: Oceanographic Research Papers, 51: 1529-1540.

Linacre, L. P., Landry, M. R., Lara-Lara, J. R., Hernández-Ayón, J. M., and Bazán-Guzmán, C. 2010. Picoplankton dynamics during contrasting seasonal oceanographic conditions at a coastal upwelling station off Northern Baja California, México. Journal of Plankton Research, 32: 539-557.

Lochte, K., Ducklow, H. W., Fasham, M. J. R., and Stienen, C. 1993. Plankton succession and carbon cycling at 47°N 20°W during the JGOFS North Atlantic Bloom Experiment. Deep Sea Research Part II: Topical Studies in Oceanography, 40: 91-114.

Loick-Wilde, N., Bombar, D., Doan, H. N., Nguyen, L. N., Nguyen-Thi, A. M., Voss, M., and Dippner, J. W. 2017. Microplankton biomass and diversity in the Vietnamese upwelling area during SW monsoon under normal conditions and after an ENSO event. Progress in Oceanography, 153: 1-15.

Mann, K. H., and Lazier, J. R. N. 2006. Dynamics of Marine Ecosystems: Biological-physical interactions in the oceans, Blackwell Science, Oxford.

Martiny, A. C., Kathuria, S., and Berube, P. M. 2009. Widespread metabolic potential for nitrite and nitrate assimilation among *Prochlorococcus* ecotypes. Proceedings of the National Academy of Sciences, 106: 10787-10792.

McClatchie, S., Middleton, J. F., and Ward, T. M. 2006. Water mass analysis and alongshore variation in upwelling intensity in the eastern Great Australian Bight. Journal of Geophysical Research: Oceans, 111: doi:10.1029/2004JC002699.

Middleton, J. F., and Bye, J. A. T. 2007. A review of the shelf-slope circulation along Australia's southern shelves: Cape Leeuwin to Portland. Progress in Oceanography, 75: 1-41.

Mignot, A., Claustre, H., Uitz, J., Poteau, A., D'Ortenzio, F., and Xing, X. 2014. Understanding the seasonal dynamics of phytoplankton biomass and the deep chlorophyll maximum in

oligotrophic environments: A Bio-Argo float investigation. Global Biogeochemical Cycles, 28: 856-876.

Morán, X. A. G., Estrada, M., Gasol, J. M., and Pedrós-Alió, C. 2002. Dissolved primary production and the strength of phytoplankton-bacterioplankton coupling in contrasting marine regions. Microbial Ecology, 44: 217-223.

Murray, S., and Suthers, I., M. 1999. Population ecology of *Noctiluca scintillans* Macartney, a red-tide-forming dinoflagellate. Marine and Freshwater Research, 50: 243-252.

Nagata, T. 2000. Production mechanisms of dissolved organic matter. *In* Microbial Ecology of the Oceans, pp. 121-151. Ed. by D. L. Kirchman. Wiley-Liss, New York.

Not, F., Latasa, M., Marie, D., Cariou, T., Vaulot, D., and Simon, N. 2004. A single species, *Micromonas pusilla* (Prasinophyceae), dominates the eukaryotic picoplankton in the Western English Channel. Applied and Environmental Microbiology, 70: 4064-4072.

Not, F., Latasa, M., Scharek, R., Viprey, M., Karleskind, P., Balagué, V., Ontoria-Oviedo, I., et al. 2008. Protistan assemblages across the Indian Ocean, with a specific emphasis on the picoeukaryotes. Deep Sea Research Part I: Oceanographic Research Papers, 55: 1456-1473.

Painting, S. J., Lucas, M. I., Peterson, W. T., Brown, P. C., Hutchings, L., and Mitchell-Innes, B. A. 1993. Dynamics of bacterioplankton, phytoplankton and mesozooplankton communities during the development of an upwelling plume in the southern Benguela. Marine Ecology Progress Series, 100: 35-53.

Partensky, F., Blanchot, J., and Vaulot, D. 1999. Differential distribution and ecology of *Prochlorococcus* and *Synechococcus* in oceanic waters: a review. *In* Marine cyanobacteria, pp. 457-475. Ed. by L. Charpy, and A. Larkum, W,D. Museé Océanographique, Monaco.

Paterson, J. S., Nayar, S., Mitchell, J. G., and Seuront, L. 2013. Population-specific shifts in viral and microbial abundance within a cryptic upwelling. Journal of Marine Systems, 113–114: 52-61.

Patten, N. L., and van Ruth, P. D. In Review. Environmental driven shifts in picoplankton and viral community composition in slope and offshore waters of the Great Australian Bight (southern Australia) Deep Sea Research Part II: Topical Studies in Oceanography.

Pomeroy, L. R., and Wiebe, W. J. 2001. Temperature and substrates as interactive limiting factors for marine heterotrophic bacteria. Aquatic Microbial Ecology, 23: 187-204.

Quevedo, M., Gonzalez-Quiros, R., and Anadon, R. 1999. Evidence of heavy predation by *Noctiluca scintillans* on *Acartia clausi* (Copepoda) eggs off the central Cantabrian coast (NW Spain). Oceanologica Acta, 22: 127-131.

Rogers, P. J., Ward, T. M., van Ruth, P. D., Williams, A., Bruce, B. D., Connell, S. D., Currie, D. R., et al. 2013. Physical processes, biodiversity and ecology of the Great Australian Bight region: a literature review.

Romagnan, J.-B., Legendre, L., Guidi, L., Jamet, J.-L., Jamet, D., Mousseau, L., Pedrotti, M.-L., et al. 2015. Comprehensive Model of Annual Plankton Succession Based on the Whole-Plankton Time Series Approach. PLOS ONE, 10: e0119219.

Round, F. E. 1981. The ecology of algae, Cambridge University Press, Cambridge, UK. 653 pp.

Ryther, J. H. 1969. Photosynthesis and fish production in the sea. Science, 166: 72-76.

Scanlan, D. J., Ostrowski, M., Mazard, S., Dufresne, A., Garczarek, L., Hess, W. R., Post, A. F., et al. 2009. Ecological genomics of marine picocyanobacteria. Microbiology and Molecular Biology Reviews, 73: 249-299.

Sieracki, M. E., Verity, P. G., and Stoecker, D. K. 1993. Plankton community response to sequential silicate and nitrate depletion during the 1989 North Atlantic spring bloom. Deep Sea Research Part II: Topical Studies in Oceanography, 40: 213-225.

Simpson, J. H., and Bowers, D. 1981. Models of stratification and frontal movement in shelf seas. Deep Sea Research Part A. Oceanographic Research Papers, 28: 727-738.

Siokou-Frangou, I., Christaki, U., Mazzocchi, M. G., Montresor, M., Ribera d'Alcalá, M., Vaqué, D., and Zingone, A. 2010. Plankton in the open Mediterranean Sea: a review. Biogeosciences, 7: 1543-1586.

Sommer, U., and Stibor, H. 2002. Copepoda – Cladocera – Tunicata: The role of three major mesozooplankton groups in pelagic food webs. Ecological Research, 17: 161-174.

Stockner, J. G. 1988. Phototrophic picoplankton: an overview from marine and freshwater ecosystems. Limnology and Oceanography, 33: 765-775.

Stoecker, D. K. 1999. Mixotrophy among Dinoflagellates. Journal of Eukaryotic Microbiology, 46: 397-401.

Suttle, C. A., and Chan, A. M. 1995. Viruses infecting the marine Prymnesiophyte *Chrysochromulina* spp.:isolation, preliminary characterization and natural abundance. Marine Ecology Progress Series, 118: 275-282.

Sverdrup, H. 1953. On conditions for the vernal blooming of phytoplankton. Journal du Conseil, 18: 287-295.

Tai, V., and Palenik, B. 2009. Temporal variation of *Synechococcus* clades at a coastal Pacific Ocean monitoring site. ISME J, 3: 903-915.

Tarran, G. A., Burkill, P. H., Edwards, E. S., and Woodward, E. M. S. 1999. Phytoplankton community structure in the Arabian Sea during and after the SW monsoon, 1994. Deep Sea Research Part II: Topical Studies in Oceanography, 46: 655-676.

Taylor, A. G., Landry, M. R., Selph, K. E., and Yang, E. J. 2011. Biomass, size structure and depth distributions of the microbial community in the eastern equatorial Pacific. Deep Sea Research Part II: Topical Studies in Oceanography, 58: 342-357.

Tudela, S., and Palomera, I. 1995. Diel feeding intensity and daily ration in the anchovy Engraulis encrasicolus in the northwest Mediterranean Sea during the spawning period. Marine Ecology Progress Series, 129: 55-61.

Turner, J. T. 2004. The importance of small planktonic copepods and their roles in pelagic marine food webs. Zoological Studies, 43: 255-266.

Uitz, J., Huot, Y., Bruyant, F., Babin, M., and Claustre, H. 2008. Relating phytoplankton photophysiological properties to community structure on large scales. Limnology and Oceanography, 53: 614-630.

Uye, S., Aoto, I., and Onbé, T. 2002. Seasonal population dynamics and production of Microsetella norvegica, a widely distributed but little-studied marine planktonic harpacticoid copepod. Journal of Plankton Research, 24: 143-153.

Van Der Lingen, C. D. 2002. Diet of sardine *Sardinops sagax* in the southern Benguela upwelling ecosystem. South African Journal of Marine Science, 24: 301-316.

van Dongen-Vogels, V., Seymour, J. R., Middleton, J. F., Mitchell, J. G., and Seuront, L. 2011. Influence of local physical events on picophytoplankton spatial and temporal dynamics in South Australian continental shelf waters. Journal of Plankton Research, 33: 1825-1841.

van Dongen-Vogels, V., Seymour, J. R., Middleton, J. F., Mitchell, J. G., and Seuront, L. 2012. Shifts in picophytoplankton community structure influenced by changing upwelling conditions. Estuarine, Coastal and Shelf Science, 109: 81-90.

Van Heukelem, L., and Thomas, C., S. 2001. Computer-assisted high-performance liquid chromatography method development with applications to the isolation and analysis of phytoplankton pigments. Journal of Chromatography A, 910: 31-49.

van Ruth, P. D., Ganf, G. G., and Ward, T. M. 2010a. Hot-spots of primary productivity: An Alternative interpretation to Conventional upwelling models. Estuarine, Coastal and Shelf Science, 90: 142-158.

van Ruth, P. D., Ganf, G. G., and Ward, T. M. 2010b. The influence of mixing on primary productivity: A unique application of classical critical depth theory. Progress in Oceanography, 85: 224-235.

van Ruth, P. D., and Ward, T. M. 2009. Meso-Zooplankton Abundance, Distribution and Community Composition in the Eastern Great Australian Bight. Transactions of the Royal Society of South Australia, 133: 274-283.

Vargas, C. A., Martínez, R. A., Cuevas, L. A., Pavez, M. A., Cartes, C., GonzÁlez, H. E., Escribano, R., et al. 2007. The relative importance of microbial and classical food webs in a highly productive coastal upwelling area. Limnology and Oceanography, 52: 1495-1510.

Vidussi, F., Claustre, H., Manca, B. B., Luchetta, A., and Marty, J.-C. 2001. Phytoplankton pigment distribution in relation to upper thermocline circulation in the eastern Mediterranean Sea during winter. Journal of Geophysical Research: Oceans, 106: 19939-19956.

Ward, T., M., McLeay, L. J., Dimmlich, W. F., Rogers, P., J., McClatchie, S. A. M., Matthews, R., Kampf, J., et al. 2006. Pelagic ecology of a northern boundary current system: effects of upwelling on the production and distribution of sardine (*Sardinops sagax*), anchovy (*Engraulis australis*) and southern bluefin tuna (*Thunnus maccoyii*) in the Great Australian Bight. Fisheries Oceanography, 15: 191-207.

Weinbauer, M., G., Bonilla-Findji, O., Chan, A., M., Dolan, J., R., Short, S., M., Šimek, K., Wilhelm, S., W., et al. 2011. *Synechococcus* growth in the ocean may depend on the lysis of heterotrophic bacteria. Journal of Plankton Research, 33: 1465-1476.

Weinbauer, M. G., and Suttle, C. A. 1996. Potential significance of lysogeny to bacteriophage production and bacterial mortality in coastal waters of the Gulf of Mexico. Applied and Environmental Microbiology, 62: 4372-4380.

Weitz, J. S., Stock, C. A., Wilhelm, S. W., Bourouiba, L., Coleman, M. L., Buchan, A., Follows, M. J., et al. 2015. A multitrophic model to quantify the effects of marine viruses on microbial food webs and ecosystem processes. ISME J, 9: 1352-1364.

Wilhelm, S. W., and Suttle, C. A. 1999. Viruses and nutrient cycles in the sea. Bioscience, 49: 781-788.

Worden, A. Z., and Binder, B. J. 2003. Application of dilution experiments for measuring growth and mortality rates among *Prochlorococcus* and *Synechococcus* populations in oligotrophic environments. Aquatic Microbial Ecology, 30: 159-174.

Worden, A. Z., Follows, M. J., Giovannoni, S. J., Wilken, S., Zimmerman, A. E., and Keeling, P. J. 2015. Rethinking the marine carbon cycle: Factoring in the multifarious lifestyles of microbes. Science, 347.

Wright, S. W., Thomas, D. P., Marchant, H. J., Higgins, H. W., Mackey, M. D., and Mackey, D. J. 1996. Analysis of phytoplankton of the Australian sector of the Southern Ocean: comparisons of microscopy and size frequency data with interpretations of pigment HPLC data using the 'CHEMTAX' matrix factorisation program. Marine Ecology Progress Series, 144: 285-298.

Zhang, S., Liu, H., Guo, C., and Harrison, P. J. 2016. Differential feeding and growth of *Noctiluca scintillans* on monospecific and mixed diets. Marine Ecology Progress Series, 549: 27-40.

4.2 Drivers of variation in meso-zooplankton abundance, biomass and size distribution, and sardine egg densities, in shelf waters of the Great Australian Bight (van Ruth, P.D., Everett, J., Patten, N.L., McGarvey, R., Ward, T.M)

4.2.1 Introduction

Shelf waters of the eastern Great Australian Bight (GAB), support Australia's largest fishery by weight, the South Australian Sardine Fishery (SASF) (Goldsworthy et al. 2013; Rogers et al. 2013). Since 1995, the South Australian Research and Development Institute (SARDI) has been conducting surveys during the peak of the summer upwelling season (February/March) to estimate the spawning biomass of sardine (*Sardinops sagax*) in South Australian waters (Ward et al. 1998, 2011a). Application of data collected during these surveys through the Daily Egg Production Method (DEPM, Parker 1980) has facilitated the rapid and sustainable development of the SASF, despite the effects of two mass mortality events that killed over 70% of the adult sardine population in waters off South Australia (e.g. Ward et al. 2001a, 2011a, b). Although sardine eggs and larvae are the targets of these surveys, the nature of the sampling methods (using 330 µm mesh CalVET nets) obligate the concurrent collection of meso-zooplankton community samples. While regarded as "by-catch" for the spawning biomass studies, the meso-zooplankton were retained, preserved, and samples were archived for future analysis.

Meso-zooplankton size frequency distributions can be used to characterise ecosystem dynamics, and can provide predictions about the effect of changes in microbial and planktonic community structure on pelagic fish (Jennings and Mackinson 2003). To date, there have been few investigations of the meso-zooplankton community in the GAB. van Ruth and Ward (2009), and van Ruth (2009), examined spatial and temporal variations in meso-zooplankton abundance and community composition in the region in 1999 and 2000, and in 2004 and 2005, respectively. These studies found increased meso-zooplankton abundance and biomass were associated with a cold, upwelled water mass, but did not examine variations in meso-zooplankton size structure, or try to link it to fishery (SASF) production. This study used a suite of meso-zooplankton parameters (abundances, biomass and size distributions), together with environmental parameters, to improve the understanding of the factors influencing the distributions and densities of sardine eggs. This work aims to improve our ability to model and manage the marine ecosystems of the region. The specific aims of the study were:

1. To examine differences in meso-zooplankton abundance, biomass and size distribution between regions in the GAB, location on the shelf, or survey years.
2. To characterise environmental drivers of meso-zooplankton abundance, biomass and size distributions.
3. To examine differences in sardine egg densities between regions in the GAB, location on the shelf, or survey years.
4. To determine the environmental drivers and meso-zooplankton community parameters which best predict sardine egg densities.

4.2.2 Methods

Sample collection

Samples used in this study were collected during sardine biomass surveys conducted in South Australian shelf waters aboard the *RV Ngerin* in February/March 2009, 2011, 2013 and 2014 (Fig. 4.2-1). On these surveys, plankton samples were collected at >300 sites on 24 transects across the GAB using paired Californian Vertical Egg Tow (CalVET) plankton nets. Each 330 µm mesh CalVET net had an internal diameter of 0.3 m. CalVET nets were deployed to within 10 m of the seabed at depths <80 m or to a depth of 70 m at depths >80 m, and retrieved vertically at a speed of ~1 m s^{-1}. General Oceanics 2030 flow-meters and factory calibration coefficients were used to estimate the distance travelled by the net during each tow. Upon retrieval of the nets the samples from each of the two cod-ends were washed into a sample container and fixed using 5% buffered formaldehyde and seawater.

Physical and chemical water column characteristics

Vertical profiles of physical and biological parameters were measured at each site using a Sea-Bird Conductivity, Temperature, Depth (CTD) recorder fitted with a Chelsea Aquatrakka fluorometer, which was lowered to a depth of 70 m, or to 10 m from the bottom in waters less than 80 m deep.

The depth of the subsurface chlorophyll fluorescence maximum (FM) was determined from the maximum peak in fluorescence. The FM was then used as a proxy for Chlorophyll *a* biomass in linear models (outlined below). Mixed Layer Depths (Z_m) were calculated using CTD-derived potential density profiles and a hybrid method modified from the algorithm of Holte and Talley (2009). The algorithm models the general shape of the profile and selects Z_m from a number of possible values, including the de Boyer Montégut et al. (2004) threshold criteria (a density difference of 0.03 kg m^{-3} and the measurement closest to the 10 dbar as the reference value) and Dong et al. (2008) gradient method criteria (0.0005 kg m^{-3} $dbar^{-1}$).

Sample analysis

Sardine eggs were identified in each sample according to White and Fletcher (1996) and Neira et al. (1998). Egg density was calculated as the number of eggs in a sample divided by the volume of water swept through the net, with results expressed in eggs m^{-3}.

A sub-set of samples from each survey year were processed through the Laser Optical Plankton Counter (LOPC ™). Samples were chosen to provide broad spatial coverage across the GAB to allow the examination of variations in meso-zooplankton parameters with longitude and water depth across the GAB shelf. Sixty samples were processed from each of the years 2009, 2011, and 2013, and with 143 samples processed from the 2014 survey (Fig. 4.2-1). The LOPC provides size based abundance data in 15 µm bins of particulate matter and is capable of quantifying particles with an Equivalent Spherical Diameter (ESD) between 0.1 - 10 mm (Herman et al. 2004). While providing informative information on the size spectrum of mesozooplankton, the counter does not provide any taxonomic information.

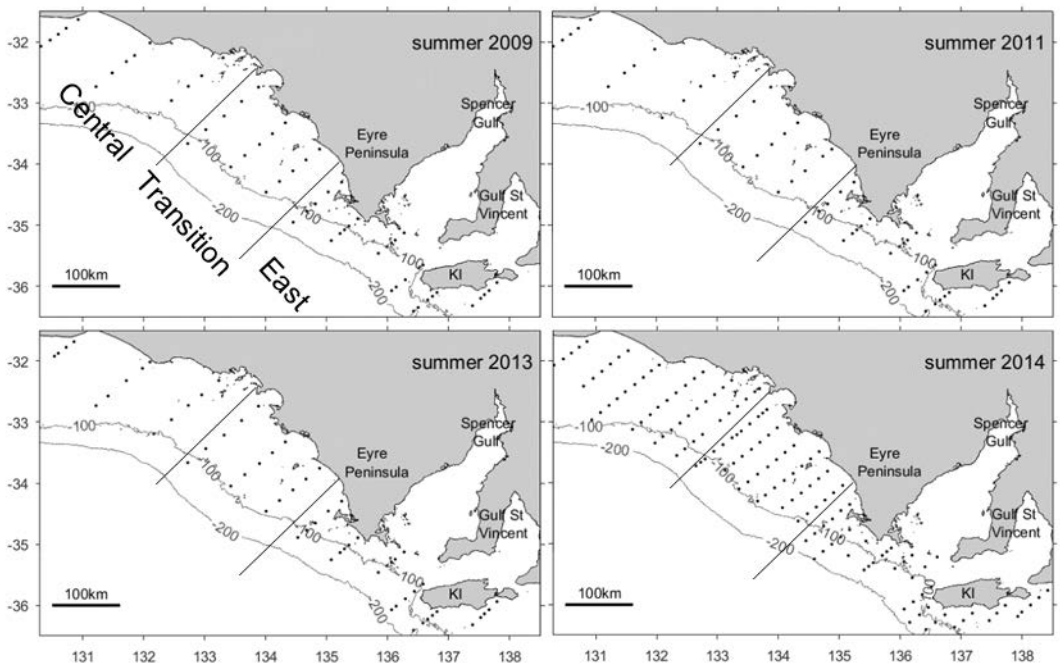

Figure 4.2-1 Station locations for the sub-set of samples used in this study. Samples were collected during sardine biomass surveys in February/March 2009, 2011, 2013, and 2014. Note the division of the survey area into regions for spatial analysis.

Meso-zooplankton community characteristics

Zooplankton communities were quantified from LOPC data using four metrics; abundance (ind. m^{-3}), biomass (mg m^{-3}), geometric mean size (GMS; ESD; µm); and the slope of the normalised biomass size spectrum (NBSS; $NBSS_{slope}$). Biomass was calculated using the volume equation of a prolate spheroid (size ratio of 3:1) and a specific gravity of 1 (Moore and Suthers 2006). The summed biomass for each net tow was standardised by the processed volume.

In order to calculate the $NBSS_{slope}$, the particle-biomass data from each deployment was binned into a series of logarithmically equal size intervals of 0.2 mg. This resulted in a total of 32 bins. This biomass size spectrum was then normalised by dividing the biomass of each bin by the width of the bin (mg m^{-3}/Δ mg). The NBSS is independent of any specified body size interval allowing for comparison across different studies and systems (Sprules and Munawar 1986). The $NBSS_{slope}$ was derived by fitting a least-squares polynomial regression to the normalised biomass size spectrum (Krupica et al. 2012).

Statistical analysis

Spatial and temporal variations in the meso-zooplankton abundance, biomass, GMS and $NBSS_{slope}$ as well as sardine egg densities, were examined by calculating mean values for these parameters across a range of spatial scales, and by survey year. The survey area was split into three regions (Fig. 4.2-1), based on previous understanding of dominant circulation patterns (Middleton and Bye 2007; van Ruth et al. 2010). The influence of the depth in which samples were collected was also considered, with the shelf split into three areas, defined as the Inner shelf (depth <75 m), Mid shelf (depth >75 m and <110 m) and Outer shelf (depth >110 m). Differences in meso-zooplankton abundance, biomass, GMS and $NBSS_{slope}$ and sardine egg densities between regions, location on the shelf and survey years

(Region × Shelf location × Year) were tested using a PERmutational Multivariate Analysis of VAriance (PERMANOVA) in in Primer Version 6 (PRIMER-E, Plymouth, UK), which relies on the analysis of similarities between samples (Anderson et al. 2008). To do this, data were $\log_{10}$ transformed (x + 1 for sardine egg densities) and Bray Curtis similarity matrices computed. P-values for the PERMANOVA were obtained for each term of the model, using 9999 permutations, with Type III (partial) sum of squares and permutation of residuals under a reduced model. P values <0.05 were considered statistically significant.

Linear models were used to examine the influence of environmental variables (water depth, Z_m, depth of FM, surface temperature, surface salinity, surface fluorescence, temperature at Z_m, salinity at Z_m, density at Z_m, fluorescence at the FM) on meso-zooplankton abundance, biomass, and $NBSS_{slope}$. The drivers of variations in sardine egg density were examined using linear models with the above detailed environmental parameters, together with meso-zooplankton abundance and biomass, and the parameters of the NBSS. Data were log transformed, where required, prior to all statistical analysis, to meet assumptions of normality and homoscedasticity. A significance level of 0.05 was used for all tests.

4.2.3 Results

Meso-zooplankton community characteristics

The meso-zooplankton community in the GAB was highly variable in space and time, with significant differences in abundance, biomass, GMS and NBSS slope parameters between regions, areas of the shelf, and survey years. For both zooplankton abundance and biomass, there was significant interaction between region and survey year (all P <0.05). The high meso-zooplankton abundances and biomass observed in the central and eastern GAB were driven by data from the 2014 survey year, which were the highest abundances and biomass recorded in this study (all P <0.05). Significantly higher zooplankton abundance (but not biomass; P >0.05) occurred on the inner shelf in the eastern and central GAB (both P <0.05).

Trends for GMS were even more complex than for zooplankton abundance and biomass, with significant interactions occurring between region, slope location and survey year (P < 0.05). Highest GMS occurred in 2013 (when meso-zooplankton abundance and biomass was lowest), with GMS in the east significantly higher than in the central or transition region over the inner shelf (for survey years 2011 and 2014; all P < 0.05) and mid shelf (for the survey year of 2014; P < 0.05).

Similarly complex interactions occurred for $NBSS_{slope}$, with an overall steeper slope in the central GAB, and in the inner shelf across the GAB, but with differences occurring between years (all P < 0.05). For example, a steeper slope occurred in 2014 in the central GAB on the mid and outer shelf region compared to the transition region or the eastern GAB (all P < 0.05). This was also apparent on the inner shelf for the survey year 2011 and 2014, but statistical differences only occurred between the central and transition region for these years (P <0.05).

The Normalised Biomass Anomaly shows size classes which deviate from the mean NBSS. The Central region had a high biomass of smaller zooplankton, but a lower biomass of larger zooplankton (Fig. 4.2-5). The reverse was observed in the eastern region, while the transition zone had lower than average biomass of all sizes. Similarly, the outer shelf area had a lower biomass of small zooplankton and a high biomass of larger size classes. The reverse was true for the inner shelf, while

the mid shelf had lower than average biomass of all sizes. Zooplankton biomass in 2009 and 2011 was generally lower than average in all size classes, with the exception of the smallest size class. The survey year 2013 showed higher biomass in the larger size classes, while in the survey year 2014, biomass in all size classes was overall, higher than for any other survey year.

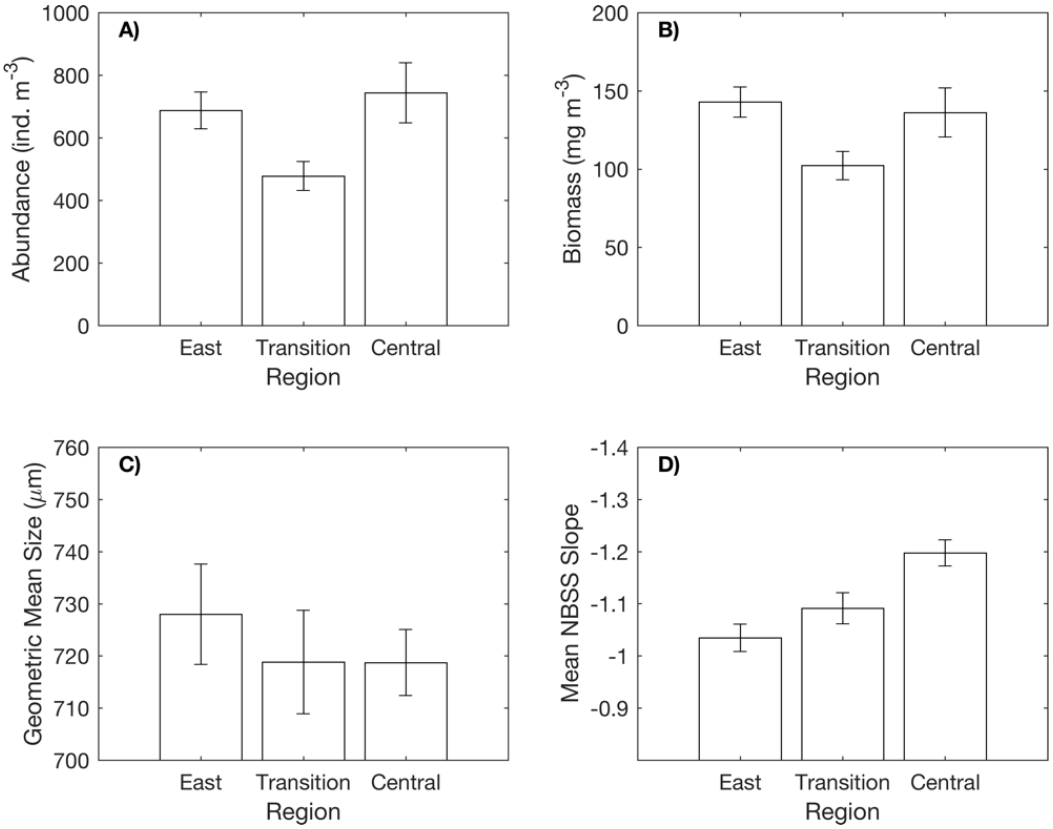

Figure 4.2-2 The mean (± standard error) Abundance (A), Biomass (B), Geometric Mean Size (C) and Mean NBSS Slope (D) for each of the 3 GAB regions – East, Transition, and Central.

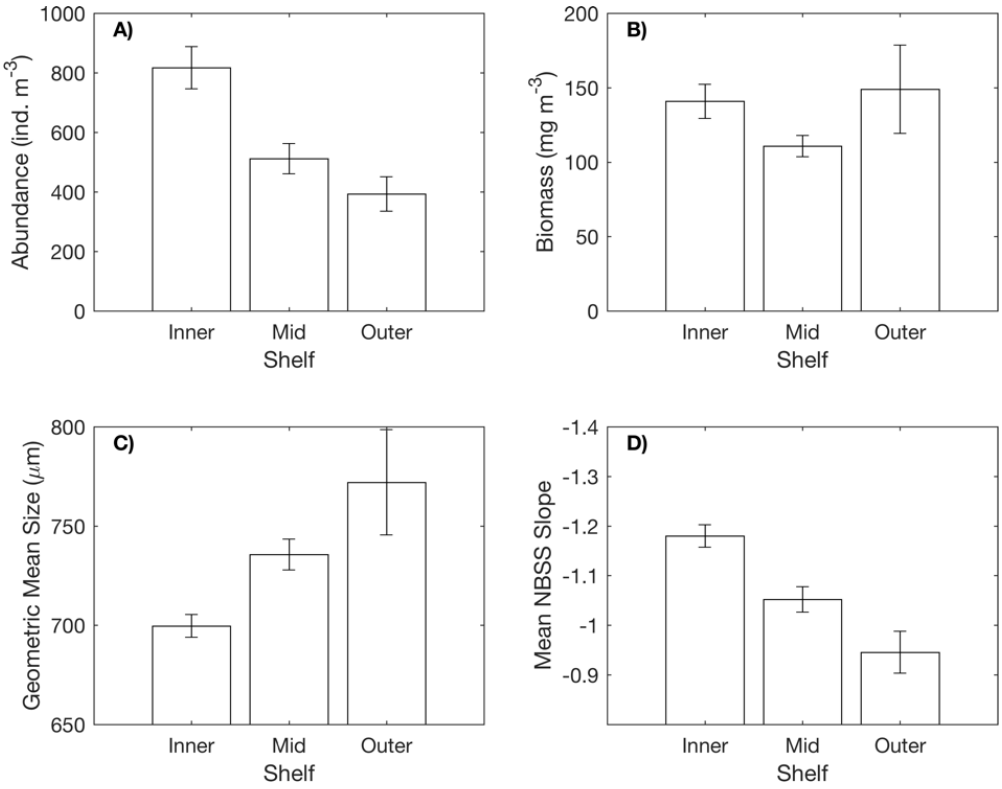

Figure 4.2-3 The mean (± standard error) Abundance (A), Biomass (B), Geometric Mean Size (C) and Mean NBSS Slope (D) for 3 shelf areas – Inner (Depth < 75 m), Mid (75 > Depth < 110) and Outer (Depth > 110 m).

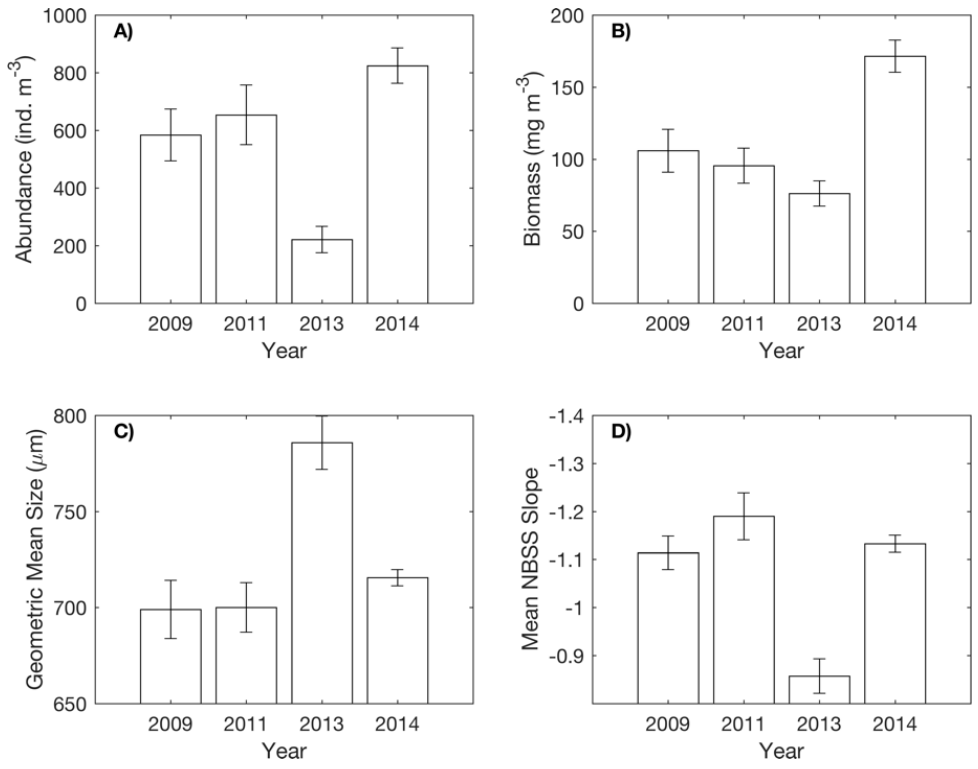

Figure 4.2-4 The mean (± standard error) Abundance (A), Biomass (B), Geometric Mean Size (C) and Mean NBSS Slope (D) for the 4 years of sampling.

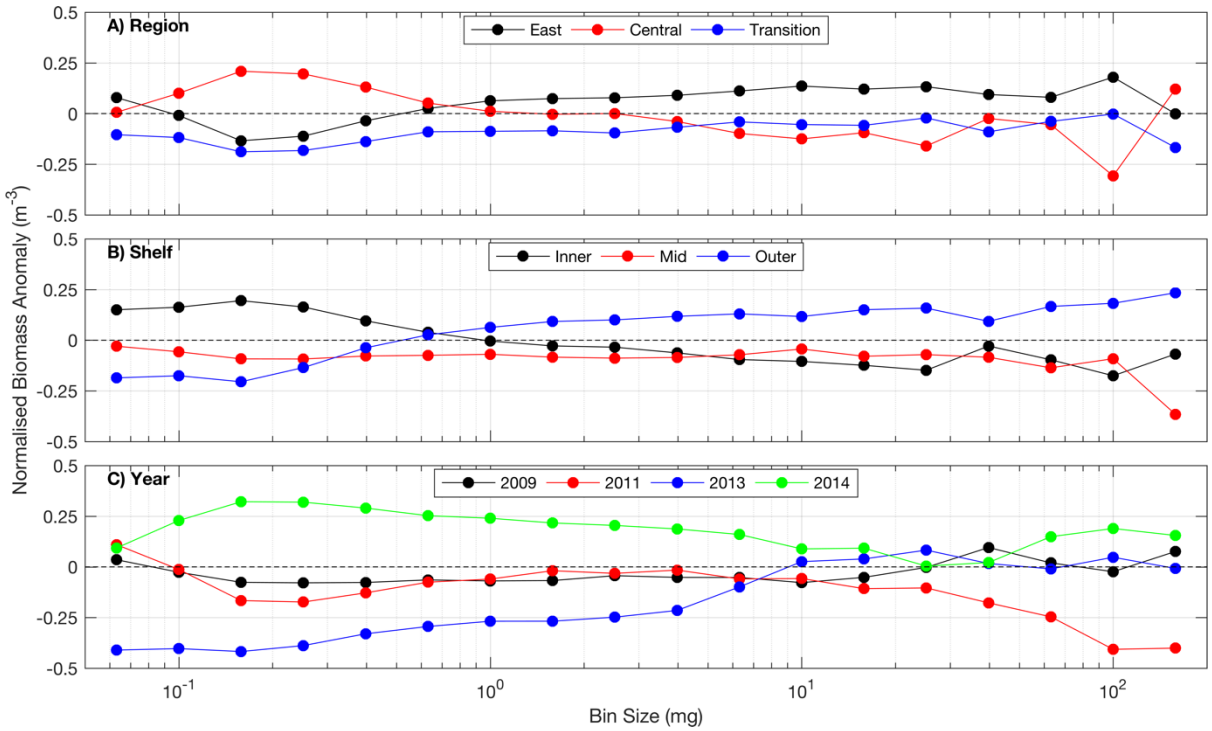

Figure 4.2-5 The Normalised Biomass Anomaly (m^{-3}) for each Region (A), Shelf Area (B), and Year (C).

The best fit model of log_{10}Abundance data indicated that variations in meso-zooplankton abundance were best described by changes in surface temperature and water depth (Table 4.2-1), though this only explained ~ 23% of the variation in the community. Abundances significantly increased with decreasing temperature (P <0.001) and decreasing depth (P <0.05).

The best fit model of log_{10}Biomass data showed that differences in meso-zooplankton biomass were best described by changes in surface temperature and salinity (Table 4.2-2). This model only explained ~ 13% of the variation in the community. Meso-zooplankton biomass significantly increased with decreasing temperature (p <0.001).

The best fit model of $NBSS_{Slope}$ data revealed that changes in surface temperature, surface salinity, and depth best described differences in $NBSS_{Slope}$ (Table 4.2-3), but this model only explained ~ 9% of the variation. Meso-zooplankton $NBSS_{Slope}$ significantly increased with increasing temperature (p <0.05), and increasing depth (p <0.001).

Table 4.2-1 Linear model of log_{10}meso-zooplankton abundance data. Temp = surface temperature (°C), Depth = water depth (m).

	Estimate	Std. Error	t value	Pr(>|t|)	
(Intercept)	6.25138	0.43634	14.327	< 2e-16	***
Temp	-0.18275	0.022825	-8.006	4.41E-14	***
Depth	-0.00233	0.001172	-1.99	0.0476	*

Multiple R-squared: 0.2259, Adjusted R-squared: 0.2197

F-statistic: 36.62 on 2 and 251 DF, p-value: 1.107e-14

Table 4.2-2 Linear model of log_{10}meso-zooplankton biomass data. Temp = surface temperature (°C), Salt = surface salinity (psu).

	Estimate	Std. Error	t value	Pr(>|t|)	
(Intercept)	13.2815	5.56926	2.385	0.0178	*
Temp	-0.09687	0.02292	-4.226	3.33E-05	***
Salt	-0.26434	0.16148	-1.637	0.1029	

Multiple R-squared: 0.1333, Adjusted R-squared: 0.1264

F-statistic: 19.3 on 2 and 251 DF, p-value: 1.593e-08

Table 4.2-3 Linear model of $NBSS_{slope}$ data. Temp = surface temperature (°C), Salt = surface salinity (psu), Depth = water depth (m).

	Estimate	Std. Error	t value	Pr(>|t|)	
(Intercept)	4.095698	3.898915	1.05	0.29459	
Temp	0.042465	0.016508	2.572	0.010723	*
Salt	-0.17301	0.112897	-1.532	0.126762	
Depth	0.002429	0.000718	3.386	0.000833	***

Multiple R-squared: 0.09133, Adjusted R-squared: 0.07963

F-statistic: 7.806 on 3 and 233 DF, p-value: 5.483e-05

Sardine egg densities

Mean sardine egg densities were overall highest in the central GAB (Fig. 4.2-6) but were driven by significantly higher densities occurring in the survey year 2014 ($P < 0.05$) and by higher densities occurring at the outer shelf at this location (all $P < 0.05$).

The best fit model of log_{10}Egg density data indicated that changes in log_{10}fluorescenec at FM, temperature at MLD, GMS, log_{10}Abundance, and distance from shore best described differences in egg density (Table 4.2-4). However, this model only explained ~19% of the variation in this data. Egg densities significantly increased with increasing meso-zooplankton abundance ($p < 0.001$), increasing fluorescence at the FM ($P < 0.05$), and decreasing GMS ($P < 0.05$).

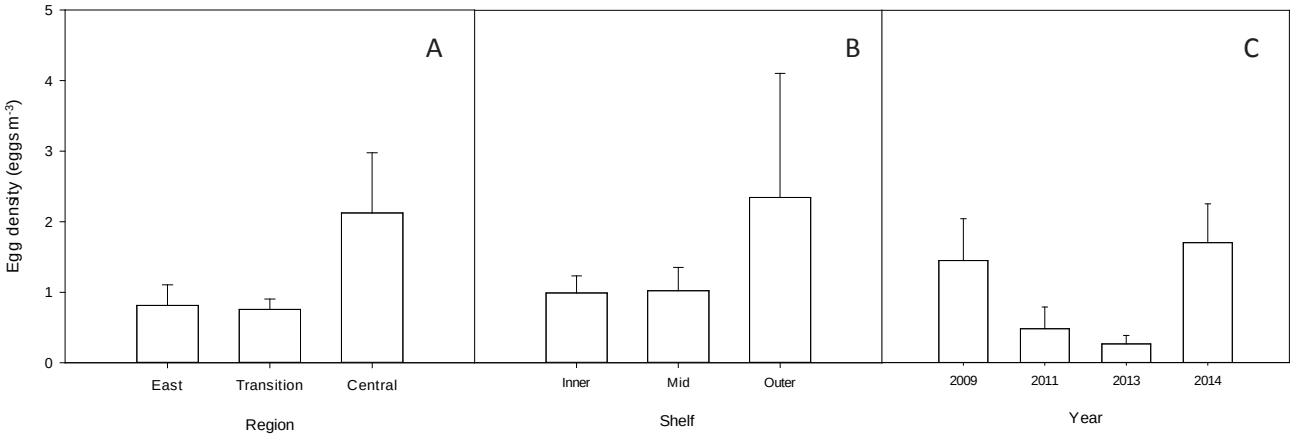

Figure 4.2-6 Variations in mean (± standard error) sardine egg density (eggs m^{-3}) in different regions (A) and shelf areas (B) in the GAB, and in different survey years (C).

Table 4.2-4 Linear Model of log_{10}Egg density. DCM_Chl = chlorophyll concentration at DCM (µg L^{-1}), MLD_Temp = temperature at MLD (°C), GeoMn = Geometric mean size (µm), Abundance = meso-zooplankton abundance (ind. m^{-3}), Dist_Shore = distance from shore (m).

	Estimate	Std. Error	t value	Pr(>|t|)	
(Intercept)	-0.67321	0.627276	-1.073	0.285323	
Log_{10}FM_Fluor	0.202608	0.100286	2.02	0.045579	*
MLD_Temp	0.045455	0.026294	1.729	0.086431	.
GMS	-0.00095	0.000471	-2.018	0.04584	*
Log_{10}Abundance	0.253445	0.069367	3.654	0.000385	***
Dist_Shore	0.001724	0.001151	1.498	0.13669	

Multiple R-squared: 0.1933, Adjusted R-squared: 0.1597

F-statistic: 5.751 on 5 and 120 DF, p-value: 8.564e-05

4.2.4 Discussion

The meso-zooplankton community in the GAB was highly variable in space and time, with significant differences in abundance, biomass, GMS, and $NBSS_{slope}$ between regions, areas of the shelf, and survey years. Overall, the GAB meso-zooplankton community was characterised by a higher biomass of small zooplankton in the central GAB, and with higher biomass of larger zooplankton in the upwelling region in the east. The $NBSS_{slope}$ was significantly steeper in the central region, further indicating the presence of a community dominated by smaller meso-zooplankton, likely feeding on pico and nano-phytoplankton (Marcolin et al. 2015). The $NBSS_{slope}$ was flatter in the east, indicative of a larger meso-zooplankton community, likely feeding on larger phytoplankton (i.e. diatoms), as previously reported for productive upwelling systems like the Humboldt current system (Iriarte and Gonza 2004). Together, these results support our findings from Project 2.2 (Chapter 4.1) of a longer microbial food web operating in the central GAB, with a shorter, classical food web in the east.

There were also significant annual differences in the meso-zooplankton community present in the GAB during the upwelling season. The clearest difference was in the 2013 survey year, when there were significantly larger meso-zooplankton in the community than in other years examined in this study, as indicated by the highest GMS and the flatter $NBSS_{slope}$ in this year. The presence of a flatter slope in 2013 may indicate that the zooplankton community is dominated by carnivorous and or omnivorous zooplankton at this time (Zhou et al. 2009). A community dominated by larger meso-zooplankton did not translate to highest mesozooplankton biomass for this region. In the survey year of 2014 for example, the highest meso-zooplankton abundance and biomass occurring for the study period, was reflected in a meso-zooplankton community dominated by relatively smaller sized individuals than in 2013. Such a community would likely be herbivorous/omnivorous, feeding on smaller particles and phytoplankton (Zhou et al. 2009; Marcolin et al. 2015). The central GAB phytoplankton community is dominated by pico- and nano-size particles, as well as abundant heterotrophic and/or mixotrophic dinoflagellates. Zooplankton taxa previously identified in the central GAB are known in other regions to feed preferentially on pico- and nano-sized organisms (see Patten and van Ruth, Project 2.2, Chapter 4.1).

Variations in meso-zooplankton abundance, biomass and size distributions by region and shelf area, and drivers of differences between regions, shelf areas and years, were in agreement with findings from previous studies where increases in abundance and biomass were associated with the presence of the cold upwelled water mass (van Ruth 2009, van Ruth and Ward 2009). However, measured environmental parameters explained at most 23% of the variation (i.e. temperature and shelf depth with meso-zooplankton abundances) and suggest other parameters not measured were also important drivers of the meso-zooplankton community. Alternatively, the low (but significant) explanatory power may be due to the time lag between key environmental parameters and the measured zooplankton parameters. High biomass in a given region for example, is the response to environmental conditions occurring in the ~weeks prior to sampling and do not necessarily match the *in situ* environmental conditions measured at the time of sampling.

Highest sardine egg densities occurred in the central GAB shelf in 2014, concomitant with highest meso-zooplankton abundances and biomass, with the meso-zooplankton dominated by relatively smaller individuals. In the GAB, copepods represent a significant fraction of the zooplankton community (see Patten and van Ruth, Project 2.2, Chapter 4.1). While the prey items of sardine adults in the GAB region are not well defined, in other regions (e.g. Adriatic Sea, Mediterranean Sea, Benguela and Humboldt current systems) copepod nauplii and copepodites represent major prey items for this group (Tudela and Palomera 1995).

The key enviromental drivers of fluorescence and temperature (at the MLD), together with the increased meso-zooplankton abundance provided a significant, yet overal low (19%), explanatory power for describing sardine egg density distributions. Nonetheless, these results support previous studies showing positive links between cold upwelled water and trophic biomass transfer from phytoplankton to meso-zooplankton to sardines, culminating in high sardine egg densities (Ward et al. 2006).

Through this work we have discovered that meso-zooplankton size distributions and the parameters of the NBSS provide valuable information that improves our understanding of the drivers of sardine egg density distributions. The analysis of plankton “bycatch” collected during sardine biomass surveys will provide additional information that will assist in the management of this valuable fishery and the GAB marine ecosystem.

References

Anderson, M. J., Gorley, R. N., and Clarke, K. N. 2008. PERMANOVA+ for PRIMER; a guide to software and statistical methods, PRIMER-E, Plymouth, UK.

de Boyer Montégut, C. B., G. , Madec, G., Fischer, A. S., Lazar, A., and D., L. 2004. Mixed layer depth over the global ocean: An examination of profile data and a profile-based climatology. Journal of Geophysical Research, 109: doi:10.1029/2004JC002378.

Dong, S., Sprintall, J., Gille, S. T., and Talley, L. 2008. Southern Ocean mixed-layer depth from Argo float profiles. Journal of Geophysical Research, 113: C06013, doi:06010.01029/02006JC004051.

Goldsworthy, S., D., Page, B., Rogers, P., J., Bulman, C., Wiebkin, A., McLeay, L. J., Einoder, L., et al. 2013. Trophodynamics of the eastern Great Australian Bight ecosystem: Ecological change associated with the growth of Australia's largest fishery. Ecological Modelling, 255: 38-57.

Herman, A. W., Beanlands, B., and Phillips, E. F. 2004. The next generation of Optical Plankton Counter: the Laser-OPC. Journal of Plankton Research, 26: 1135-1145.

Holte, J., and Talley, L. 2009. A New Algorithm for Finding Mixed Layer Depths with Applications to Argo Data and Subantarctic Mode Water Formation. Journal of Atmospheric and Oceanic Technology, 26: 1920-1939.

Iriarte, J., Luis., and González, H. E. 2004. Phytoplankton size structure during and after the 1997/98 El Niño in a coastal upwelling area of the northern Humboldt Current System. Marine ecology progress series, 269: 83-90.

Jennings, S., and Mackinson, S. 2003. Abundance–body mass relationships in size-structured food webs. Ecology Letters, 6: 971-974.

Krupica, K., L., Sprules, W. G., and Herman, A., W. 2012. The utility of body size indices derived from optical plankton counter data for the characterization of marine zooplankton assemblages. Continental Shelf Research, 36: 29-40.

Marcolin, C., R., Gaeta, S., and Lopes, R. M. 2015. Seasonal and interannual variability of zooplankton vertical distribution and biomass size spectra off Ubatuba, Brazil. Journal of Plankton Research, 37: 808-819.

Middleton, J. F., and Bye, J. A. T. 2007. A review of the shelf-slope circulation along Australia's southern shelves: Cape Leeuwin to Portland. Progress in Oceanography, 75: 1-41.

Moore, S., K., and Suthers, I., M. 2006. Evaluation and correction of subresolved particles by the optical plankton counter in three Australian estuaries with pristine to highly modified catchments. Journal of Geophysical Research: Oceans, 111: C05S04, doi:10.1029/2005JC002920.

Neira, F., J., Miskiewicz, A., G., and Trnski, T. 1998. Larvae of temperate Australian fishes: laboratory guide for larval fish identification, UWA Publishing.

Parker, K. 1980. A direct method for estimating northern anchovy, Engraulis mordax, spawning biomass. Fisheries Bulletin, 84: 541-544.

Rogers, P. J., Ward, T. M., van Ruth, P. D., Williams, A., Bruce, B. D., Connell, S. D., Currie, D. R., et al. 2013. Physical processes, biodiversity and ecology of the Great Australian Bight region: a literature review.

Sprules, W. G., and Munawar, M. 1986. Plankton Size Spectra in Relation to Ecosystem Productivity, Size, and Perturbation. Canadian Journal of Fisheries and Aquatic Sciences, 43: 1789-1794.

Suthers I, M., Taggart C, T., Rissik, D., and Baird, M. E. 2006. Day and night ichthyoplankton assemblages and the zooplankton biomass size spectrum in a deep ocean island wake. Marine ecology progress series, 322: : 225-238.

Tudela, S., and Palomera, I. 1995. Diel feeding intensity and daily ration in the anchovy Engraulis encrasicolus in the northwest Mediterranean Sea during the spawning period. Marine ecology progress series, 129: 55-61.

Van Ruth, P. D. 2009. Spatial and temporal variation in primary and secondary prodcuvity in the eastern Great Australian Bight. PhD Thesis. The University of Adelaide. p. 189.

van Ruth, P. D., Ganf, G. G., and Ward, T. M. 2010. Hot-spots of primary productivity: An Alternative interpretation to Conventional upwelling models. Estuarine, Coastal and Shelf Science, 90: 142-158.

van Ruth, P. D., and Ward, T. M. 2009. Meso-Zooplankton Abundance, Distribution and Community Composition in the Eastern Great Australian Bight. Transactions of the Royal Society of South Australia, 133: 274-283.

Ward, T. M., Burch, P., and Ivey, A. R. 2011a. Spawning biomass of Sardine, *Sardinops sagax*, in water off South Australia in 2011. Report to PIRSA Fisheries and Aquaculture. South Australian Research and Development Institute (Aquatic Sciences), Adelaide. SARDI Publication No. F2007.000566-4. SARDI Research Report Series No. 584. 31p pp.

Ward, T. M., Burch, P., McLeay, L. J., and Ivey, A. R. 2011b. Use of the Daily Egg Production Method for stock assessment of sardine, *Sardinops sagax*; lessons learnt over a decade of application off southern Australia. Reviews in Fisheries Science, 19: 1-20.

Ward, T. M., Hoedt, F., McLeay, L. J., Dimmlich, W. F., Jackson, G., Rogers, P. J., and Jones, K. 2001. Have recent mass mortalities of the sardine Sardinops sagax facilitated an expansion in the distribution and abundance of the anchovy *Engraulis australis* in South Australia. Marine ecology progress series, 220: 241-251.

Ward, T. M., Kinloch, M., G.K., J., and Neira, F. J. 1998a. A Collaborative Investigation of the Usage and Stock Assessment of Baitfish in Southern and Eastern Australian Waters, with Special Reference to Pilchards (*Sardinops sagax*). Final Report to FRDC. 324 pp.

Ward, T. M., Kinloch, M., Jones, G. K., and Neira, F. J. 1998b. A Collaborative Investigation of the Usage and Stock Assessment of Baitfish in Southern and Eastern Australian Waters, with Special Reference to Pilchards (*Sardinops sagax*). Final Report to FRDC. 324 pp.

Ward, T., M., McLeay, L. J., Dimmlich, W. F., Rogers, P., J., McClatchie, S. A. M., Matthews, R., Kampf, J., et al. 2006. Pelagic ecology of a northern boundary current system: effects of upwelling on the production and distribution of sardine (*Sardinops sagax*), anchovy (*Engraulis australis*) and southern bluefin tuna (*Thunnus maccoyii*) in the Great Australian Bight. Fisheries Oceanography, 15: 191-207.

White, K. V., and Fletcher, W. J. 1996. Identifying the developmental stages for eggs of the Australian sardine, Sardinops sagax. Fisheries Western Australia. Fisheries Research Report No. 103.

Zhou, M., Tande, K. S., Zhu, Y., and Basedow, S. 2009. Productivity, trophic levels and size spectra of zooplankton in northern Norwegian shelf regions. Deep Sea Research Part II :Topical Studies in Oceanography, 56: 1934-1944

5. SYNTHESIS / DISCUSSION
(Van Ruth, P.D. and Patten, N.L.)

Shelf waters of the eastern GAB support Australia's largest fishery by weight, the Australian Sardine Fishery, and the valuable Commonwealth Southern Bluefin Tuna Fishery, as well as the highest densities of seabirds and marine mammals in the Australian region. The enhanced pelagic productivity of this ecosystem is driven by seasonal upwelling of nutrient rich water from the Flinders Current. Despite the economic importance and conservation values of the region, few studies have investigated the effects of upwelling on the structure and function of the microbial and planktonic communities of the GAB or levels of primary, secondary and tertiary production. This project (Project 2.1) was designed to: 1) characterise the structure and function of the microbial and planktonic assemblages in the shelf waters of the eastern GAB, 2) provide enhanced understanding of the key environmental drivers of pelagic productivity, especially inter-annual variation in upwelling strength, and 3) provide the capacity to assess potential future impacts on pelagic ecosystem processes, including the implications of climate change for future management of the region's valuable pelagic fisheries. We utilized a suite of physical, chemical and biological data sets collected over a range of spatial and temporal scales to address the key project hypotheses. Section 3 of this report characterised spatial and temporal variations in physical and chemical drivers of food web dynamics in shelf waters across the GAB. Section 4 examined variations in microbial and planktonic abundance, size structure and community composition, and was more focussed on the data rich eastern GAB region. Key findings from each section, and their role in the evaluation of project hypotheses and objectives, are outlined below.

Hypothesis 1: "That the microbial food web is the dominant planktonic food web in shelf waters of the eastern GAB, and that the more efficient classic food web only occurs during periods of nutrient-rich upwelling. Spatial and temporal shifts in the influence of upwelling and downwelling in the eastern GAB trigger shifts in food web structure between the microbial food web, and the classic, diatom dominated food web"

> *Objective 1: Identify and compare inter-annual, seasonal and spatial variability in the taxonomic composition and size distribution of the microbial, phytoplankton and zooplankton assemblage in shelf waters of the eastern GAB to test the hypothesis that spatial and temporal shifts in the influence of upwelling and downwelling trigger shifts in food web structure between the microbial loop and the classic diatom dominated food web.*
>
> *Objective 3: Identify key environmental drivers of observed variability in species composition and size spectrum of microbes and plankton (e.g. upwelling strength, nutrient concentrations, primary productivity).*

Chapter 3.1 analysed a ten-year data set of wind stress and remote sensed primary productivity, and coupled this with a five-year data set of *in situ* water column measurements (seawater temperature, salinity, irradiance and dissolved nutrients) to assess key drivers of variation in enrichment and primary productivity in the eastern GAB. Consistent with previous research (Kämpf et al. 2004, Middleton and Bye 2007, van Ruth et al. 2010b, a) we found that:

- Seasons can be characterised by the dominant alongshore windstress (AWS), with upwelling favourable winds prevailing through summer/autumn (November-April), and downwelling favourable winds dominant in winter/spring (May-October).
- Inter- and intra-seasonal variability in AWS drove marked variation in seasonal primary productivity between years

- Chapter 3.1 provided new information regarding the timing, intensity and duration of upwelling, and the potential influence of upwelled waters on primary productivity.

Specifically, key findings were:

- The length of an upwelling season did not dictate its intensity or productivity, and long, intense seasons were not necessarily the most productive.
- It was important to differentiate between upwelling events (indicated from AWS) and enrichment events (as indicated by NO_x >2 µM; temperatures <15°C and salinities <35.6 psu in the euphotic zone). Specifically, AWS was not a good indicator of enrichment in the euphotic zone in the early upwelling season (November-December).
- The early upwelling season represents a pre-conditioning period that is critical in governing the intensity of enrichment in the euphotic zone during the late upwelling season. The intensity and number of upwelling/downwelling events through the pre-conditioning period will dictate the volume of nutrient rich water drawn onto the shelf in the Kangaroo Island pool that is available to be brought into the euphotic zone during subsequent, late season upwelling events.
- The eastern GAB can be considered a region subject to moderate enrichment and, generally, moderate rates of primary productivity on a global scale.

With a clearer understanding of the influence of event scale variations in upwelling and downwelling on enrichment and primary productivity in the eastern GAB, we propose a refined conceptual model for the region (Fig. 3.1-6), building on the work of van Ruth et al. (2010a, b). The model details five different meteorological/oceanographic scenarios that are likely to occur in the eastern GAB, and their influence on lower trophic ecosystem dynamics and productivity:

- Winter-mixing: Downwelling conditions, well mixed water column, no enriched water entering the euphotic zone.
- Preconditioning: Upwelling favourable winds with an enriched bottom layer of water on the shelf, but no enrichment of euphotic zone.
- Moderate upwelling: Upwelling favourable conditions, moderate enrichment of ~ the bottom third of the euphotic zone.
- Strong upwelling: Upwelling favourable conditions with significant enrichment of ~ the bottom two thirds the euphotic zone, at times approaching the surface.
- Suppression: downwelling conditions, enhanced mixing, suppression of enrichment.

Total ecosystem productivity in the eastern GAB will depend on the combination of these scenarios that occurs in the region in a given season/year, and will be further influenced by variations in the duration and intensity of individual events (i.e. within scenario variation).

Further information on water mass characteristics and spatial variations in the influence of upwelling and downwelling across the wider GAB shelf region was provided through Chapter 3.2. Data analysed in Chapter 3.2 consisted of over 10 years of data obtained from CTD instruments that were attached to Australian sea lions, with ~20,000 temperature and salinity profiles across ~1,000 km of shelf, covering up to 10 months of the year, including the 4 – 6 months through the upwelling season. All the data are free to access, and are stored on the IMOS Ocean Current web portal (see http://oceancurrent.imos.org.au/aatams.php). This dataset was critical for evaluating the objectives of this project as it represents the only source of sub-surface data available in some areas of the GAB, especially the more remote regions in the central GAB where there is a paucity of ship-based CTD profiles, and the only source of near-real time sub-surface observations in the GAB region. Key

findings from Chapter 3.2 regarding spatial and temporal variations in water mass characteristics across the broader GAB shelf include:

- The water column was well-mixed from surface to bottom during winter (June to September). The set-up of stratification occurred in Spring (November), with wide spread stratification of the water column over the shelf in Summer (December to February). The breakdown of stratification occurred in Autumn (March to May).
- Cold water originating from the slope present on the shelf south of Eyre Peninsula in December, which then moves north-westerly toward Cape Bauer by March/April, after which slope water no longer observed on the shelf.
- The rare occurrence of cold (<15°C) water reaching the surface during the upwelling season, a phenomenon that was not observed in the datasets analysed in Chapters 3.1 and 4.1.
- The maximum spatial extent of upwelled water occurs over the GAB shelf during March and April.
- The westward extent of upwelled water reaches along the coast as far as ~133.5°E.
- The long time series data analysed in Chapter 3.2 confirm that the upwelled water mass, and thus significant enrichment of waters in the euphotic zone, is restricted to the eastern GAB region, and areas close to the coast as far west as Cape Bauer. Aside from these nearshore regions, water mass characteristics in the central GAB reveal little evidence of upwelled water (temperatures < 15°C and salinities < 35.6 psu), which implies the absence of significant enrichment from physical processes in the region. This further suggests that enrichment through biological processes associated with the microbial food web may be more important in supporting productivity in the central GAB, as discovered in project 2.2, Chapter 4.1.

The results of Chapter 4.1 represent the first holistic view of the lower trophic food web in the eastern GAB. An ~8 year time series of chemical and biological parameters was used to characterise variation in the composition of the lower trophic ecosystem (viruses, bacteria, phytoplankton through to mesozooplankton) in the region, in order to capture the responses of organisms at the base of the food web over a spectrum of sizes and trophic modes, to changes in hydrographic conditions and the degree of enrichment of waters in the euphotic zone. Sampling events were assigned to one of five scenarios likely to occur in the eastern GAB, as defined in the conceptual model in Chapter 3.1 (Fig. 3.1-6). We then compared observed community biomass, abundance, composition and structure with predictions made in the conceptual model. Key features of the food web during winter-mixing, moderate and strong upwelling best aligned with the predictions of the conceptual model, but there were inconsistencies between the predicted and observed plankton community. For example, during winter-mixing, a picophytoplankton community was predicted to dominate. Instead, nanophytoplankton comprised the bulk of autotrophic biomass and with high numbers of flagellates and dinoflagellates occurring (Table 4.1-5). Together, these results indicated a food web better described as multivorous, rather than strictly microbial. The predictions for a shift towards a classical food web during moderate upwelling were consistent with observed plankton communities, with a co-dominance of pico- and micro-phytoplankton at this time (Table 4.1-5). Clear classical food webs were also apparent during strong upwelling, as predicted, with micro-phytoplankton (specifically diatoms) comprising the bulk of abundance and biomass (Table 4.1-5). During suppression, the prediction of a multivorous food web, with a combination of microbial and classical food webs operating together, was somewhat matched with observations. However, this food web is better described as microbial/multivorous, given the dominance of nanophytoplankton (as biomass) and relatively high numbers of the small picophytoplankton, bacteria and viruses (Chapter 4.1). Furthermore, given the low autotrophic biomass at this time, concomitant with low

zooplankton biomass, primary productivity might be lower than predicted in the conceptual model. Predictions of the food web structure and likely levels of primary productivity did not match well during preconditioning. Predictions in Chapter 3.1 were based solely on the fact that during pre-conditioning, enriched water rarely (if ever) reached the euphotic zone, suggesting a microbial food web would likely occur. Instead, we observed moderate to high levels of autotrophic biomass together with highest abundances of diatoms and flagellates (and bacteria) (Table 4.1-5), which are hypothesised to represent a newly documented "spring bloom" scenario, commencing during the winter to spring transition period, when irradiance levels increase and the water column begins to stratify. Coincident high zooplankton abundances and biomass suggest efficient trophic transfer from primary producers to secondary consumers. These results further indicate higher levels of primary productivity during the pre-conditioning period than predicted in the conceptual model in Chapter 3.1.

Other novel findings from Chapter 4.1 include:

- Possible additional SiO_2 sources in the eastern GAB, not linked to upwelled water (e.g. groundwater intrusion, benthic resuspension).
- The importance of nanophytoplankton to overall phytoplankton biomass and food web dynamics year-round in eastern GAB shelf waters.
- The occurrence of relatively high numbers of dinoflagellates which appear to be mixotrophic/heterotrophic, and are proposed as an important trophic link between pico-, nano-, and micro-plankton and copepods and other zooplankton taxa.
- Viruses likely exert, at times, strong pressures on the bacteria, picophytoplankton and nanophytoplankton communities.
- The microbial food web is a persistent feature of the eastern GAB, with growth and biomass buildup of larger phytoplankton concomitant with smaller cells during periods of enrichment (i.e. not replacement of small cells with larger cells).
- Efficient biomass transfer from primary to secondary producers occurs during preconditioning, strong upwelling and, at times, at the end of the upwelling season.
- The importance of the winter to spring transition period for "kick starting" productivity and trophic transfer in the system.

Hypothesis 2: "That shifts in food web structure will have implications for the size structure of the zooplankton community in shelf waters of the GAB and, consequently, the biomass of upper trophic levels."

Objective 2: Derive empirical relationships between taxonomic composition and size structure of plankton to test the hypothesis that shifts in food web structure will have implications for the size structure of the zooplankton community and, consequently, the biomass of upper trophic levels.

Objective 4: Compare inter-annual patterns in microbial and planktonic ecosystem structure and sardine egg density.

Chapter 4.2 used a suite of meso-zooplankton parameters (abundances, biomass and size distributions), together with environmental parameters, to improve the understanding of the factors influencing the distributions and densities of sardine eggs.

Key results for the meso-zooplankton community showed that there were:

- Differences in the size distributions of meso-zooplanton in the central and eastern GAB; with the meso-zooplankton comprised of smaller individuals in the central GAB, and larger

individuals in the eastern GAB. These results suggest a longer chained 'microbial' food web may be occurring in the central GAB and a shorter chained, more efficient, classical food web may be occurring in the east during upwelling.

- Clear annual differences in the meso-zooplankton community present in the GAB during the upwelling season. For example, a significantly larger sized meso-zooplankton community occurred in 2013 compared to any other year. In survey year 2014, the highest meso-zooplankton abundance and biomass recorded for the study period was reflected in a meso-zooplankton community dominated by relatively smaller sized individuals than in 2013.
- Temperature was a key driver overall of meso-zooplankton abundance, biomass and size distribution, as shown in previous studies (e.g. van Ruth 2009, van Ruth and Ward 2009). However, the low explanatory power was likely due to additional parameters not measured and/or time lags in the responses of the meso-zooplankton community to key environmental drivers.

The key findings for the sardine egg densities were that:

- Highest sardine egg densities occurred in the central GAB shelf in 2014, concomitant with highest meso-zooplankton abundances and biomass, with the meso-zooplankton dominated by relatively smaller individuals.
- The key enviromental drivers of fluorescence and temperature (at the MLD), together with the increased meso-zooplankton abundance provided a significant yet, overal low (19%) explanatory power for describing sardine egg densities distributions.

Together these results highlight the difficulty in unravelling the responses of lower trophic organisms influenced by environmental drivers occurring over various time scales (i.e. days to weeks). However, these results support previous findings of the link between cold upwelled water, increased phytoplankton biomass, increased zooplankton biomass and increased sardine egg densities (Ward et al. 2006).

References

Kämpf, J., Doubell, M., Griffin, D., Matthews, R., L., and Ward, T. M. 2004. Evidence of a large seasonal coastal upwelling system along the southern shelf of Australia. Geophysical Research Letters, 31: 31:doi:1029/2003GL019221.

Middleton, J. F., and Bye, J. A. T. 2007. A review of the shelf-slope circulation along Australia's southern shelves: Cape Leeuwin to Portland. Progress in Oceanography, 75: 1-41.

Van Ruth, P. D. 2009. Spatial and temporal variation in primary and secondary prodcuvity in the eastern Great Australian Bight. PhD Thesis. The University of Adelaide. p. 189.

van Ruth, P. D., Ganf, G. G., and Ward, T. M. 2010a. Hot-spots of primary productivity: An Alternative interpretation to Conventional upwelling models. Estuarine, Coastal and Shelf Science, 90: 142-158.

van Ruth, P. D., Ganf, G. G., and Ward, T. M. 2010b. The influence of mixing on primary productivity: A unique application of classical critical depth theory. Progress in Oceanography, 85: 224-235.

van Ruth, P. D., and Ward, T. M. 2009. Meso-Zooplankton Abundance, Distribution and Community Composition in the Eastern Great Australian Bight. Transactions of the Royal Society of South Australia, 133: 274-283.

Ward, T., M., McLeay, L. J., Dimmlich, W. F., Rogers, P., J., McClatchie, S. A. M., Matthews, R., Kampf, J., et al. 2006. Pelagic ecology of a northern boundary current system: effects of upwelling on the production and distribution of sardine (*Sardinops sagax*), anchovy (*Engraulis australis*) and southern bluefin tuna (*Thunnus maccoyii*) in the Great Australian Bight. Fisheries Oceanography, 15: 191-207.

6. CONCLUSION

This study was focused primarily on shelf waters of the eastern GAB, using existing time series data to examine temporal variations in food web dynamics linked to changes in physical processes. In addition, datasets collected in shelf waters of the central GAB were used to identify the spatial and temporal extent of the influence of upwelled water, and examine variations in the distributions of higher order planktonic organisms across the region.

Our findings indicate that enrichment via upwelling is a key environmental driver of variation in food web dynamics in the eastern GAB. However, the situation is more complex than first thought, and our findings deviate somewhat from our hypotheses. There are three food webs operating in the eastern GAB, all of which vary significantly in their influence on productivity in the region, and are enhanced by enrichment via upwelling. The microbial food web is present year-round in the eastern GAB, but as a background signal underlying other important food webs in the region, effectively "keeping the lights on" in productivity terms. The dominant food web in the eastern GAB, underpinning moderate rates of primary productivity year-round, is a previously undocumented (for GAB waters) food web based on nanophytoplankton and heterotrophic dinoflagellates. The importance of dinoflagellates representing a significant trophic pathway has been highlighted across the wider GAB region (Kloser et al. 2017). The efficient, classic food web only occurs during upwelling, when enrichment drives spikes in rates of primary productivity that are comparable to highly productive eastern boundary current upwelling systems. Of particular note is that during periods of enrichment, growth and biomass buildup of larger phytoplankton occurs together with increased growth and biomass of smaller cells (i.e. not simply the replacement of small cells with larger cells).

We have detailed, for the first time, the importance of the preconditioning period that characterises the early upwelling season in governing the intensity of enrichment in the euphotic zone during the late upwelling season. In addition, we have discovered a previously undocumented "spring bloom" scenario which develops during the winter-spring transition, and provides a critical "kick-start" for productivity and trophic transfer in the system. Physical and chemical drivers of this phenomenon are yet to be described. Future studies should focus on examining the influence of variations in the duration and intensity of individual events (i.e. within scenario variation) on enrichment, primary productivity, and food web dynamics in the eastern GAB, and the physical, chemical, and biological processes underlying the spring bloom.

Variations in the size structure of the zooplankton community in the GAB are implicitly related to the underlying dominant food webs, and shifts in food web structure drive changes in meso-zooplankton size structure. The meso-zooplankton community found in the central GAB was smaller than that found in the east. This same finding has been shown to occur using different data sets in the early austral summer (December, Kloser et al. 2017). Highest sardine egg densities are linked with years and locations having highest zooplankton abundances and biomass. Our work highlights the influence of enrichment via upwelling on biomass transfer from primary producers to primary and secondary consumers in eastern GAB waters.

References

Kloser R, van Ruth P.D, Doubell M, Downie R, Flynn A, Gershwin L, Patten N, Revill A, Richardson A.E, Ryan T.E and Sutton C.A (2017). Characterisation of spatial variability of offshore/slope plankton and micronekton communities. Final Report GABRP Project 2.2. Great Australian Bight Research Program, Great Australian Bight Research Report Series Number 22, 297pp.

7. APPENDIX 1: DATA MANAGEMENT

7.1 Raw dataset created

Type	Description	Data security and privacy issues	Nominated data custodian	Institute
Dissolved nutrients	NO_2 + NO_2 (NO_x), NH_4, PO_4 and SiO_2 from various depths through the water column but usually corresponding with a surface (5 – 10 m), cmax (as defined from fluorescence profiles) and deep samples (below the cmax)		Australian Ocean Data Network (AODN)	Integrated Marine Observing System (IMOS)
CTD profiles	Conductivity temperature and depth profiles obtained via shipboard oceanographic sampling		Australian Ocean Data Network (AODN)	Integrated Marine Observing System (IMOS)
CTD profiles (from seals)	Temperature, salinity and depth profiles obtained from seal dives		Australian Ocean Data Network (AODN)	Integrated Marine Observing System (IMOS)
Viruses, bacteria and picophytoplankton	Samples were analysed with flow cytometry and raw FSC files obtained. FSC files were subsequent analysed with FlowJo software to differentiate and determine abundances of groups viruses, bacteria and picophytoplankton.		Australian Ocean Data Network (AODN)	Integrated Marine Observing System (IMOS)
Phytoplankton	Enumeration and taxonomic identification of phytoplankton		Australian Ocean Data Network (AODN)	Integrated Marine Observing System (IMOS)
Pigments/Chlorophyll a	Filtered water samples processed via High Performance Liquid Chromatography (HPLC)		Australian Ocean Data Network (AODN)	Integrated Marine Observing System (IMOS)
LOPC	Mesozooplankton size distributions		Paul van Ruth	SARDI

7.2 Data processing and derived datasets

Reference Chapter	Description			Institute
3.1	Physical (Wind stress) and chemical data sets were processed as described in chapter 3.1. Remote sensed Primary productivity data was obtained as outlined in Chapter 3.1.		Paul van Ruth	SARDI
3.2	Conductivity, temperature and salinity data were processed as described in Chapter 3.2. Three main water masses were identified and further temporal and spatial patterns/ranges over the GAB were described.		Fred Ballieul	SARDI
4.1	Physical (Wind stress, stratification), chemical, microbial and plankton data sets were processed as described in chapter 4.1. Sampling dates were assigned to one of five scenarios based on *in situ* temperatures within the water column as described in chapter 4.1.		Nicole Patten	SARDI
4.2	LOPC data was processed as described in Chapter 4.2. Mesozooplankton abundance, biomass, geometric mean size and NBSS slope determined were then determined. Sardine egg density data was also used together with physical parameters in generalised linear models.		Paul van Ruth	SARDI

7.3 Data curation and archive

A metadata record will be created and registered on AODN catalogue for all raw and derived datasets generated as part of the GABRP. Where possible, datasets will be lodged with IMOS / IMOS Ocean Portal.

7.4 Data access, use agreements and licensing

Where possible, datasets will be made publicly available (e.g. through the AODN / IMOS portal). In the event that a dataset can't be made publicly available, an electronic copy of the dataset will be supplied to GABRP partners.

7.5 Publication of datasets

Data generated by this study will be made publicly available via the SARDI and CSIRO data portals (as per SARDI and CSIRO data management policies) and via the Integrated Marine Observing System's Australian Ocean Data Network.

8. APPENDIX 2: STUDENT PROJECTS

8.1 Student name

8.2 Degree type, project title and institution

8.3 Status of student project

9. APPENDIX 3: PROJECT PUBLICATIONS

9.1 Papers

Patten, N. L., van Ruth, P. D., and Redondo Rodriguez, A. In review. Environmental driven shifts in picoplankton and viral community composition in slope and offshore waters of the Great Australian Bight (southern Australia). Deep Sea Research Part II: Topical Studies in Oceanography.

Bailleul, F., Richardson, L., van Ruth P.D., McMahon, C.R., Harcourt, R.G., Middleton, J., Ward, T., and Goldsworthy, S.D. In review. Animal-borne instruments provide new observations of seasonal subsurface oceanographic features over the continental shelf of the Great Australian Bight. Deep Sea Research Part II: Topical Studies in Oceanography.

9.2 Presentations

Patten, N. L., and van Ruth, P. D. 2015. Picoplankton and virioplankton in offshore waters of the Great Australian Bight. Australian Marine Science Association conference, Geelong, Vic, July 2015.

Patten, N. L., Doubell, M.D., and van Ruth, P. D. 2017. Shifts in plankton community composition as indicators of enrichment processes in the Great Australian Bight (southern Australia), Australian Marine Science Association conference, Darwin, N.T. July 2017

van Ruth, P., Patten, N., and Redondo, A. (2017) Variations in productivity in the Great Australian Bight: Uncovering hidden influences on the food web. Australian Marine Sciences Association annual conference, July 2017, Darwin, Northern Territory.

9.3 Patents

Not applicable

9.4 Media Releases

Refer to program summary

10. APPENDIX 4: INTELLECTUAL PROPERTY

10.1 Unique discoveries

Not applicable

10.2 Action plan

TBD


bp


CSIRO


SOUTH AUSTRALIA
Government
of South Australia
Primary Industries
and Regions SA


SARDI
SOUTH AUSTRALIAN
RESEARCH AND
DEVELOPMENT
INSTITUTE


SUB CRUCE LUMEN
THE UNIVERSITY
of ADELAIDE


Flinders
UNIVERSITY